AD_____

Award Number: DAMD17-02-1-0336

TITLE: Functional Disruption of the Netrin-1 Guidance Cue Leads to Disruption in Mammary Gland Development and Increased Tumor Incidence

PRINCIPAL INVESTIGATOR: Lindsay Hinck, Ph.D.

CONTRACTING ORGANIZATION: University of California, Santa Cruz
Santa Cruz, CA 95064

REPORT DATE: July 2005

TYPE OF REPORT: Annual Summary

PREPARED FOR: U.S. Army Medical Research and Materiel Command
Fort Detrick, Maryland 21702-5012

REPORT DOCUMENTATION PAGE

Form Approved
OMB No. 0704-0188

1. REPORT DATE *(DD-MM-YYYY)*	2. REPORT TYPE	3. DATES COVERED *(From - To)*
01-07-2005	Annual Summary	1 Jul 2002 – 30 Jun 2005

4. TITLE AND SUBTITLE
Functional Disruption of the Netrin-1 Guidance Cue Leads to Disruption in Mammary Gland Development and Increased Tumor Incidence

5a. CONTRACT NUMBER

5b. GRANT NUMBER
DAMD17-02-1-0336

5c. PROGRAM ELEMENT NUMBER

6. AUTHOR(S)
Lindsay Hinck, Ph.D.

E-mail: hinck@biology.ucsc.edu

5d. PROJECT NUMBER

5e. TASK NUMBER

5f. WORK UNIT NUMBER

7. PERFORMING ORGANIZATION NAME(S) AND ADDRESS(ES)
University of California, Santa Cruz
Santa Cruz, CA 95064

8. PERFORMING ORGANIZATION REPORT NUMBER

9. SPONSORING / MONITORING AGENCY NAME(S) AND ADDRESS(ES)
U.S. Army Medical Research and Materiel Command
Fort Detrick, Maryland 21702-5012

10. SPONSOR/MONITOR'S ACRONYM(S)

11. SPONSOR/MONITOR'S REPORT NUMBER(S)

12. DISTRIBUTION / AVAILABILITY STATEMENT
Approved for Public Release; Distribution Unlimited

13. SUPPLEMENTARY NOTES

14. ABSTRACT
My laboratory discovered a mammary receptor for the "axon guidance" cue netrin-1 (Ntn1) called neogenin, and I proposed to examine the stromal phenotype associated with the loss of function of neogenin using transplant analysis. Analysis of homozygous null mammary tissue versus wildtype revealed no changes in tissue morphology due to the loss of neogenin function during any stage of mammary gland development. During these studies, we observed a synergistic relationship between netrin-1 and another "axon guidance" cue, Slit2. Importantly, many studies have linked misexpression of Slit proteins with breast cancer progression. While Slit2 null mammary glands displayed a phenotype similar to Ntn1 null glands, glands harboring homozygous null mutations in both Ntn1 and Slit2 showed an enhanced phenotype that extended through the ducts and was characterized by separated cell layers, occluded lumens and hyperplasia. Our data demonstrate that these new proteins, originally identified in the nervous system, play critical roles during gland development and disease.

15. SUBJECT TERMS
Netrin-1, tumor suppressor, neogenin, Slit2

16. SECURITY CLASSIFICATION OF:			17. LIMITATION OF ABSTRACT	18. NUMBER OF PAGES	19a. NAME OF RESPONSIBLE PERSON
a. REPORT	b. ABSTRACT	c. THIS PAGE			19b. TELEPHONE NUMBER *(include area code)*
U	U	U	UU	89	

Table of Contents

Introduction: In the first year, we discovered a mammary receptor for netrin-1 (Ntn1). On the basis of this discovery, the advice of my grant reviewers and the recommendation after my first annual summary, I revised my Statement of Work (SOW) to focus my studies on the function of this receptor during mammary gland development. I specifically proposed to examine the stromal phenotype associated with the loss of neogenin using transplant analysis. I completed these studies by examining the phenotypes in mature animals during pregnancy, lactation and involution. The results were negative but in the course of the studies we made the intriguing observation that glands carrying homozygous null mutations in Slit2, which encodes another "axon guidance" cue, displayed phenotypes strikingly similar to the Ntn1-/- glands. We pursued these observations and discovered that Netrin1 and Slit2 act synergistically during mammary ductal development to mediate adhesive interactions between the luminal and myoepithelial cell layers.

Body: I analyzed transplants harboring neogenin homozygous loss of function mutations (Neo1-/-) during all stages of mammary gland development (pregnancy, lactation and involution) as specified in my revised and approved Task 3 of my SOW. No differences were observed between Neo1-/- and +/+ tissue, suggesting that stromally-expressed neogenin does not play a significant role in mediating outgrowth of the gland.

During these studies, we observed a synergistic relationship between netrin-1 and another "axon guidance" cue, Slit2. Importantly, many studies have linked mis-expression of Slit proteins with breast cancer progression. While Slit2 null mammary glands displayed a phenotype similar to Ntn1 null glands, glands harboring homozygous null mutations in both Ntn1 and Slit2 showed an enhanced phenotype that extended through the ducts and was characterized by separated cell layers, occluded lumens and hyperplasia. I pursued these results using in vitro aggregation assays and showed that Slit2-/-;Ntn1-/- cells, in contrast to +/+ cell, do not form bi-layered organoids, a defect rescued by addition of SLIT2. NTN1 has no effect alone but synergistically enhances this rescue. These data establish a new role for SLIT2 as an adhesive cue during mammary development, and show that NTN1 and SLIT2 act synergistically to generate cell boundaries along ducts during the formation of the bi-layered mammary tube.

Key Research Accomplishments:

- Transplanted +/+ and Neo1-/- epithelium into Neo1-/- stroma and compared this to wildtype control. Obtained negative results showing no differences between +/+ and Neo1-/- tissue during any stage of mammary development.
- During course of study, observed that glands harboring Slit2 loss-of-function mutations displayed phenotypes reminiscent of those present in Ntn1-/- and Neo1-/- glands.
- Pursued these new results and demonstrated that Slit2 functions synergistically with Ntn1 during mammary gland development.

Reportable Outcomes (Bibliography):

Presentations:

Lindsay Hinck, Phyllis Strickland, Grace Shin. 2005. *Axon guidance cues in mammary gland development,* Era of Hope Breast Cancer Research Program, Pennsylvania.

Lindsay Hinck, Phyllis Strickland, Grace Shin, Andrew Plump, Marc Tessier-Lavigne. 2005. *Generating at tubular bilayer: Slit2 and Netrin1 act as short-range attractants,* Mammary Gland and Breast Cancer Gordon Conference, Rhode Island.

Lindsay Hinck, Grace Shin, Phyllis Strickland, 2005. *The role of axon guidance molecules in mammary gland development,* Salivary Glands and Exocrine Secretion Gordon Conference, California.

Lindsay Hinck, Grace Shin, Phyllis Strickland, 2004. *The role of axon guidance molecules in mammary gland development,* Basement Membrane Gordon Conference, New Hampshire.

Lindsay Hinck, Grace Shin, Phyllis Strickland, 2004. *The role of axon guidance molecules in mammary gland development,* Mammary Gland and Breast Cancer Gordon Conference, Italy.

Lindsay Hinck, Grace Shin, Phyllis Strickland, 2004 *The role of axon guidance molecules in mammary gland development,* Keystone Symposium, Signaling in Vertebrate Organogenesis, New Mexico.

Lindsay Hinck, Phyllis Strickland, 2003. *Netrin and slit axon guidance molecules play a role during mammary gland developemnt,* Mammary Gland and Breast Cancer Gordon Conference, Rhode Island.

Manuscripts:

*Strickland P., *Shin G., Plump A., Tessier-Lavigne M., Hinck L., Slit2 and Netrin1 act synergistically as adhesive cues to generate tubular bi-layers during ductal morphogenesis. Development, in review.

Hinck, L. 2004. The versatile roles of "axon guidance' cues in tissue morphogenesis. Developmental Cell. 7: 783-793.

*Srinivasan K., *Strickland P., Valdes A., Shin, G.C., Hinck, L. 2003. Netrin-1/neogenin interaction stabilizes multipotent progenitor cap cells during mammary gland development. Developmental Cell 4: 1-20.

List of personnel receiving pay:

Lindsay Hinck

Conclusions:

At the beginning of this grant, I was new to the mammary gland/breast cancer field having done my post-doctoral training in a neuroscience lab. A major goal of this DOD Career Grant was to facilitate my entry into this new field. In my statement of work, task 1 was to master techniques of mammary gland manipulation and I have accomplished this. Task 2 was to generate tissue for experiments and I accomplished this. Based on reviewers suggestion, Task 3 was revised after the first year to become analyzing neogenin null mammary gland at all developmental stages: virgin development, pregnancy, lactation and involution. I performed these experiments but the results were negative. During the course of the investigation, however, we made and pursued an intriguing observation about another "axon guidance" cue Slit2. The final task in my SOW, Task 4 scheduled for the final year, was to analyze data and write papers.

With the conclusion of the grant, I have successfully entered the mammary gland/ breast cancer field as evidenced by my involvement in the community, invitations to speak at meetings and write reviews, and research papers either published or in submission. Our work on "axon guidance" cues in the mammary gland has progressed steadily. My laboratory has discovered novel adhesive roles for two families of cues, the Netrin and Slit families, during mammary gland development. The implications of these new findings are very important because they suggest that significant and complex roles exist for "neurogenic" signaling systems in the mammary gland. Because these systems appear to target cell adhesion and potentially cell motility, their disfunction in the mammary gland could be pro-metastatic. Our findings lay the foundation for future studies to examine the role that Netrin and Slit loss play in the etiology of breast cancer and whether this loss serves as a prognostic indicator of disease outcome.

Appendixes:

Netrin-1/Neogenin Interaction Stabilizes Multipotent Progenitor Cap Cells During Mammary Gland Morphogenesis

Karpagam Srinivasan §, Phyllis Strickland §,

Ana Valdes, Grace C. Shin and Lindsay Hinck*

Department of Molecular, Cell and Developmental Biology

University of California, Santa Cruz

Santa Cruz, CA 95064

*** Corresponding author: hinck@biology.ucsc.edu**

§ These authors contributed equally to the work

Running title: **Netrin-1/Neogenin in Mammary Gland Morphogenesis**

SUMMARY

Netrin-1 and its receptors play an essential role patterning the nervous system by guiding neurons and axons to their targets. To explore whether netrin-1 organizes non-neural tissues, we examined its role in mammary gland morphogenesis. Netrin-1 is expressed in prelumenal cells and its receptor, neogenin, in a complementary pattern in adjacent cap cells of terminal end bud (TEBs). We discovered that loss of either gene results in disorganized TEBs characterized by exaggerated subcapsular spaces, breaks in basal lamina, dissociated cap cells and an increased influx of cap cells into the prelumenal compartment. Cell aggregation assays demonstrate that neogenin mediates netrin-1 dependent cell clustering. Thus netrin-1 appears to act locally through neogenin to stabilize the multipotent progenitor (cap) cell layer during mammary gland development. Our results provide a new perspective on netrin-1 and its receptor neogenin by demonstrating an adhesive rather than guidance function for them during non-neural organogenesis.

INTRODUCTION

Netrin-1 (*ntn1*) plays a well-established role both as a short-and long-range guidance cue directing neurons and their axons to targets during development of the nervous system (Tessier-Lavigne and Goodman, 1996). It is bifunctional, acting either as an attractant or a repellent depending on the receptors expressed on neurons and the levels of intracellular cAMP (Hong et al., 1999; Ming et al., 1997). Two vertebrate families of netrin-1 receptors have been identified, the Deleted in Colorectal Cancer family comprising *DCC* and *neo1* (Keino-Masu et al., 1996), and the UNC5H family comprising *unc5h1-h4* (Engelkamp, 2002; Leonardo et al., 1997; Przyborski et al., 1998). The DCC family mediates attraction to netrin-1 while the UNC5H family forms a netrin-1 dependent complex with DCC to mediate repulsion (Hong et al., 1999). The function of DCC as a neuronal attractant receptor for netrin-1 has been well established (Fazeli et al., 1997; Keino-Masu et al., 1996), but relatively little is known about the function of neogenin. Although widely expressed during development (Gad et al., 1997), no phenotype has been reported for the *neo1* -/- mouse (Leighton et al., 2001). Indeed, no functional role for neogenin has been demonstrated in either an *in vitro* or *in vivo* context.

While netrin-1 is primarily thought of as an axon guidance cue, guidance is unlikely to be its only function since expression studies have shown that many netrins are widely expressed outside the nervous system (Koch et al., 2000; Meyerhardt et al., 1999; Salminen et al., 2000; Wang et al., 1999). Nevertheless, the developmental role of netrin-1 and its receptors in the morphogenesis of non-neuronal organs remains largely unexplored. Since netrin-1 is an early cue that patterns the nervous system by guiding millions of growth cones

on their journeys, one way to think about its function in morphogenesis is as a molecule that provides spatial and temporal information to shape tissue and organ development.

The mammary gland is an organ that undergoes an elaborate and regulated morphogenesis (Silberstein, 2001). During development, mammary epithelium grows from the nipple subdermally to invade the fat pad, establishing a mammary tree through a process of ductal elongation and branching. The ducts of the mammary gland comprise an outer tube of myoepithelial cells juxtaposing an inner tube of lumenal epithelial cells surrounding a central lumen. Terminal end buds (TEBs) are the enlarged termini of ducts responsible for prodigious pubertal growth controlled by hormones and growth factors (Fig. 1H). During development, the motile TEB penetrates the stromal fat pad at a rapid pace (0.5 mm/day), establishing the complex ductal architecture of the virgin mammary gland (Williams and Daniel, 1983). This growth is driven by the proliferation of a single layer of cells, termed cap cells, at the tip of the TEB, and by the underlying prelumenal epithelium. Cap cells are multipotent progenitor cells of the virgin mammary gland (Williams and Daniel, 1983). As the TEB grows rapidly toward the edge of the fat pad, cap cells translocate laterally to differentiate into myoepithelial cells (Williams and Daniel, 1983). In addition, a fraction detach and move into the subjacent prelumenal cell population where they are thought to give rise to a fraction of lumenal epithelial cells (Williams and Daniel, 1983). Cap and prelumenal cell layers are maintained as distinct populations through different adhesion systems. Cap cells adhere to each other through P-cadherin, and prelumenal cells through E-cadherin (Daniel et al., 1995). However, the mechanism that maintains the close apposition of the cap and prelumenal layers during the dynamic growth of the TEB has not been identified.

Here we analyze the functional role of netrin-1 and neogenin in mammary gland morphogenesis. We examine *in vivo* localization of both proteins in the TEB and defects resulting from loss of either gene product. We also explore the mechanism underlying the netrin-1/neogenin interaction using *in vitro* assays. The results show that in the developing mammary gland netrin-1 acts locally through neogenin to maintain close apposition of cap cells and prelumenal cells at the leading edge of the TEB. Furthermore our results suggest that in this context netrin-1 acts as a short-range attractant and has an adhesive rather than guidance function.

RESULTS

Ntn1 and *neo1* display non-overlapping, complementary expression patterns in the TEB

For *ntn1* to play a role in regulating early mammary gland development, it must normally be expressed during this stage. Since the construct used to generate *ntn1*-/- mice inserted *lacZ* under the control of the *ntn1* promoter (Serafini et al., 1996), we assayed +/- glands and -/-outgrowths at 3 weeks for b-galactosidase activity. Accumulation of b-galactosidase reaction product revealed that *ntn1* is present exclusively in the prelumenal epithelial cell compartment; cap cells do not stain positive (Fig. 1A). We confirmed this pattern by *in situ* hybridization (data not shown). Since netrin-1 is a secreted glycoprotein, we determined the distribution of netrin-1 protein by performing immunohistochemistry (Deiner et al., 1997). This reveals strong staining of

netrin-1 around all cells of the TEB, including cap cells (Fig. 1B), showing that, even though cap cells do not express *ntn1* mRNA, they are surrounded by secreted netrin-1 protein. Light staining is also seen in the stroma immediately adjacent to the TEB, but not at a distance. Using the same antibody, little or no background staining is observed in *ntn1* -/- glands (Fig. 1C). Unlike netrin-4, which is detected in the basement membrane surrounding various organs (Koch et al., 2000), we do not detect netrin-1 in basal lamina surrounding the TEB.

We next examined the expression of known netrin-1 receptors and discovered the presence of neogenin. Using *neo1* -/- mice which also have *LacZ* inserted downstream of the *neo1* promoter (Leighton et al., 2001), we assayed +/- glands and -/-outgrowths at 3 weeks for b-galactosidase activity and observe *neo1* expression in the cap cell layer (Fig. 1D). A fraction of cells in the prelumenal compartment underlying the cap cells also stain positive for the b-galactosidase reaction product. It is likely that these are cap cells that have detached and migrated down into this region (Williams and Daniel, 1983). We also detected neogenin in cap cells using immunohistochemistry, including the occasional cap cell in the prelumenal compartment (Fig. 1E, F). Analysis of netrin-1 protein distribution in *neo1* -/- outgrowths reveals netrin-1 staining around cap cells of the TEB similar to the staining in +/+ TEBs (Fig. 1G, B), suggesting that neogenin does not simply bind and distribute netrin-1. Thus the expression studies show that netrin-1 and neogenin are expressed in complementary expression patterns in the TEB. Together with the fact that netrin-1 binds neogenin (Keino-Masu et al., 1996; Wang et al., 1999) (Fig. 7A, B), the data suggest that they function as ligand and receptor to signal between prelumenal and cap cell layers during mammary gland development. The *neo1* homolog, *DCC*, is not expressed in the mammary gland at this stage of development as determined by *in situ* hybridization and immunohistochemistry (data not shown). *Unc5h* receptors are detected by *in situ* hybridization, but only in fibroblasts that encircle the mammary ducts and not in epithelial cells (Fig. 1I-N).

Loss of either *ntn1* or *neo1* results in abnormal TEBs

The perinatal lethality of both *ntn1* -/- and *neo1* -/- mutations prevented the study of mammary glands in mice carrying the homozygous mutation. To circumvent this problem, we followed standard protocols (Robinson et al., 2000; Young, 2000), and harvested mammary anlage from *ntn1* -/- embryos and transplanted them into cleared fat pads of immuno-compromised mice. The contralateral fat pad received control anlage from +/+ embryos from the same litter. To ensure that only the epithelial compartment of the anlage was transplanted, we performed serial transplants of tissue fragments to generate outgrowths. At least three independently derived lines were isolated and serially transplanted for up to three generations to provide outgrowths for experiments. In all studies, littermate control +/+ outgrowths were generated on the contralateral side for comparison so that both +/+ and -/- outgrowths were subject to the same systemic environment.

We sectioned *ntn1* -/- outgrowths 2-3 weeks post-transplantation to analyze TEBs. The sections were stained with Fast green and Sirius red to visualize the epithelial compartment and basement membrane respectively. Compared to TEBs from control +/+ transplants (Fig. 2A), *ntn1* -/- TEBs displayed severe

abnormalities. In *ntn1* -/- TEBs , cap cells are significantly pulled away from prelumenal cells (Fig. 2B, C, D) creating an exaggerated subcapsular space ranging from 5- 20 mm, compared to 0.1-1 mm typically observed in +/+ TEBs (Fig. 2A). There are often detached cells in this subcapsular space (Fig. 2C), and in some morphologically abnormal TEBs, the basal lamina in front of the cap cell layer is disrupted (Fig. 2D). The structure of the prelumenal compartment of many -/- TEBs is also disturbed with epithelial cells appearing disorganized. Analysis of outgrowths at different time points post-transplantation reveal such defects throughout the ductal growth phase. The phenotype is 100% penetrant and, within any given outgrowth, approximately 60% of TEBs are affected (60% +/-5.5, n=60 TEBs, 5 animals). TEBs at the leading edge of the array display the most severe phenotype. These TEBs have the largest subcapsular space, the greatest number of detached cells and also breaks in basal lamina. The severity of the phenotype in these TEBs is most likely due to the fact that they are the largest and most proliferative in the array. Although netrin-1 is expressed in ductal epithelial cells (data not shown), examination of ducts did not reveal any obvious defects in either lumen formation or stromal investment.

A similar analysis was performed on *neo1* -/- outgrowths (Fig. 2E, F). These TEBs are also disorganized and we observe all the characteristics of *ntn1* -/- TEBs (Fig. 2E, F). The phenotype is 100% penetrant and approximately 58% of TEBs are affected (58.25+/-8.8, n=61 TEBs, 4 animals). The observation that *neo1* -/- TEBs phenocopy *ntn1* -/- TEBs strongly support the notion that *neo1* is the receptor for *ntn1*.

Netrin-1 expressing +/+ cells restore normal TEB topology

The data document the functional involvement of netrin-1 in organizing the leading edge of the TEB. A stringent confirmation that the observed phenotype is solely due to lack of netrin-1 is to rescue disorganized TEBs by adding it back. Since mammary glands can be reconstituted using suspensions of mammary epithelial cells (Young, 2000), netrin-1 can be added back by reconstituting outgrowths with mixtures of +/+ (netrin-1 secreting) and -/- cells. We injected *ntn1* -/- cell suspensions and determined that these outgrowths have a similar phenotype to those generated from ductal fragments (disorganized TEBs/outgrowth = 88.6+/-1.5% n=114 TEBs, 4 outgrowths).

To rescue the phenotype, we injected mixtures of cell suspensions containing different ratios of +/+ and *ntn1* -/- cells into cleared fat pads. Analysis of these mosaic outgrowths reveal TEBs that are composed entirely of +/+ cells, -/- cells, and mixtures of +/+ and -/- cells (Fig. 3A, B). As a result, every outgrowth displays both normal and morphologically abnormal TEBs, but the ratio depends on the starting ratio of +/+ and -/- cells used to reconstitute the outgrowth. For example, outgrowths generated with 90% -/- cells have more disorganized TEBs compared to outgrowths generated with 50% -/- cells. Within each TEB, the location of +/+ cells does not correlate with rescue, but the number of +/+ cells does. To determine the minimum number of +/+ cells required for rescue, we counted +/+ versus -/- cells in each TEB and discovered a striking trend. With fewer than 50% netrin-1 expressing cells, the majority of TEBs display the *ntn1* -/- phenotype (Fig. 3A, C). In contrast, with

greater than 50% netrin-1 expressing cells, the majority of TEBs are normal (Fig. 3B, C). The ability to restore normal TEB structure demonstrates that netrin-1 is responsible for the observed phenotype.

The observation that some TEBs containing 50% netrin-1 still display the phenotype suggests that *ntn1* is haploinsufficient. To confirm *ntn1* haploinsufficiency, we analyzed heterozygous mammary glands and discovered the phenotype (86% penetrance) (Fig. 3D). However, compared to *ntn1* -/- outgrowths, which display approximately 60% expressivity, the expressivity of the heterozygous phenotype is reduced to only 17% TEBs displaying morphological abnormalities (17% +/-12.6, n=128 TEBs, 7 animals). This analysis provides strong evidence that a strict requirement for adequate levels of netrin-1 in the TEB is not met by a single functional allele.

Detached cells are multipotent progenitor cells from the cap cell layer

Having confirmed the observed phenotype is due to absence of *ntn1*, we next characterized the nature of the phenotype. First, we determined the origin of detached cells in disorganized TEBs. These cells could either be cap cells that move downward or prelumenal cells that move upward into the subcapsular space. To distinguish between these two, we used an immunohistochemical marker.

Smooth muscle actin (sma) is a marker for both cap and myoepithelial cells (Deugnier et al., 1995), but cap cells can be distinguished based on their location and morphology. Using an antibody to sma, we performed immunohistochemistry on +/+, *ntn1* -/- and *neo1* -/- outgrowths. As expected, cap and myoepithelial cells in the +/+ TEBs stain positive for sma (Fig. 4A). A fraction of cells present within the prelumenal cell population also stain positive for sma and very likely represent cap cells that have migrated into this region (Williams and Daniel, 1983). Importantly, a majority of non-adherent cells present within the subcapsular space of disorganized *ntn1* -/- and *neo1* -/- TEBs stain positive for sma, confirming their identity as cap cells and further demonstrating the similarity of *ntn1* and *neo1* phenotypes (Fig. 4B, C). A few detached cells do not stain positive, but their nuclei appear shrunken and it is likely that these cells are dying by detachment-induced apoptosis (Fig. 6A, B).

Lack of either *ntn1* or *neo1* leads to breaks in the basal lamina

While performing the analysis of *ntn1* -/- and *neo1* -/- outgrowths, we frequently observe breaks in basal lamina (Fig. 2D, F), and occasionally observe cells in the stroma that stain positive for sma (data not shown). Cap cells make and secrete the basal lamina, depositing it at the stromal interface. Therefore their disorganization may destabilize the laminin network in front of the TEB, allowing cap cells to escape their boundaries in the morphologically abnormal TEBs. We examined this possibility by staining both *ntn1* -/- and *neo1* -/- outgrowths with an antibody to laminin-1, which is the major laminin in the basal lamina at the leading edge (Klinowska et al., 1999). This antibody can also be used to identify cap cells since it intracellularly stains these cells, but not lumenal or myoepithelial cells (Daniel and Silberstein, 2000).

Immunohistochemistry on +/+ control outgrowths using laminin antibody reveals staining in the basal lamina extracellularly and cap cells intracellularly (Fig. 4D). We also observe a fraction of cells staining positive intracellularly within the prelumenal compartment, providing additional evidence that during normal development cap cells migrate into this region (Williams and Daniel, 1983). A majority of detached cells in *ntn1*-/- and *neo1* -/- TEBs stain positive for intracellular laminin further confirming their identity as cap cells (Fig. 4E, F). In many disorganized TEBs we see striking breaks in laminin staining indicating that basal lamina has been compromised (Fig. 4E, F). Detached cells that have escaped their boundaries, presumably by migrating through breaks in basal lamina, are occasionally observed in the stroma and also stain positive for intracellular laminin (Fig. 6D).

Cadherin systems are intact in the TEBs

In TEBs, cells of the cap and myoepithelial layers adhere to each other through P-cadherin while prelumenal and lumenal epithelial cells adhere through E-cadherin (Daniel et al., 1995). Since we observe loose cap cells in disorganized TEBs, we examined if the cadherin adhesion systems are intact in these TEBs. Immunohistochemistry on +/+ control outgrowths with E-cadherin antibody reveals, as expected, membrane staining only on prelumenal cells (Fig. 5A). Similarly, in disorganized *ntn1* -/- and *neo1* -/- TEBs, prelumenal cells stain positive (Fig. 5B, C). Cap cells in the cap cell layer, in the exaggerated subcapsular space and in the prelumenal compartment do not stain positive for E-cadherin (Fig. 5B, C). Since two-fold more cap cells migrate into the prelumenal compartment in both *ntn1* -/- and *neo1* -/- TEBs (Fig. 6C), patches of E-cadherin negative (cap) cells are observed (Fig. 5B, C), but contacts between prelumenal cells do not appear dramatically altered.

We performed a similar analysis using a P-cadherin antibody. This reveals normal P-cadherin staining in cells of the intact cap cell layer in both +/+ and -/- TEBs, providing evidence that *ntn1* -/- and *neo1* -/- TEBs maintain their P-cadherin adhesion systems (Fig. 5D, E, F). The majority of detached cap cells also stain positive for P-cadherin suggesting that they have not downregulated it (Fig. 5E, F). We also observe an increased fraction of cells staining positive for P-cadherin in the prelumenal cell population of *ntn1* -/- and *neo1* -/- TEBs (Fig. 5E, F), reflecting the increased number of cap cells that migrate into this region (Fig. 6C). Together, the E- and P-cadherin staining demonstrate that prelumenal and cap cell layers maintain their distinct adhesion systems, even though the interaction between these two layers is compromised in *ntn1*-/- and *neo1* -/- TEBs.

A fraction of detached cap cells die by detachment induced apoptosis

Having established that detached cells are cap cells, we next wanted to determine their destiny. Normally, cap cells exhibit a high rate of proliferation and low rate of apoptosis (Humphreys et al., 1996). However, since some cap cells in the *ntn1* -/- and *neo1* -/- TEBs are detached, they might die by detachment-induced apoptosis (anoikis) as many non-adherent cells do (Boudreau et al., 1995), or continue their downward

migration. The appearance of shrunken nuclei in a fraction of these detached cells suggested that at least some detached cap cells are apoptotic. Cap cells from +/+ TEBs and morphologically normal *ntn1* -/- TEBs display a low apoptotic index (Fig. 6A). In contrast in disorganized TEBs, cap cells, both attached to the cap cell layer and detached, display an approximately 5-fold higher apoptotic index (Fig. 6A). If this increased apoptosis is due to anoikis, then the apoptotic index of detached cap cells should be significantly greater than the apoptotic index of attached cap cells. Quantitation of these indices reveals a 17-fold greater apoptotic index in the detached cap cell fraction of disorganized -/- TEBs compared to the attached cap cell fraction of the same TEBs or +/+ TEBs (Fig. 6A, inset). These data strongly support the idea that detached cap cells die by anoikis, resulting in the increased overall apoptotic index observed in disorganized TEBs. Examination of the apoptotic index of cells in the prelumenal fraction of *ntn1* -/- compared to +/+ TEBs shows no statistically significant difference (data not shown). Furthermore, examination of the proliferation rate of *ntn1* -/- compared to +/+ also shows no statistically significant difference (-/-: 36.5% +/-6.7, n=24 TEBs, 3 animals; +/+: 40.8% +/-5.0, n=21 TEBs, 3 animals).

We performed a similar TUNEL analysis on the *neo1* -/- TEBs and find a similar low rate of apoptosis in +/+ and normal -/- TEBs (Fig. 6B). Examination of disorganized -/- TEBs (attached and detached cap cells), reveals an approximately 8-fold increase in apoptosis (Fig. 6B). Again, the increase in death may be due to anoikis of detached cap cells since we observe an approximately 18-fold greater apoptotic index in detached versus attached cap cells in these TEBs (Fig. 6B, inset).

The increased cell death observed in detached cap cells of -/- outgrowths likely explains the slightly slower growth observed in -/- compared to +/+ outgrowths. For example, at 3 weeks post transplantation, the average percent fat pad filled (%fpf) by *ntn1* -/- outgrowths is 18% less than the %fpf by contralateral +/+ outgrowths (n=5 contralaterally transplanted animals, $P< 0.0005$). Despite the slower growth rate, *ntn1* -/- outgrowths eventually fill the fat pad and establish normal looking ductal architecture (data not shown).

Increased influx of cap cells into the prelumenal compartment

Since only 30% of detached cells die by apoptosis, we investigated whether the remaining cells migrate into the stroma when the basal lamina is compromised, or into the prelumenal compartment. We occasionally observe a few cap cells in the stroma ahead of the TEB (Fig. 6D), but we always observe more cap cells in the prelumenal compartment whether the basal lamina is intact or compromised. We counted these cells in both *ntn1* -/- and *neo1* -/- TEBs (Fig. 6C) and discovered a two-fold increase compared to +/+ TEBs (Fig. 6C). As a result of this influx, the prelumenal compartment contains a mixed population making it appear disorganized. The propensity of cap cells to migrate into the prelumenal compartment in the absence of *ntn1* or *neo1*, suggests that netrin-1 is not responsible for guiding individual neogenin expressing cap cells into this compartment. Lack of a point source of netrin-1 in the TEB likely precludes a traditional long-range guidance role for netrin-1. Instead, the close apposition of receptor-expressing cap cells with ligand-expressing prelumenal cells, suggest a

short-range role for *ntn1* in maintaining and stabilizing the layer of *neo1* expressing cap cells at the leading edge.

Neogenin mediates netrin-1 dependent cell aggregation

To determine the nature of interaction between netrin-1 and neogenin, we shifted to an *in vitro* cell culture system using L1 mouse fibroblast cells. L1 cells do not express netrin-1 or DCC (data not shown) but endogenously express neogenin (Fig. 7A). This indicates that neogenin does not function as a homotypic cell adhesion protein in the absence of ligand since L1 cells are well known to be non-adherent. We established that neogenin expressing L1 cells bind netrin-1 (Fig. 7B, C), and then performed cell aggregation assays to determine if these cells cluster in the presence of netrin-1 protein (Albelda et al., 1991; DeLisser et al., 1993). In the absence of netrin-1, approximately 10% of L1 cells are in aggregates of greater than three cells, similar to previous observations (Albelda et al., 1991; DeLisser et al., 1993). Addition of netrin-1 leads to a two-fold increase in aggregation (Fig. 7E, F, G). This aggregation is blocked in the presence of an antibody against the extracellular domain of neogenin, but not a control antibody (Fig. 7E, H, I). Thus neogenin mediates netrin-1 dependent aggregation of L1 cells, suggesting that the short-range attractive interaction between netrin-1 and neogenin may be adhesive rather than instructive in nature.

DISCUSSION

In the developing mammary gland, we discovered that netrin-1 is expressed by prelumenal cells and its receptor neogenin is expressed by the adjacent cap cell layer raising the possibility that their interaction mediates local, short-range attraction between these two epithelial layers. Several lines of evidence support this hypothesis. First, netrin-1 and neogenin are expressed in close opposition and netrin-1 appears to diffuse a short distance surrounding cap cells that do not express it (Fig. 1G). Second, absence of either *ntn1* or *neo1* results in detached and inappropriately migrating cap cells as may be expected when a stabilizing interaction is lost. Third, expression of *unc5h* family members is not detected in cap cells, suggesting that neogenin functions alone as a short-range attractant receptor for netrin-1 rather than as a component of a repellent complex. Fourth, E- and P-cadherin mediated contacts in the prelumenal and cap cell layers, respectively, are maintained even though the two layers lose their interaction. This suggests a local mechanism, distinct from cadherin mediated adhesion, maintains the apposition between these two layers. Finally, neogenin acts as a ligand dependent, cell adhesion protein in cell aggregation assays. Together the data support a model in which netrin-1, secreted by prelumenal cells stabilizes and maintains the close proximity of neogenin expressing cap cells.

Netrin-1 acts as a short-range attractant through neogenin

The TEB is the highly invasive growth structure of the developing mammary gland and cap cells present at the leading edge direct this rapid growth. Cap cells are very motile and the mechanism that restrains their

motility is unknown. Here, we present a model where cap cell motility is kept in check by neogenin mediated attraction of the cap cell layer to the underlying prelumenal compartment. In the absence of this attractive force, there is an overall destabilization of the cap cells at the leading edge. One result of this destabilization is that cap cells pull away from the prelumenal compartment creating exaggerated subcapsular spaces. Another result is the inappropriate influx of cap cells into the prelumenal compartment. Binding of netrin-1 to neogenin presumably triggers downstream signaling molecules, which ultimately lead to cytoskeletal reorganization of cap cells and their stabilization at the leading edge. Thus in the TEB, neogenin expressing cap cells are not guided to a netrin-1 source, rather they are kept in place at the stromal interface and prevented from moving inappropriately.

We describe the interaction between netrin-1 and neogenin as short-range attraction because netrin-1 is a secreted ligand which binds to receptors with relatively low affinity (Keino-Masu et al., 1996; Wang et al., 1999). This description is also consistent with the short-range activity of netrin-1 in the nervous system. For example in the optic disc, netrin-1 acts locally as a short-range attractant to ensure the proper exit of DCC expressing retinal ganglion cell axons from the eye (Deiner et al., 1997). In the mammary gland, it seems likely that short-range attraction between netrin-1 and neogenin subserves a low affinity adhesive rather than guidance function. In this context, we propose that the interaction between them preserves the structure of the end bud and the compartmentalization of cap cells without compromising the dynamic nature of these highly proliferative, multipotent cells.

Neogenin is not a netrin-1 dependence receptor in the TEB

DCC has been reported to induce cell death in the absence but not the presence of netrin-1 (Mehlen et al., 1998). This dependence on ligand to prevent constitutive cell death raises the possibility that the phenotype of the *ntn1* -/- outgrowths is simply due to neogenin acting as a dependence receptor and inducing apoptosis in cap cells in the absence of netrin-1. However it is unlikely for the following reasons. First, all cap cells express *neo1*, but we show the increase in apoptosis in *ntn1* -/- outgrowths is due to anoikis of detached cap cells. The apoptotic index of the attached cap cell fraction is unaffected by the loss of netrin-1 (Fig. 6A, B). Second, myoepithelial cells also express *neo1* (Srinivasan, Strickland and Hinck, unpublished data), but we do not observe any apoptosis in these cells in *ntn1* -/- outgrowths. Third, our TUNEL data on *neo1* -/- TEBs show a similar amount of apoptosis compared to *ntn1* -/- TEBs which is inconsistent with a dependence role for neogenin (Fig. 6A, B). In fact, all of our analyses of the phenotype demonstrate that *ntn1* -/- and *neo1* -/- TEBs have very similar defects, strongly indicating neogenin is a netrin-1 signaling receptor in the TEB.

Signaling pathways that are activated by DCC-mediated attraction to netrin-1 have been identified and it seems likely that similar molecules would be activated by neogenin. In the nervous system, netrin-1 signaling through DCC has been shown to activate two different second messenger pathways: small GTPases (Li et al.,

2002; Shekarabi and Kennedy, 2002) and MAPK (Forcet et al., 2002). Furthermore, levels of intracellular cAMP play a key role in determining the response of a growth cone to netrin-1(Ming et al., 1997). In mammary epithelium, cAMP induces proliferation and new TEB formation (Ethier et al., 1989; Silberstein et al., 1984) and MAPK signaling is associated with cytoskeletal reorganization (Subbaramaiah et al., 2000). Furthermore, p190B, a Rho-GTPase that promotes motility by cytoskeletal reorganization is preferentially expressed by cap cells (Chakravarty et al., 2000). Thus molecules that are potential transducers of a neogenin signal are present in the mammary gland. Future studies will focus on whether these molecules mediate neogenin signaling in the TEB.

Physiological relevance of netrin-1 and neogenin loss in the mammary gland

We show that during early mammary development, absence of *ntn1* and *neo1* removes the constraints on cap cells and increases the number of these motile cells migrating into the underlying prelumenal compartment (Fig. 6C). This change in population dynamics of cap cells may have long-term consequences for the mammary gland. Cap cells are multipotent progenitor cells of the TEB and retaining this type of cell in the gland during maturation and aging is implicated in an increased risk for tumorigenesis in both humans and mice (Boulanger and Smith, 2001; Russo et al., 1999). These cells may retain their mitotic potential and accumulate genetic alterations over time. Since *ntn1* -/- and *neo1* -/- outgrowths also display breaks in basal laminin (Fig. 6D), these alterations would occur in a 'primed' background as breaks in basal lamina have been linked to cancer progression in the uterus and breast (Gudjonsson et al., 2002; Nair et al., 1997). Experiments are in progress to study whether there is an increased incidence of tumorigenesis due to loss of *ntn1* and *neo1*.

While we focused on the stabilizing function of *ntn1* and *neo1* in the TEB, both genes are expressed during pregnancy, lactation and involution of the mammary gland (Srinivasan, Strickland and Hinck, unpublished). Detailed analyses of these stages may provide further insights into the biology of netrin-1 and its receptors during epithelial remodeling. Furthermore, *ntn1* and its receptors are expressed in other developing organs. For example, *neo1* is expressed in simple epithelia of the developing lung, gut and stomach, and in stem/progenitor cells of the nervous system (Gad et al., 1997). Future studies will elucidate whether netrin-1 and neogenin stabilize inter-epithelial interactions in other tissues during remodeling and organogenesis.

METHODS

Animals: The study conformed to guidelines set by the UCSC animal care committee (CARC). *Ntn1* severe hypomorphs, +/- and +/+ controls were generated and genotyped as described (Serafini et al., 1996). Mice carrying gene trap insertions in *neo1* were genotyped and maintained as described (Leighton et al., 2001).

Transplant techniques: Female athymic mice (nu/nu) were obtained at 21 days of age and both #4 fat pads were cleared for use as transplant host (Young, 2000). Embryonic anlage rescue and fragment transplants were done as described (Robinson et al., 2000). Reconstitution experiments were performed as described (Brisken et al.,

1999; Emerman et al., 1977) with the following modifications. Donor mice were primed with a single injection of both 5 mg Depo-Estradiol and 5 mg Depo-Provera (Upjohn) 8 days prior to use. Donor glands were mixed based on wet weight prior to mincing. 2.5X 10^4cells were injected into each cleared fat pad and analyzed after 18 days. Glands were stained for b-galactosidase activity prior to sectioning (Brisken et al., 1999). Numbers shown were pooled data from 4 different outgrowths generated in 4 individual mice. As a control, the contralateral sides were injected with 100% -/- cells.

Tissue Analysis: Whole gland preparations were analyzed with hematoxylin or b-galactosidase staining as described (Brisken et al., 1999). Phenotype was characterized using 6 mm serial sections. Fat pad filling was calculated as a relative percentage compared to +/+ control outgrowth as described (Wiesen et al., 1999). Standard deviation was reported when animals from one transplant generation were analyzed. Standard error was reported when animals from more than one transplant generation were analyzed.

Expression studies: The following protocols were performed as described: in situ hybridization (Friedmann and Daniel, 1996); b-galactosidase staining (Brisken et al., 1999); immunohistochemistry using anti-netrin-1, 11760 (Salminen et al., 2000), anti-smooth muscle actin (Deugnier et al., 1995), anti-E-cadherin (ECCD-2, a gift from Dr.Takeichi) (Daniel et al., 1995). The following antibody staining used standard protocols: anti-neogenin (SCBT, #sc-15337), anti-P-cadherin (SCBT, #sc-1501) and anti-laminin (Sigma L9393). For all quantitation purposes, tissue was sectioned (6-10 mm) and mounted serially. To ensure that cells were counted only once, TEBs were followed through serial sections and the number of positively stained cells were counted in every third section.

BrdU and TUNEL: BrdU and TUNEL analyses and quantitation were performed as described (Gavrieli et al., 1992; Humphreys et al., 1996) with the following modifications. Zymed kit was used to detect incorporation of BrdU. TUNEL positive cells were detected using Vectastain ABC elite HRP kit.

Netrin-1 Binding, Cell Aggregation: Netrin-1 binding assays were performed as described (Keino-Masu et al., 1996), and neogenin was visualized using a specific antibody (SCBT, #sc-15337). Cell aggregation assays were performed as described (Albelda et al., 1991; DeLisser et al., 1993) using 7-10 X 10^5 cell/ml in HBSS with calcium. 3mg of netrin-1 protein was added and for antibody blocking, cells were pre-incubated with 3mg of antibody for 20 minutes followed by 1X HBSS wash and resuspension prior to netrin-1 addition (neogenin antibody, SCBT, #sc-15337; PLAP antibody, SCBT, #sc-15337). Aggregation was quantified in a blind manner in triplicate by examining representative aliquots (at least 10) from each sample on a hemocytometer grid. The number of particles containing cells in aggregates > 3 versus total number of particles were counted (at least 1200 cells) from four 1mm squares.

ACKNOWLEDGEMENTS

We gratefully acknowledge Dr. Mark Tessier-Lavigne for his kind gift of *ntn1* -/- and *neo1* -/- mice. We thank Dr. Tim Kennedy and Dr. Mark Tessier-Lavigne for the 11760 antibody. We acknowledge Dr. Gary Silberstein, Dr. Charles Daniel, Dr. Andrew Chisholm, Kathy Vanhorn for critical input and Dr. Gumi Thordarson for technical advice. We acknowledge SCBT for their gift of P-cadherin, neogenin and PLAP antibodies.

Supported by Research Scholar Grant #RSG0218001MGO from the American Cancer Society.

REFERENCES

Albelda, S. M., Muller, W. A., Buck, C. A., and Newman, P. J. (1991). Molecular and cellular properties of PECAM-1 (endoCAM/CD31): a novel vascular cell-cell adhesion molecule, J Cell Biol *114*, 1059-68.

Boudreau, N., Sympson, C. J., Werb, Z., and Bissell, M. J. (1995). Suppression of ICE and apoptosis in mammary epithelial cells by extracellular matrix, Science *267*, 891-3.

Boulanger, C. A., and Smith, G. H. (2001). Reducing mammary cancer risk through premature stem cell senescence, Oncogene *20*, 2264-72.

Brisken, C., Kaur, S., Chavarria, T. E., Binart, N., Sutherland, R. L., Weinberg, R. A., Kelly, P. A., and Ormandy, C. J. (1999). Prolactin controls mammary gland development via direct and indirect mechanisms, Dev Biol *210*, 96-106.

Chakravarty, G., Roy, D., Gonzales, M., Gay, J., Contreras, A., and Rosen, J. M. (2000). P190-B, a Rho-GTPase-activating protein, is differentially expressed in terminal end buds and breast cancer, Cell Growth Differ *11*, 343-54.

Daniel, C. A., and Silberstein, G. B. (2000). Working with the Mouse Mammary End Bud (New York, Kluwer Academic/Plenum Press).

Daniel, C. W., Strickland, P., and Friedmann, Y. (1995). Expression and functional role of E- and P-cadherins in mouse mammary ductal morphogenesis and growth, Dev Biol *169*, 511-9.

Deiner, M. S., Kennedy, T. E., Fazeli, A., Serafini, T., Tessier-Lavigne, M., and Sretavan, D. W. (1997). Netrin-1 and DCC mediate axon guidance locally at the optic disc: loss of function leads to optic nerve hypoplasia, Neuron *19*, 575-89.

DeLisser, H. M., Yan, H. C., Newman, P. J., Muller, W. A., Buck, C. A., and Albelda, S. M. (1993). Platelet/endothelial cell adhesion molecule-1 (CD31)-mediated cellular aggregation involves cell surface glycosaminoglycans, J Biol Chem *268*, 16037-46.

Deugnier, M. A., Moiseyeva, E. P., Thiery, J. P., and Glukhova, M. (1995). Myoepithelial cell differentiation in the developing mammary gland: progressive acquisition of smooth muscle phenotype, Dev Dyn *204*, 107-17.

Emerman, J. T., Enami, J., Pitelka, D. R., and Nandi, S. (1977). Hormonal effects on intracellular and secreted casein in cultures of mouse mammary epithelial cells on floating collagen membranes, Proc Natl Acad Sci U S A *74*, 4466-70.

Engelkamp, D. (2002). Cloning of three mouse Unc5 genes and their expression patterns at mid-gestation., Mech Dev *118*, 191-7.

Ethier, S. P., van de Velde, R. M., and Cundiff, K. C. (1989). cAMP levels in proliferating rat mammary epithelial cells in vitro and in vivo, Exp Cell Res *182*, 653-8.

Fazeli, A., Dickinson, S. L., Hermiston, M. L., Tighe, R. V., Steen, R. G., Small, C. G., Stoeckli, E. T., Keino-Masu, K., Masu, M., Rayburn, H., *et al.* (1997). Phenotype of mice lacking functional Deleted in colorectal cancer (Dcc) gene, Nature *386*, 796-804.

Forcet, C., Stein, E., Pays, L., Corset, V., Llambi, F., Tessier-Lavigne, M., and Mehlen, P. (2002). Netrin-1-mediated axon outgrowth requires deleted in colorectal cancer- dependent MAPK activation, Nature *417*, 443-7.

Friedmann, Y., and Daniel, C. W. (1996). Regulated expression of homeobox genes Msx-1 and Msx-2 in mouse mammary gland development suggests a role in hormone action and epithelial- stromal interactions, Dev Biol *177*, 347-55.

Gad, J. M., Keeling, S. L., Wilks, A. F., Tan, S. S., and Cooper, H. M. (1997). The expression patterns of guidance receptors, DCC and Neogenin, are spatially and temporally distinct throughout mouse embryogenesis, Dev Biol *192*, 258-73.
Gavrieli, Y., Sherman, Y., and Ben-Sasson, S. A. (1992). Identification of programmed cell death in situ via specific labeling of nuclear DNA fragmentation, J Cell Biol *119*, 493-501.
Gudjonsson, T., Ronnov-Jessen, L., Villadsen, R., Rank, F., Bissell, M. J., and Petersen, O. W. (2002). Normal and tumor-derived myoepithelial cells differ in their ability to interact with luminal breast epithelial cells for polarity and basement membrane deposition, J Cell Sci *115*, 39-50.
Hong, K., Hinck, L., Nishiyama, M., Poo, M. M., Tessier-Lavigne, M., and Stein, E. (1999). A ligand-gated association between cytoplasmic domains of UNC5 and DCC family receptors converts netrin-induced growth cone attraction to repulsion, Cell *97*, 927-41.
Humphreys, R. C., Krajewska, M., Krnacik, S., Jaeger, R., Weiher, H., Krajewski, S., Reed, J. C., and Rosen, J. M. (1996). Apoptosis in the terminal endbud of the murine mammary gland: a mechanism of ductal morphogenesis, Development *122*, 4013-22.
Keino-Masu, K., Masu, M., Hinck, L., Leonardo, E. D., Chan, S. S., Culotti, J. G., and Tessier-Lavigne, M. (1996). Deleted in Colorectal Cancer (DCC) encodes a netrin receptor, Cell *87*, 175-85.
Klinowska, T. C., Soriano, J. V., Edwards, G. M., Oliver, J. M., Valentijn, A. J., Montesano, R., and Streuli, C. H. (1999). Laminin and beta1 integrins are crucial for normal mammary gland development in the mouse, Dev Biol *215*, 13-32.
Koch, M., Murrell, J. R., Hunter, D. D., Olson, P. F., Jin, W., Keene, D. R., Brunken, W. J., and Burgeson, R. E. (2000). A novel member of the netrin family, beta-netrin, shares homology with the beta chain of laminin: identification, expression, and functional characterization, J Cell Biol *151*, 221-34.
Leighton, P. A., Mitchell, K. J., Goodrich, L. V., Lu, X., Pinson, K., Scherz, P., Skarnes, W. C., and Tessier-Lavigne, M. (2001). Defining brain wiring patterns and mechanisms through gene trapping in mice, Nature *410*, 174-9.
Leonardo, E. D., Hinck, L., Masu, M., Keino-Masu, K., Ackerman, S. L., and Tessier-Lavigne, M. (1997). Vertebrate homologues of *C. elegans* UNC-5 are candidate netrin receptors, Nature *386*, 833-8.
Li, X., Saint-Cyr-Proulx, E., Aktories, K., and Lamarche-Vane, N. (2002). Rac1 and Cdc42 but not RhoA or Rho kinase activities are required for neurite outgrowth induced by the Netrin-1 receptor DCC (deleted in colorectal cancer) in N1E-115 neuroblastoma cells, J Biol Chem *277*, 15207-14.
Mehlen, P., Rabizadeh, S., Snipas, S. J., Assa-Munt, N., Salvesen, G. S., and Bredesen, D. E. (1998). The DCC gene product induces apoptosis by a mechanism requiring receptor proteolysis, Nature *395*, 801-4.
Meyerhardt, J. A., Caca, K., Eckstrand, B. C., Hu, G., Lengauer, C., Banavali, S., Look, A. T., and Fearon, E. R. (1999). Netrin-1: interaction with deleted in colorectal cancer (DCC) and alterations in brain tumors and neuroblastomas, Cell Growth Differ *10*, 35-42.
Ming, G. L., Song, H. J., Berninger, B., Holt, C. E., Tessier-Lavigne, M., and Poo, M. M. (1997). cAMP-dependent growth cone guidance by netrin-1, Neuron *19*, 1225-35.
Nair, S. A., Nair, M. B., Jayaprakash, P. G., Rajalekshmy, T. N., Nair, M. K., and Pillai, M. R. (1997). The basement membrane and tumor progression in the uterine cervix, Gen Diagn Pathol *142*, 297-303.
Przyborski, S. A., Knowles, B. B., and Ackerman, S. L. (1998). Embryonic phenotype of Unc5h3 mutant mice suggests chemorepulsion during the formation of the rostral cerebellar boundary, Development *125*, 41-50.
Robinson, G. W., Accili, D., and Hennighausen, L. (2000). Rescue of Mammary Epithelium of Early Lethal Phenotypes by Embryonic Mammary Gland Transplantation as Exemplified with Insulin Receptor Null Mice. (New York, Kluwer Academic/Plenum Press).
Russo, J., Ao, X., Grill, C., and Russo, I. H. (1999). Pattern of distribution of cells positive for estrogen receptor alpha and progesterone receptor in relation to proliferating cells in the mammary gland, Breast Cancer Res Treat *53*, 217-27.
Salminen, M., Meyer, B. I., Bober, E., and Gruss, P. (2000). Netrin 1 is required for semicircular canal formation in the mouse inner ear, Development *127*, 13-22.

Serafini, T., Colamarino, S. A., Leonardo, E. D., Wang, H., Beddington, R., Skarnes, W. C., and Tessier-Lavigne, M. (1996). Netrin-1 is required for commissural axon guidance in the developing vertebrate nervous system, Cell *87*, 1001-14.
Shekarabi, M., and Kennedy, T. E. (2002). The netrin-1 receptor DCC promotes filopodia formation and cell spreading by activating Cdc42 and Rac1, Mol Cell Neurosci *19*, 1-17.
Silberstein, G. B. (2001). Postnatal mammary gland morphogenesis, Microsc Res Tech *52*, 155-62.
Silberstein, G. B., Strickland, P., Trumpbour, V., Coleman, S., and Daniel, C. W. (1984). In vivo, cAMP stimulates growth and morphogenesis of mouse mammary ducts, Proc Natl Acad Sci U S A *81*, 4950-4.
Subbaramaiah, K., Hart, J. C., Norton, L., and Dannenberg, A. J. (2000). Microtubule-interfering agents stimulate the transcription of cyclooxygenase-2. Evidence for involvement of ERK1/2 AND p38 mitogen-activated protein kinase pathways, J Biol Chem *275*, 14838-45.
Tessier-Lavigne, M., and Goodman, C. S. (1996). The molecular biology of axon guidance, Science *274*, 1123-33.
Wang, H., Copeland, N. G., Gilbert, D. J., Jenkins, N. A., and Tessier-Lavigne, M. (1999). Netrin-3, a mouse homolog of human NTN2L, is highly expressed in sensory ganglia and shows differential binding to netrin receptors, J Neurosci *19*, 4938-47.
Wiesen, J. F., Young, P., Werb, Z., and Cunha, G. R. (1999). Signaling through the stromal epidermal growth factor receptor is necessary for mammary ductal development, Development *126*, 335-44.
Williams, J. M., and Daniel, C. W. (1983). Mammary ductal elongation: differentiation of myoepithelium and basal lamina during branching morphogenesis, Dev Biol *97*, 274-90.
Young, L. J. T. (2000). The Cleared Mammary Fat Pad and the Transplantation of Mammary Gland Morphological Structures and Cells (New York, Kluwer Academic/Plenum Press).

FIGURE LEGEND

Figure 1: Expression patterns of *ntn1* and its receptors, *neo1*, *unc5h1* and *unc5h2* during early mammary development.

(A) *ntn1*-/- outgrowth stained for β-galactosidase activity. (B,C,G) Netrin-1 immunostaining on TEBs, (B) +/+ (C) *ntn1* -/- (G) *neo1*-/-. (D) *neo1* -/- outgrowth stained for β-galactosidase activity. (E, F) neogenin immunostaining on TEBs, (E) +/+ (F) *neo1* -/-. (H) schematic of a TEB. (I-N) *unc5h1* and *unc5h2 in situ* hybridization on +/+ tissue. (I, J) using an anti-sense (AS) probe to *unc5h1*. (K) using a sense probe to *unc5h1*. (L, M) using an anti-sense (AS) probe to *unc5h2*. (N) using a sense probe to *unc5h2*. (A-F, G, J, M) arrows point to cap cell layer. (D, E) arrowhead points to cap cells in the prelumenal compartment that stain positive for β-galactosidase and neogenin respectively. All outgrowths were generated by transplantation technique and taken at three weeks for analysis. L indicates lumen. Scale bar: 5 μm.

Figure 2: Loss of either *ntn1* or *neo1* leads to abnormal TEBs.

All the outgrowths shown in this panel were generated by serial transplantation technique. Every animal had a +/+ outgrowth in one #4 fat pad and either a *ntn1* -/- or *neo1* -/- outgrowth in the contralateral fat pad. (A) longitudinal section through +/+ TEB demonstrates the tight juxtaposition of the cap cell layer with prelumenal cells. (B-D) longitudinal sections through *ntn1* -/- TEBs. (B) shows exaggerated space between the cap cell layer and prelumenal cells. (C) loose cells detected in the subcapsular space. (D) break in basal lamina at the

leading edge of the cap cell layer (box) and loose cells outside the TEB (arrowheads). (E and F) longitudinal sections through *neo1* -/- TEBs. (E) shows exaggerated space between the cap cell layer and prelumenal cells, and loose cells detected in the subcapsular space. (F) break in basal lamina at the leading edge of the cap cell layer (box). (A-F) arrows point to the cap cell layer. Double-headed arrow indicates exaggerated subcapsular space between the cap and prelumenal cell layers. Boxed region indicates breaks in the basal lamina. L indicates the lumen of the TEB. Scale bar: 5 μm.

Figure 3: Mosaic analysis reveals that over 50% netrin-1 is required for normal TEB morphology.

(A and B) mosaic TEBs from reconstituted outgrowths generated using mixtures of -/- and +/+ cells stained for β-galactosidase and counterstained with hematoxylin (nuclei). Arrowheads point to *ntn1* -/- cells staining positive for β-galactosidase activity. (A) TEB comprising a majority of *ntn1* -/- cells displays the phenotype. (B) TEB comprising a majority of +/+ cells displays normal TEB structure. (C) distribution of TEBs with normal and abnormal morphology in reconstituted outgrowths reveals that the majority of TEBs composed of greater than 50% netrin-1 expressing cells are normal. n is the number of TEBs analyzed for each category. (D) longitudinal section of a representative TEB from *ntn1* +/- animal displays the phenotype as indicated by the exaggerated subcapsular space and dissociated cells. L indicates lumen of the TEB. Scale bar: 5 μm.

Figure 4: Immunohistochemical characterization of disorganized TEBs reveals the identity of dissociated cells and breaks in basal lamina at the leading edge of the TEB.

(A-C) immunostaining using a smooth muscle actin antibody on TEBs from three week outgrowths generated by serial transplantation. (A) cap cells stain positive for smooth muscle actin in the +/+ TEB. (B and C) cap cells and dissociated cells stain positive in TEBs, (B) *ntn1* -/- (C) *neo1* -/- . (D-F) immunostaining using a laminin-1 antibody on TEBs from three-week outgrowths generated by transplantation. (D) cap cells stain intracellularly for laminin-1 in the +/+ TEB. The basal lamina stains extracellularly for laminin-1. (E, F) cap cells in the cap cell layer and a fraction of dissociated cap cells stain intracellularly for laminin-1 in TEBs, (E) *ntn1* -/- (F) *neo1* -/- . Arrows point to the cap cell layer. Arrowheads point to the basal lamina. Asterisks point to dissociated cap cells. Circled region shows lack of basal lamina at the leading edge of the TEB. L indicates lumen of the TEB. Scale bar: 5 μm.

Figure 5: E- and P-cadherin adhesion system are intact in the cap cell layer of the disorganized TEBs.

(A-C) immunostaining using an E-cadherin antibody on TEBs from three-week outgrowths generated by transplantation. Prelumenal cells display normal E-cadherin staining in TEBs, (A) +/+ (B) *ntn1* -/- (C) *neo1* -/- .

(D-F) immunostaining using a P-cadherin antibody on TEBs from three week outgrowths. Cap cells display normal P-cadherin staining in TEBs, (D) +/+ (E) *ntn1* -/- (F) *neo1* -/- . Arrows point to cap cell layer and arrowheads point to dissociated cap cells that stain positive for P-cadherin. L indicates lumen of the TEB. Scale bar: 5 μm.

Figure 6: Cap cells detached from cap cell layer show an increased apoptotic index relative to cap cells attached to cap cell layer.

(A) TUNEL on cap cell fraction of TEBs from +/+ and contralateral *ntn1*-/- outgrowths (both normal and abnormal TEBs) reveals a 5-fold increase in apoptosis in disorganized compared to normal TEBs. (+/+: 3.9% +/- 0.6, n= 47; -/- normal TEBs: 2.6% +/- 0.6, n=22; -/- abnormal TEBs (attached and detached cap cells): 20% +/- 2.3, n= 51). Inset shows TUNEL on abnormal TEBs comparing the fraction of TUNEL positive attached versus detached cap cells (attached: 1.87% +/- 3.3, n=31; detached: 27% +/- 8.5%, n=12). (B) TUNEL on cap cell fraction from +/+ and contralateral *neo1*-/- outgrowths (both normal and abnormal TEBs) reveals a 7-fold increase in apoptosis in disorganized compared to normal TEBs. (+/+: 1.6% +/- 1.6, n= 14; -/- normal TEBs: 2.0% +/- 2.3, n= 14; -/- abnormal TEBs: 14.5% +/- 4.5, n= 12). Inset shows TUNEL on abnormal TEBs comparing the fraction of TUNEL positive attached versus detached cap cells. (attached: 1.43% +/-2.5, n=10; detached: 27% +/- 8.5, n=12). (C) 2.5-fold increase in number of cap cells in prelumenal compartment of disorganized TEBs. (+/+: 15.8 +/- 0.76%, n=19; *ntn1* -/-: 37.54 +/- 1.89%, n=25 ; *neo1* -/- : 37.15 +/- 1.5%, n=13). (D) anti-laminin staining on *neo1* -/- TEB shows break in basal lamina (circled region) and loose cells in stroma (arrowheads). Asterisks indicate cap cells that migrated into the prelumenal compartment. L indicates lumen. Scale bar: 5 μm

Figure 7: Neogenin mediates netrin-1 dependent cell aggregation.

(A) Western blot showing neogenin expression in 1) COS cells transfected with control expression vector, 2) COS cells transfected with neogenin expression vector, 3) L1 cells.

(B) immunostaining of neogenin expressed on L1 cells. (C) netrin-1 binding on the same cells shown in A was detected by an antibody specific to netrin-1. (D) background binding to L1 cells was detected using an antibody specific to netrin-1. (E) quantitation showing 2-fold increase over control in the aggregation of L1 cells in the presence of netrin-1. Application of an antibody to the extracellular domain of neogenin blocks aggregation mediated by neogenin. Application of a non-specific antibody (anti-PLAP) does not block cell aggregation mediated by neogenin. (F-I) representative L1 cells in (F) absence of netrin-1 (G-I) presence of netrin-1 (G) plus anti-neogenin (H) plus anti-PLAP (I). Scale bar: 5 μm.

FIGURES

Figure 1

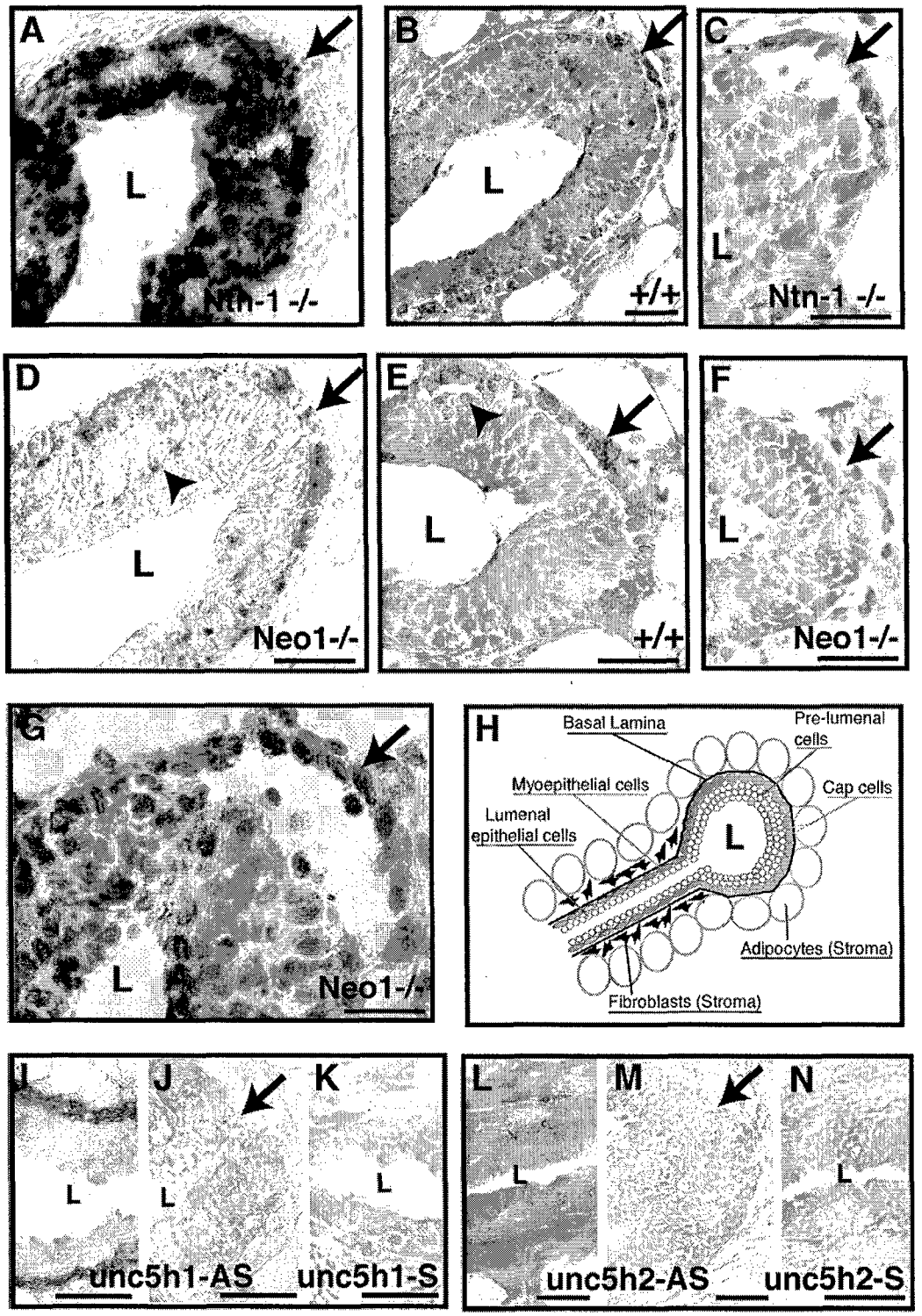
A
L
Ntn-1 -/-
B
L
+/+
C
L
Ntn-1 -/-
D
L
Neo1-/-
E
L
+/+
F
L
Neo1-/-
G
L
Neo1-/-
H
Basal Lamina
Pre-lumenal cells
Myoepithelial cells
Cap cells
Lumenal epithelial cells
L
Adipocytes (Stroma)
Fibroblasts (Stroma)
I
J
K
L
L
L
unc5h1-AS
unc5h1-S
L
M
N
L
L
unc5h2-AS
unc5h2-S

Figure 2

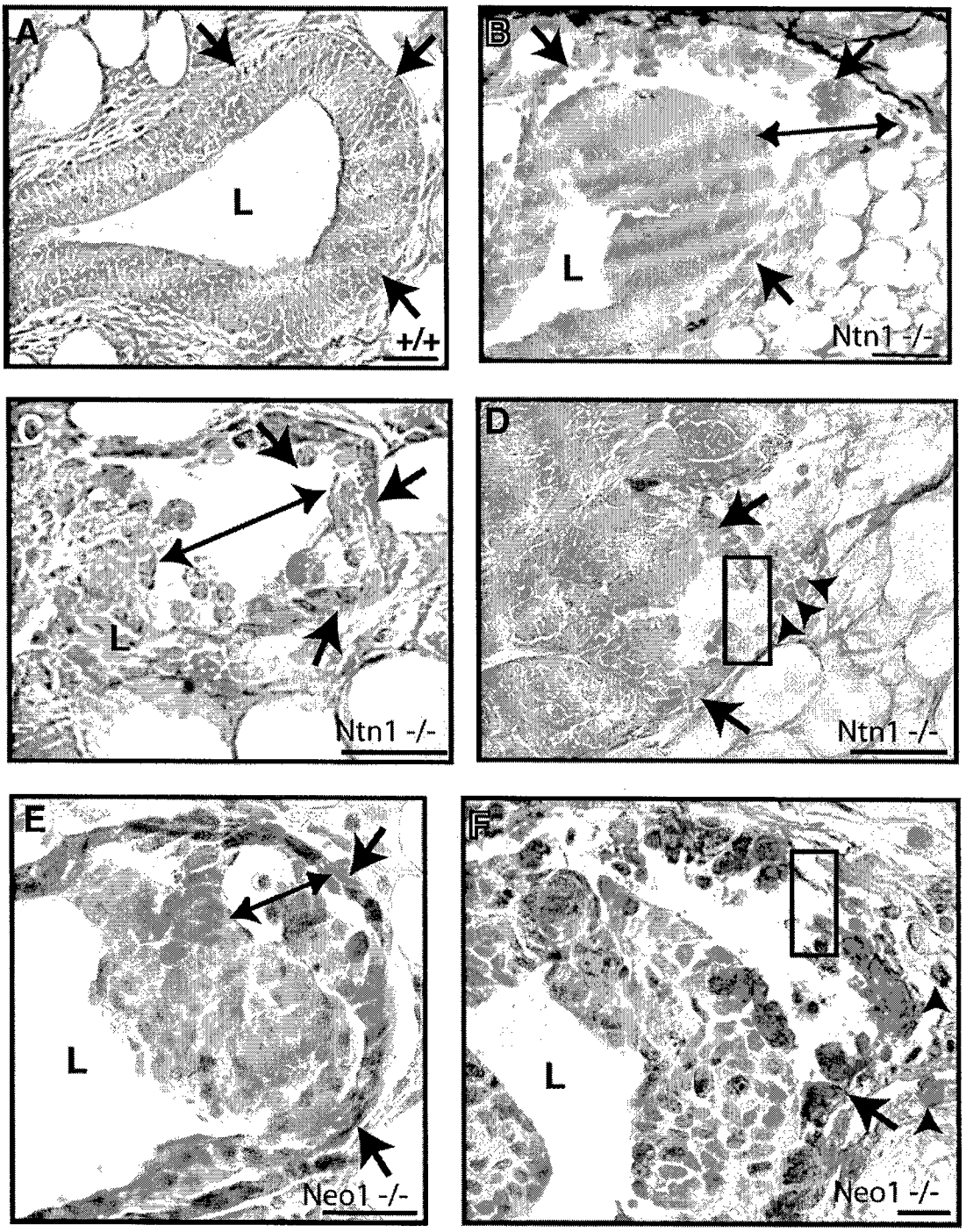

Figure 3

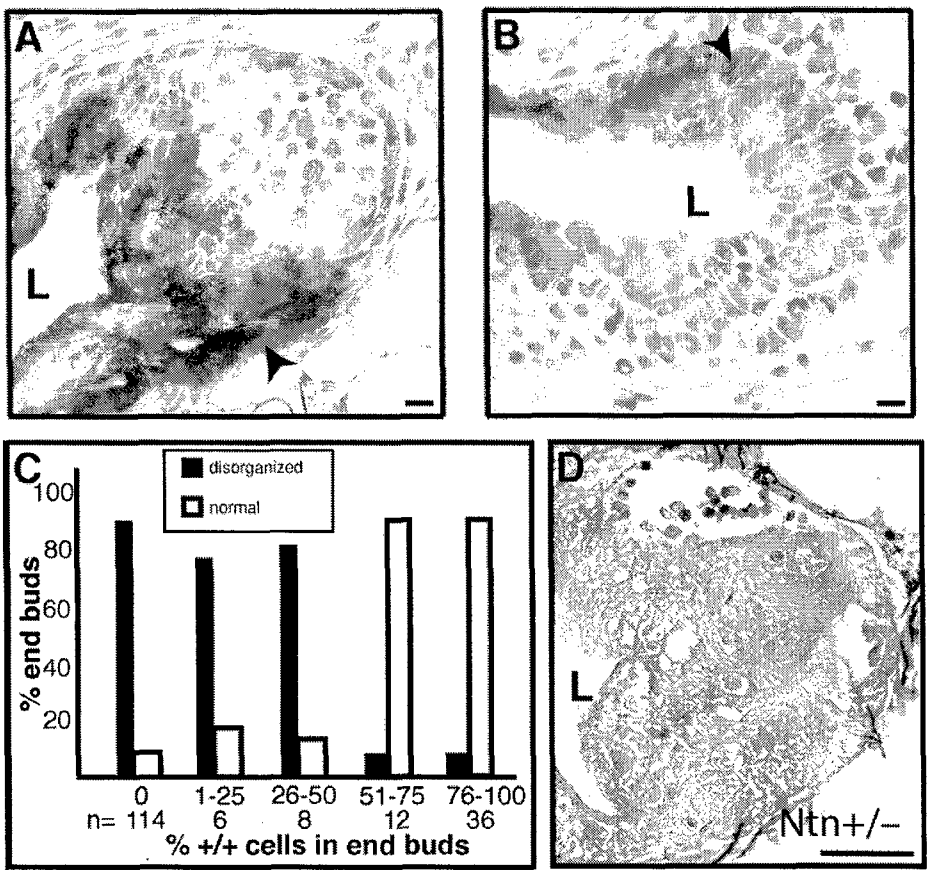
A
L
B
L
C
disorganized
normal
100
80
60
40
20
% end buds
0
1-25
26-50
51-75
76-100
n= 114
6
8
12
36
% +/+ cells in end buds
D
L
Ntn+/-

Figure 4

anti-smooth muscle actin

anti-laminin

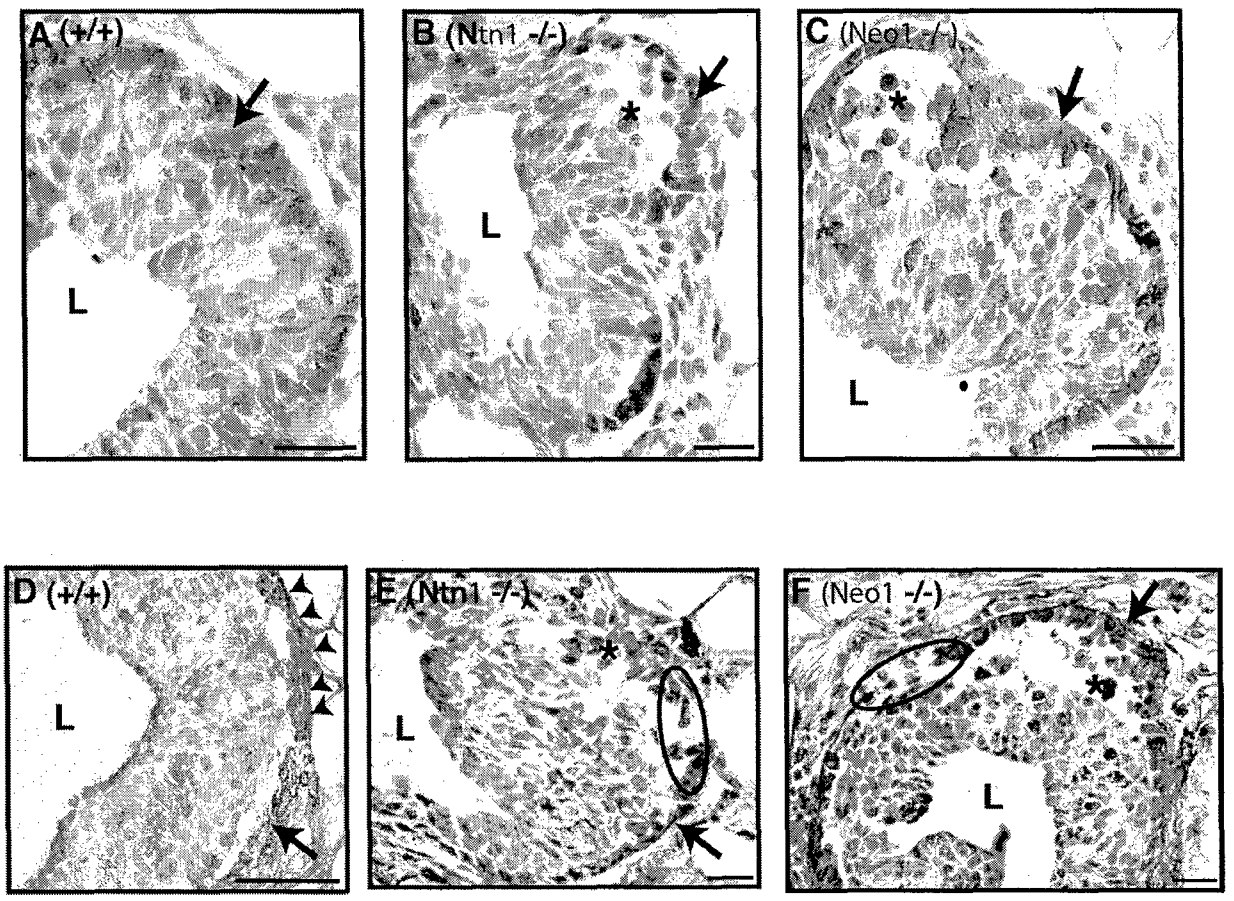

Figure 5

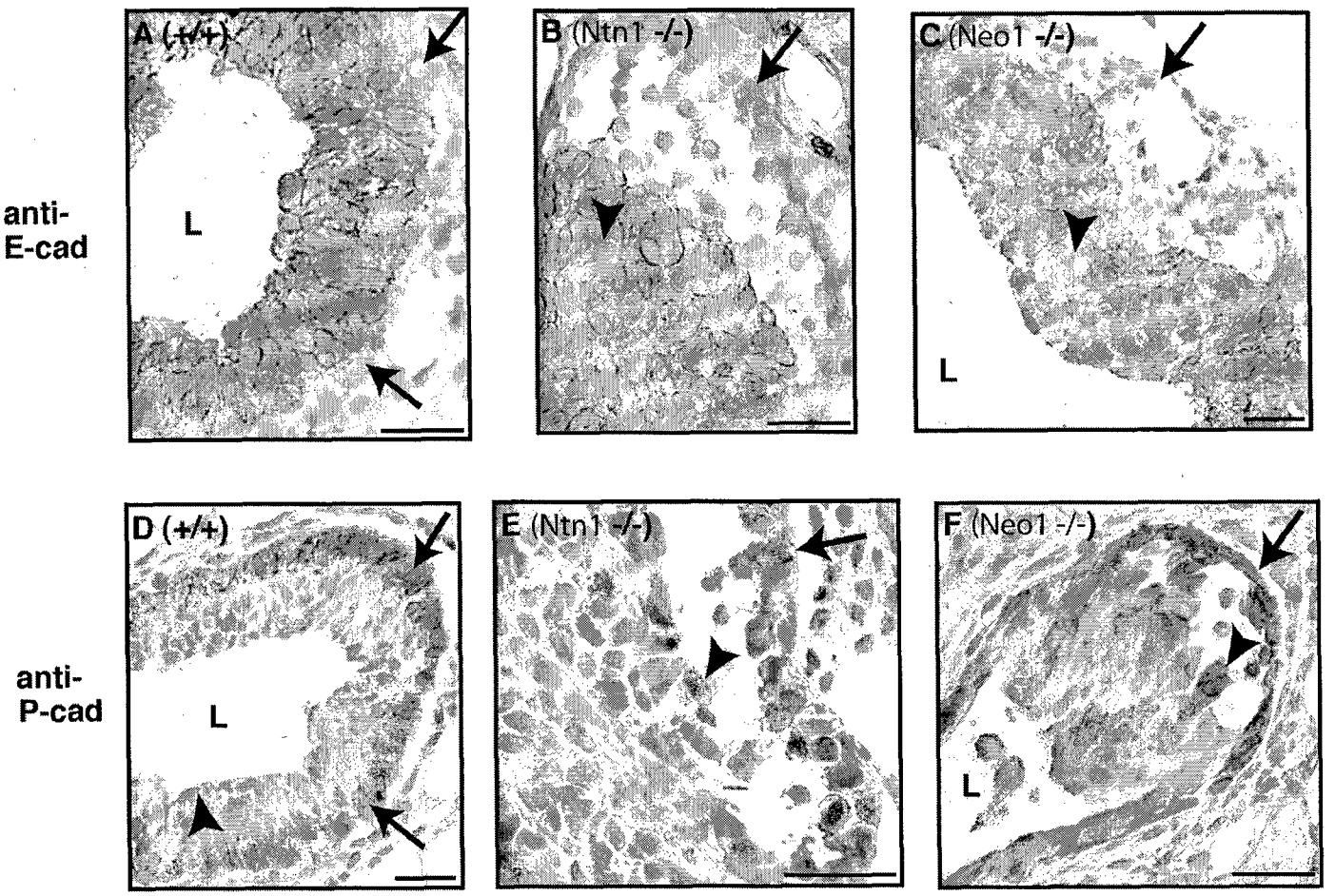

Figure 6

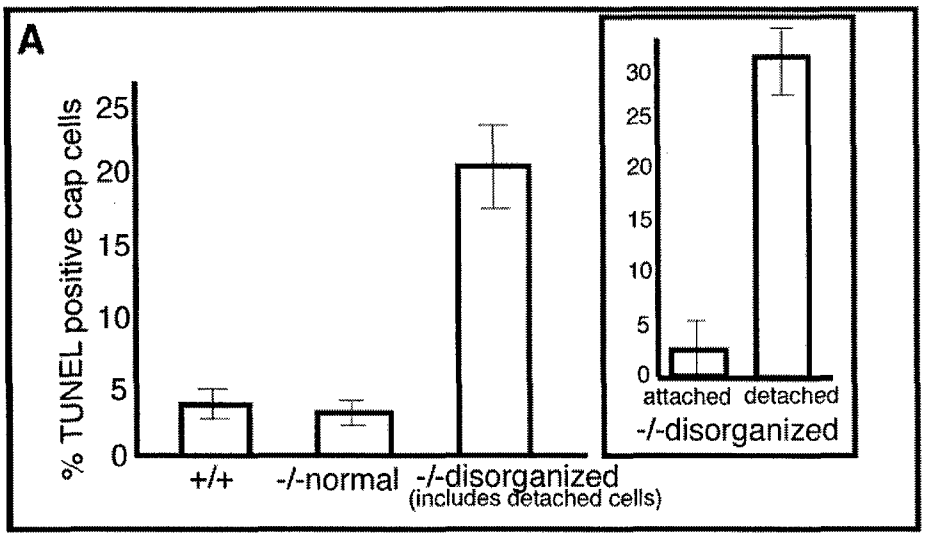
A
% TUNEL positive cap cells
25
20
15
10
5
0
+/+
-/-normal
-/-disorganized
(includes detached cells)
30
25
20
15
10
5
0
attached
detached
-/-disorganized

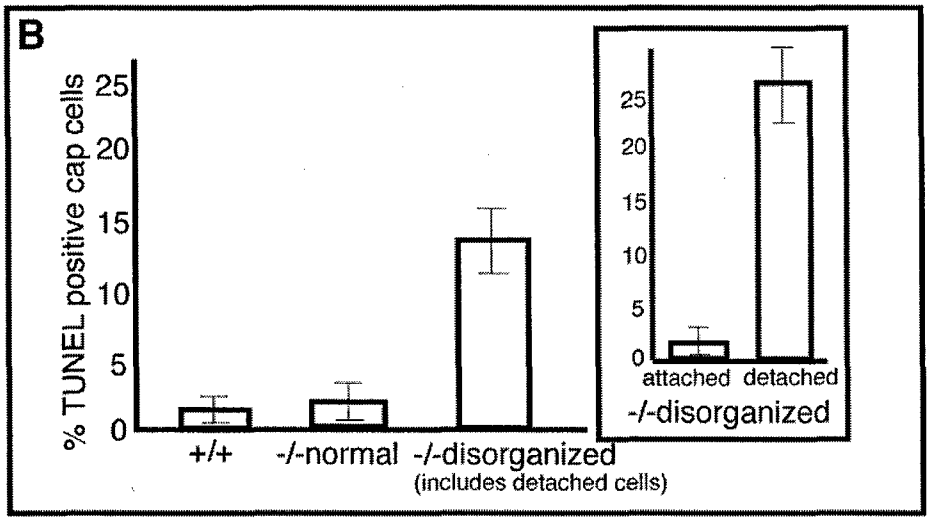
B
% TUNEL positive cap cells
25
20
15
10
5
0
+/+
-/-normal
-/-disorganized
(includes detached cells)
25
20
15
10
5
0
attached
detached
-/-disorganized

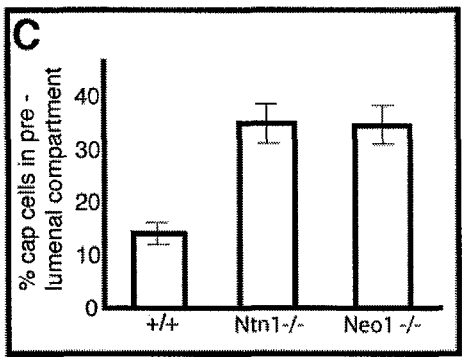
C
% cap cells in pre - lumenal compartment
40
30
20
10
0
+/+
Ntn1-/-
Neo1 -/-


D
L
Neo1-/-

Figure 7

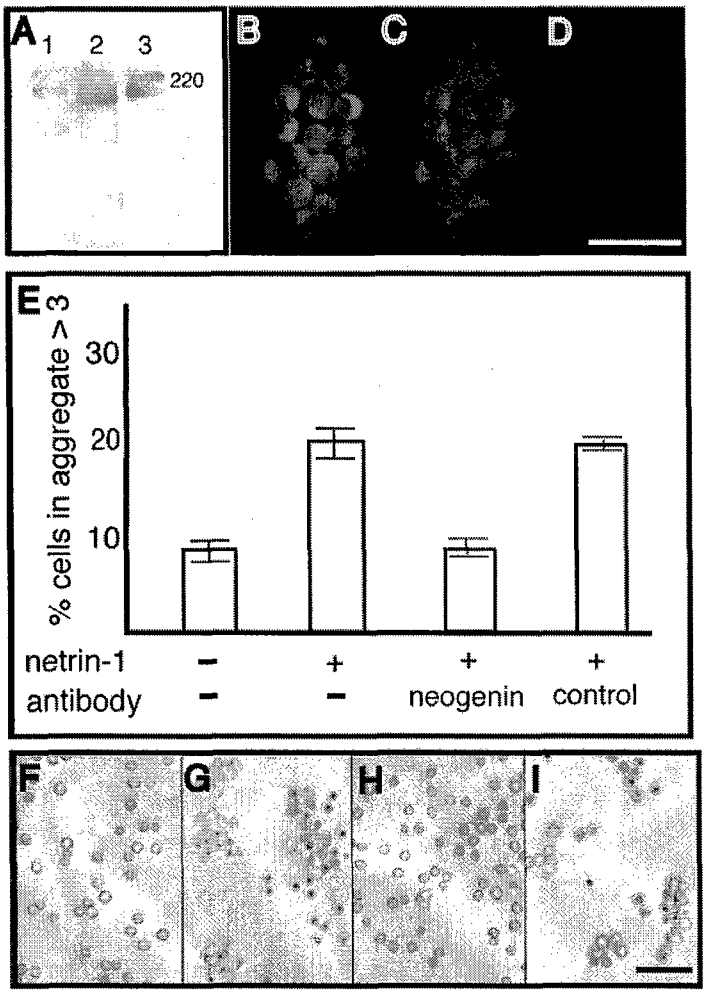
A
1 2 3
220
B
C
D
E
% cells in aggregate > 3
30
20
10
netrin-1 - + + +
antibody - - neogenin control
F
G
H
I

The versatile roles of "axon guidance" cues in tissue morphogenesis

Lindsay Hinck

Department of Molecular, Cell, and Developmental Biology,

University of California, Santa Cruz

Corresponding author: Lindsay Hinck, Ph.D. Sinsheimer Labs, University of California, Santa Cruz 95064, tel: 831-459-3139, hinck@biology.ucsc.edu

Abstract:

The Netrin, Slit, Semaphorin and Ephrin families of secreted proteins were originally characterized in the nervous system as guidance cues for axons, however recent studies demonstrate that many members of these families contribute to the development of a variety of organs. Here, the current knowledge of their roles is discussed with a focus on four tissues: lung, mammary, cardiovascular and kidney. While many studies indicate a role for "axon guidance" cues in regulating cell-cell and cell-extracellular matrix (ECM) interactions during organogenesis, there is accumulating evidence that they also contribute to tissue development by regulating the transcription and translation of genes encoding key morphogenetic factors.

Introduction:

After the three germ layers of an embryo are established in development, organogenesis begins as cells interact with each other and arrange themselves into tissues and organs. In the nervous system, guidance cues organize neural progenitor cells and direct axons into intricate networks of connections. There is a growing list of secreted proteins, including morphogens such as Wnts (Zou, 2004), that act as neuronal guidance cues. This review focuses on four families (Netrin (*Ntn*), Slit (*Slit*), Semaphorin (*Sema*) and Ephrin (*Efn*)) whose axon guidance activities have been extensively studied, but whose functions outside the nervous system are just beginning to be elucidated. These cues are present in the extracellular environment and are either expressed on the cell surface, or secreted into the ECM where they are thought to form gradients that affect neuronal behavior at long range. They can act as attractants, guiding neurons and their axons to targets, or repellents, creating exclusion zones that neurons avoid. Thus, the range and mode of action of these cues established their original classifications: Ephrins and glycosylphosphatidylinositol (GPI)-linked Semaphorins as short-range repellents; Slits and secreted Semaphorins as long-range repellents; and Netrins as long-range bifunctional cues, capable of both attraction and repulsion. But, as an increasing number of activities for these cues are discovered, stringent labels defining their function are no longer appropriate. For example, Slits act as attractants and Ephrins promote post-synaptic receptor clustering (Kramer et al., 2001) (Palmer and Klein, 2003). Furthermore, there are an increasing number of reports describing the expression of these cues outside the nervous system in a variety of developing tissues and organs. In some settings, their functions can be defined by analogous roles in the nervous system. In other settings, evidence suggests they govern tissue morphogenesis in new ways that are not simply defined in terms of their neuronal guidance functions. Here, current information is reviewed on the roles these axon guidance cues play during organogenesis with a focus on four developing tissues: lung, mammary, cardiovascular, and kidney.

Guidance Cues and their Receptors:

The response of a cell to a guidance cue depends on specific receptors expressed on the cell surface. Many of these receptors have been identified and their domain structure determined (Figure 1). There are some structural similarities between receptors, for example both Netrin and Slit receptors are members of the immunoglobulin superfamily, but for the most part the cues and their receptors are not structurally related. These differences translate into unique signaling strategies such as different ways in which co-receptors are employed. Class 3 Semaphorins have ligand-binding co-receptors, called Neuropilins (*Nrp1* and *Nrp2*), that act together with a family of signal-transducing proteins, called Plexins (*Plxn*) (Tamagnone and Comoglio, 2000). Netrins also have two families of receptors: the DCC (Deleted in Colorectal Cancer) family comprising Dcc (*Dcc*) and Neogenin (*Neo1*), and the Unc5 family comprising *Unc5a*, *Unc5b*, *Unc5c* and *Unc5d* (Engelkamp, 2002; Livesey, 1999). Members of the DCC and UNC5 family both bind ligand and transduce independent intracellular signals (Livesey, 1999). They also bind each other, acting as co-receptors for Netrin-dependent

repulsion (Hong et al., 1999). Another unique signaling strategy is bi-directional signaling employed by transmembrane Ephrins and their Eph (*Eph*) receptors (Palmer and Klein, 2003). Bi-directional signaling is different from traditional signaling between ligand and receptor in which ligand induces intracellular events only within receptor-expressing cells. In bi-directional signaling, intracellular changes can occur in both receptor-expressing cells (forward signaling) and ligand-expressing cells (reverse signaling) since the transmembrane ligand and its receptor can both send as well as receive signals. Of all the receptors that transduce guidance signals, only one, the Eph kinase receptor, has intrinsic enzymatic activity. The others rely on a variety of adaptor proteins to link them to signaling systems (Huber et al., 2003).

Despite these differences, all guidance factors direct the motility of cells and, in each case, this appears to be accomplished by a receptor interacting, directly or indirectly, with a member of the Rac family of small GTPases (Huber et al., 2003). These effector proteins in turn organize the response of receptor-expressing cells by regulating the structure and dynamics of the actin cytoskeleton. A second common feature of these cues facilitates the regulation of cell movement. Each cue interacts with its receptor with a dissociation constant in the nanomolar range. This is different from the picomolar dissociation constants that characterize many ligand/receptor interactions such as the interaction between EGF and the EGF receptor (Hurwitz et al., 1991). Interactions of this affinity apparently permit the rapid sampling of the environment observed when a growth cone actively explores its surroundings. Filopodia are extended that make and release contacts as the growth cone follows gradients of secreted cues present in the ECM. In thinking about the function of these cues during tissue morphogenesis, it is possible that such flexible interactions between receptor and cue permit active, yet constrained, mobility of cells during morphogenetic remodeling. Since these interactions between cue and receptor range from adhesive/attractive to anti-adhesive/repulsive, and occur between individual cells and between cells and their environment, they could allow for wide-ranging morphological effects; for example, they could they could participate in shaping and molding living tissue in three-dimensional space. It is therefore not surprising that, given such a potential for broad spectrum activity, guidance cues are employed in many contexts throughout development.

Lung Branching Morphogenesis: Push-Pull Mechanism of Netrins and Semaphorins

The mammalian lung exemplifies an architectural transformation as it grows from a simple epithelial bud into a complex tree-like structure designed for gas exchange. Members of all four families of guidance cues are expressed during lung development (Anselmo et al., 2003; Greenberg et al., 2004; Hafner et al., 2004; Xian et al., 2001), but functional studies relate the activity of only two families, Semaphorin and Netrin, to specific morphogenetic events (Ito et al., 2000; Kagoshima and Ito, 2001; Liu et al., 2004). One current hypothesis is that guidance cues establish permissive and restrictive zones during early steps of branching morphogenesis. The budding epithelium responds to these zones by refining the size and shape of the outgrowth, an activity similar to the role these cues play during neural development when they shape the architecture of the nervous system by directing the outgrowth of axons.

Murine lung development begins at embryonic day nine when two primordial buds composed of an inner endodermal epithelium and an outer mesenchymal jacket grow out of the primitive trachea (Cardoso, 2000). In the first stage of lung development, the bronchial tree develops through a process of elongation, branching and budding, giving rise to four bronchial stems on the right and one on the left. Development continues as dichotomous branching establishes the conducting portion of the airways and generates terminal bronchioles. Terminal bronchioles eventually give rise to primitive alveolar ducts that end in terminal sacs, and these ultimately develop into mature alveolar ducts and alveoli that compose the adult lung.

Current evidence suggests that SEMA3A, SEMA3C, NTN1 and NTN4, along with their respective receptors, play a role in defining the pattern of early branching morphogenesis (Ito et al., 2000; Kagoshima and Ito, 2001; Liu et al., 2004). From E11.5 to E13.5, these cues are expressed in overlapping patterns as the respiratory tree develops (Figure 2). *Sema3c* transcripts are expressed in the epithelium at the tips of the bronchioles, while *Sema3a* transcripts are expressed in a complementary pattern in the surrounding mesenchymal jacket (Ito et al., 2000; Kagoshima and Ito, 2001). *Ntn1* and *Ntn4* transcripts, like *Sema3c*, are expressed together in the epithelium, but rather than being expressed at the tips of the bronchi buds, Netrin transcripts are localized to the stalk regions (Liu et al., 2004). All these cues transduce signals through receptors that are present in the epithelium.

Several of these cues, SEMA3A, NTN1 and NTN4, have been shown to act repulsively in the nervous system and may have a similar function in the lung. Transcripts of *Nrp1*, which encode a receptor that mediates SEMA3A-dependent repulsion in the nervous system (He and Tessier-Lavigne, 1997; Kitsukawa et al., 1997; Kolodkin et al., 1997), are present in terminal buds adjacent to *Sema3a*-expressing mesenchyme (Kagoshima and Ito, 2001). Transcripts of *Unc5b*, which encode a Netrin receptor, are expressed along with a second Netrin receptor DCC in the epithelium (Liu et al., 2004). Together these receptors mediate repulsion in a Netrin-dependent manner (Hong et al., 1999). Given these patterns of expression, one hypothesis concerning the function of these cues is they work in concert to restrict ectopic budding and fine-tune both the size and shape of emerging buds. In this model, NTN1 and NTN4, deposited in the basal lamina surrounding the bud stalks, function in the proximal region of the duct to prevent inappropriate lateral branching. In contrast, SEMA3A, present in the mesenchyme surrounding the end of buds, acts distally to organize their shape (Figure 2). Results from *in vitro* assays, showing these cues inhibit branching, support this model (Ito et al., 2000; Liu et al., 2004). In the case of NTN1 and NTN4, this inhibition is so dramatic that buds project internally into the lumen rather than externally to form new projections (Liu et al., 2004).

These inhibitory activities could be balanced by the chemoattractant action of SEMA3C (Bagnard et al., 1998; de Castro et al., 1999), whose transcripts are expressed in the epithelium at the tips of the bronchioles (Kagoshima and Ito, 2001) (Figure 2). In the model, transcripts of *Nrp2* which encode a receptor that binds SEMA3C (Chen et al., 1997; Takahashi et al., 1998), are present in the epithelium and could receive this signal (Kagoshima and Ito, 2001). In the model, SEMA3C counters the repellent effects of SEMA3A, NTN1 and NTN4, and stimulates budding in appropriate locations. Indeed treatment of lung explants with SEMA3C

demonstrates its stimulatory effect on branching morphogenesis, resulting in a more highly branched structure and a modest increase in cell proliferation (Kagoshima and Ito, 2001).

Taken together, it is possible to generate a push-pull model of lung branching morphogenesis whereby guidance cues act in concert with other critical growth and morphogenetic factors to sculpt the architecture of the respiratory tree (Figure 2). It is, therefore, disappointing that results generated by treating lung explants with purified forms of guidance cues are not complemented by loss-of-function phenotypes in knock-out mice. There are no morphological abnormalities in mice carrying null or hypomorphic alleles of either *Sema3a*, *Ntn1*, *Ntn4* or *Dcc* (Kagoshima and Ito, 2001; Liu et al., 2004). *Nrp1* homozygous null mice display smaller lungs with significantly fewer branches, but these observations require cautious interpretation since lung explants from these animals develop normally, suggesting the defects are a secondary effect, perhaps related to cardiovascular abnormalities (see below) (Ito et al., 2000). These negative results are inconclusive and, while unsatisfying, likely indicate the high degree of similarity in the function of these factors. If the model is correct, two Netrins and a Semaphorin function as repellents, and each could compensate for the activity of another. Thus, in the lung, functional redundancy may occur among family members (e.g. NTN1 and NTN4) and between members of functionally-related families (e.g. Semaphorins and Netrins acting as repellents). This complicates the search for function as loss of multiple cues may be required for phenotypes to be displayed. Currently, there are no descriptions of phenotypes in compound null animals in which expression of more than one of these guidance cues has been eliminated.

Other families of axon guidance cues, for example transcripts of *Slit2* and *Slit3* and their *Robo*1 and *Robo2* receptors, are expressed in the lung (Anselmo et al., 2003; Greenberg et al., 2004; Xian et al., 2001). A small cell lung cancer line expresses a mutated *Robo1* gene termed *Dutt1*, for deleted in U2020, that is missing the first immunoglobulin repeat in the extracellular domain (Sundaresan et al., 1998). Mice engineered to express only *Dutt1* frequently die at birth due to respiratory failure, and histological analyses of their lungs reveal abnormally dense mesenchyme, surrounding smaller and irregularly shaped bronchioles (Xian et al., 2001). It is currently unknown how expression of the DUTT1 mutant results in this phenotype, although a likely explanation is that normal signals transduced by ROBO1 are perturbed, either through inappropriate interactions with SLIT, or another ROBO receptor, or an as yet unidentified co-factor. In the nervous system, SLIT signals through ROBO to promote axon branching (Ozdinler and Erzurumlu, 2002; Wang et al., 1999), therefore one possibility is that these irregularly shaped bronchioles are a result of inappropriate branching. This possibility, however, has not been directly tested, and additional data that could aid the interpretation of this phenotype, such as lung defects in other *Slit* or *Robo* null mice, have not yet been reported.

Mammary Gland Outgrowth: Netrin-1 as an Adhesive Cue

A second organ that undergoes branching morphogenesis is the mammary gland. A unique aspect of mammary gland development is that it occurs primarily later in life, in the juvenile and adult organism, rather than the embryo. While a simple ductal structure grows prenatally, it is only after birth that the mammary tree is

established by a process of ductal elongation and branching (Silberstein, 2001). Terminal end buds are the enlarged termini of ducts responsible for both growth and primary structure of the gland. Growth is driven by proliferation of a single layer of multi-potent progenitor cap cells at the tip of the bud and by the underlying luminal cells. As the terminal end bud grows rapidly to the edge of the fat pad, cap cells differentiate laterally into myoepithelial cells, and a fraction drop down basally to give rise to a subpopulation of luminal cells (Williams and Daniel, 1983). Mature ducts are composed of an outer tube of myoepithelial cells that eventually contract to squeeze milk from an inner tube of secretory epithelial cells into the central lumen. Under the influence of gestational hormones, acinar lobules form along the mature ductal tree in preparation for lactation. After weaning, the lobules undergo massive apoptosis leaving a ductal tree similar to one found in the gland prior to pregnancy.

The terminal end bud is highly invasive and motile, and the cap cells at the leading edge are also very motile. While cap cells adhere to each other through P-cadherin and luminal cells adhere to each other through E-cadherin, little was known of the mechanism that maintains the interactions between the cap and luminal cells layers. One clue recently came from expression studies showing that NTN1 is expressed by luminal cells of the terminal end bud and its receptor NEO1, a homolog of DCC, is expressed in a complementary pattern by cap cells (Srinivasan et al., 2003). Analysis of *Ntn1-/-* glands reveals an inappropriate space between the cap and luminal cell layers in which loose and dying cap cells accumulate (Srinivasan et al., 2003). Loss of *Neo1* results in a similar phenotype suggesting that NTN1 and NEO1 function as ligand and receptor in the same pathway. Together with results from *in vitro* assays demonstrating adhesive interactions between NTN1 and NEO1, these expression patterns and phenotypes suggest a model in which NTN1 stabilizes and maintains the close proximity of NEO1-expressing cap cells (Srinivasan et al., 2003). In this model, NTN1, secreted by luminal cells, mediates cell adhesion as a short-range attractant rather than directing cell migration as a guidance cue. This adhesive activity maintains tissue architecture during outgrowth of the gland, and it may play additional roles during the morphogenetic remodeling that occurs during pregnancy and involution.

Other cues are also expressed in the mammary gland. Similar to the expression of NTN1 and NEO1, EFNB2 is expressed by luminal cells, and its receptor, EPHB4, is expressed in a complementary pattern by myoepithelial cells (Nikolova et al., 1998). This expression pattern is dependent on estrogen and consequently regulated during the course of the estrus cycle (Nikolova et al., 1998). To examine the consequences of unscheduled EPHB4 expression on mammary gland form and function, *Ephb4* was overexpressed under the MMTV-LTR promoter, resulting in transgene expression in myoepithelial and luminal epithelial cells during pregnancy, lactation and early involution (Munarini et al., 2002). Glands overexpressing EPHB4 display reduced proliferation likely explaining an observed delay in their development. During pregnancy, fewer acinar lobules form in the transgenic animals with each lobular unit containing more but smaller alveolae (Munarini et al., 2002). Inappropriate apoptotic cell death is also observed during pregnancy followed by delayed apoptosis after weaning, suggesting an overall imbalance in the response of the tissue to proliferative/apoptotic signals

(Munarini et al., 2002). Since many of these phenotypes occur during stages when endogenous EFNB2 is expressed, one possibility is that perturbed receptor/ligand interactions are responsible. This, however, may be an oversimplification as the interactions between Ephrins and their Eph receptors are known to be promiscuous (Dodelet and Pasquale, 2000), and overexpressed EPHB4 may interact with other Ephrins in the gland. Furthermore, a ligand-independent mechanism may contribute to the observed phenotypes since Eph receptor activation is one consequence of their overexpression (Zisch et al., 1997). Thus, EPHB4 overexpression interferes with the growth response of mammary epithelial cells, however it is currently unknown whether this is a consequence of overstimulated forward signaling by EFNB2 through its overexpressed EPHB4 receptor, or unscheduled forward signaling by other Ephrins, or reverse signaling through inappropriately activated receptors.

Cardiovascular Development: Semaphorins and Ephrins Regulate Elaborate Morphogenesis

The cardiovascular system is the first functional organ system of the vertebrate embryo. From a simple tube, a four-chambered, double pump system is generated that circulates blood separately and directionally through an ordered series of vessels. Two processes can be distinguished during cardiovascular development: vasculogenesis and angiogenesis. In vasculogenesis, the heart primordia and primary capillary plexus, both tubular structures, develop from differentiating primitive angiogenic cells (Risau and Flamme, 1995). The heart develops when clusters of angiogenic cells coalesce to form an endocardial tube that bends, fuses and then becomes subdivided by septa to form two atria, two ventricles and two great vessels. The primary capillary plexus forms when a different population of angiogenic cells coalesce into a homogeneous capillary bed (Risau, 1997). This simple network of tubes is subsequently remodeled by the second process, angiogenesis, into an interconnected branched pattern characteristic of mature blood vessels. During these processes, the heart receives a critical influx of cells from the neural crest, which participate by unknown mechanisms in remodeling the great vessels, generating the endocardial cushions and creating the adult asymmetric vasculature. Not surprisingly, members of all four families of guidance cues are expressed during cardiac development and appear to regulate various aspects of endothelial cell migration (Huminiecki et al., 2002; Lu et al., 2004; Park et al., 2003), but the most extensive studies have been on the roles of Semaphorins and Ephrins during cardiovascular development.

Semaphorins:

In the Semaphorin family, a targeted mutation in *Sema3c* in the CD1 genetic background results in severe cardiac defects characterized by improper septation of the cardiac outflow tract (truncus arteriosus) and a ventricular septal defect (Feiner et al., 2001). Since disruption of cardiac neural crest cell migration leads to similar defects (Kirby et al., 1983), initial studies to understand the *Sema3c* homozygous null phenotypes focused on the migration of these cells (Brown et al., 2001; Feiner et al., 2001). Given that Semaphorins can function in the nervous system as long-range guidance cues, an attractive hypothesis concerning their function

was that cardiac neural crest cells, which express transcripts of *Plxna2*, could be guided to the cardiac outflow tract by SEMA3C, which could be encoded by the high level of transcripts detected in this region (Brown et al., 2001). An analogous long-range guidance role has been ascribed to SEMA3A in directing hindbrain and trunk neural crest cell migration (Eickholt et al., 1999). Once recruited to this destination, it seemed reasonable that these pluripotent cells could participate in cardiovascular patterning events that lead to proper outflow tract formation. This role was proved unlikely, however, by the analysis of cardiac neural crest cells in *Sema3c*-/- mice (Brown et al., 2001). These cells display only a modest disruption in their location, consistent with a role for SEMA3C in modulating their final position in the outflow tract, rather than correctly guiding them to this destination. Importantly, the disruption is not sufficient to explain the severity of cardiac defects observed in *Sema3c*-/- mice. Furthermore, targeted disruption of a different class 3 Semaphorin, *Sema3a*, also results in cardiac defects that, like the defects observed in *Sema3c*-/- mice, depend on the genetic background of the mouse (Behar et al., 1996). These defects, however, are different from those observed in *Sema3c*-/- mice since there are no defects observed in the outflow tract or great vessels (Behar et al., 1996; Takashima et al., 2002). Thus neither SEMA3C nor SEMA3A appear to simply function in the cardiovascular system as a secreted, long-range guidance cue for cardiac neural crest cells. Instead, recent work to elucidate the function of class 3 Semaphorins in the cardiovascular system has focused on three different receptors expressed during cardiac development.

Neuropilins and Plexins are co-receptors for class 3 Semaphorins, but their relationship is complicated by the fact that Neuropilins also serve as co-receptors for some forms of the vascular endothelial growth factor (VEGF) family of ligands (Soker et al., 1998). In the cardiovascular system, VEGF proteins are key regulators of vasculogenesis and angiogenesis, and VEGF^{165} (*Vegf*^{165}) likely plays overlapping roles with SEMA3C during cardiac development. This is evidenced by the phenotype of *Vegf*^{165}-/- mice which display very similar cardiac defects compared to *Sema3c*-/- mice (Brown et al., 2001; Stalmans et al., 2003). Analysis of mice carrying homozygous null mutations in the shared receptors for these ligands indicate that Neuropilins play a critical role in mediating signals during vascular development. *Nrp1*-/- mice die as embryos (~E10.5-E12.5) and exhibit defects in the heart, vasculature and nervous system (Kawasaki et al., 1999; Kitsukawa et al., 1997). In contrast, *Nrp2*-/- mice are viable, but display defects in the nervous and lymphatic systems (Chen et al., 2000; Giger et al., 2000; Yuan et al., 2002). Double homozygous null (*Nrp1*-/-;*Nrp2*-/-) embryos have severe vascular defects in both embryonic and placental blood vessels, dying earlier in gestation (~E8.5) compared to single *Nrp1*-/- mutant mice (Takashima et al., 2002). To distinguish VEGF from class 3 Semaphorin signaling through NRP1, two lines of mice were generated, one with loss of NRP1 expression only in endothelial cells (*Nrp1*$^{[endo-]}$) and the second with a mutant version of NRP1 that binds VEGF, but not SEMA3 proteins (*Nrp1*$^{[sema-]}$) (Gu et al., 2003). *Nrp1*$^{[sema-]}$ mice do not display the outflow tract and ventricular septal defects displayed in *Nrp1*$^{[endo-]}$ or *Vegf*^{165}-/- animals, suggesting that normal cardiac development requires VEGF signaling through NRP1

expressed in the endothelium. In contrast, atrial enlargement, similar to that observed in *Sema3a*-/- mice (Behar et al., 1996), was observed in *Nrp1*$^{[sema-]}$ and *Nrp1*$^{[endo-]}$ mice, suggesting that proper atrial development requires SEMA3A/ NRP1 signaling (Gu et al., 2003).

While these elegant experiments shed light on VEGF and SEMA3A signaling, the question of how SEMA3C signals during cardiac development still remained. Mice carrying homozygous mutations in both *Nrp1*$^{[sema-]}$ and *Nrp2* display outflow tract and ventricular septal defects that are not present in either single mutant animal. These defects are very similar to those displayed in *Sema3c*-/- mice in certain genetic backgrounds, raising the possibility that either NRP1 or NRP2 can serve as SEMA3C receptors during cardiac development, with each receptor able to compensate for the loss of the other. A breakthrough occurred with the identification of *Plxnd1*, a gene encoding a putative Neuropilin co-receptor (Gitler et al., 2004; Torres-Vazquez et al., 2004). PLXND1 is expressed in vascular endothelium (Gitler et al., 2004; Torres-Vazquez et al., 2004), and can enhance the binding of SEMA3C to NRP1 and NRP2, and SEMA3A to NRP1 (Gitler et al., 2004). The cardiac outflow tract and ventricular septal defects in *Plxnd1*-/- animals are very similar to those present in *Sema3c*-/-, *Nrp1*$^{[endo-]}$ and *Vegf*^{165}-/- animals, leading the authors to suggest a model in which both SEMA3C and VEGF^{165} are required for proper cardiac development (Gitler et al., 2004). In this model, SEMA3C and VEGF ^{165} signal through PLXND1 and the VEGF receptor, KDR, respectively, while Neuropilins serve as co-receptors for both pathways. Thus, SEMA3C may signal through PLXND1 to play a direct role in cardiac development (Gitler et al., 2004; Gu et al., 2003; Torres-Vazquez et al., 2004), rather than simply refining VEGF signaling through competitive inhibition of Neuropilin signaling (Miao et al., 1999). Certainly in zebrafish vascular development, a related class 3 Semaphorin, SEMA3A, appears to signal directly as a chemorepellent through PLXND1 to generate and organize developing blood vessels (Childs et al., 2002; Torres-Vazquez et al., 2004). Thus, current data suggest a direct role for SEMA3/PLXN signaling, coordinated with VEGF signaling, in mediating numerous aspects of cardiovascular development.

Since SEMA3C plays a critical role during cardiac development, the question of its function arises. In the developing nervous system, distinguishing attractive versus repellent roles for guidance cues such as the Semaphorins has been relatively straightforward. Expression analysis reveals the source of a cue relative to the neurons that express its receptors. *In vitro* collagen gel assays show whether axons, extending from tissue explants containing the cell bodies of these neurons, are attracted or repelled by the cue. These activities can then be confirmed by examining whether the axons are misguided in mice carrying homozygous null mutations in genes encoding either the cue or its receptor. In contrast, *in vitro* assays for cardiac development are not well developed, and while the analysis of knock-out phenotypes illuminates specific defects, it is difficult to extrapolate from these defects how a specific morphogenetic event went awry. Consequently, it is much more difficult to tease out the precise activity of a guidance cue. Take, for example, the formation of the outflow tract which is disrupted in *Sema3c*, *Nrp1*$^{[endo-]}$, *Plxnd1*, and *Vegf*^{165} single homozygous null animals and in *Nrp1*$^{[sema-]}$

;Nrp2 double null homozygotes. By a number of developmental events that are still poorly understood, this bi-layered tubular structure is transformed into two spiraling tubes that are capped by valves (Webb et al., 2003). While expression analysis reveals that *Sema3c* transcripts are expressed by the outer layer of cardiomyocytes and transcripts of its receptors by the inner layer of endothelial cells (Feiner et al., 2001), it is unclear how and when Semaphorin signaling occurs during outflow tract development. One clue comes from *in vitro* studies in which PLXND1-expressing endothelial cells are treated with SEMA3A, leading to the loss of actin stress fibers, a response associated with the loss of cell adhesion and repulsion (Torres-Vazquez et al., 2004). These data suggests that at least one class 3 Semaphorin may act at short-range to disrupt adhesion between two cell layers, allowing sheets of cells to slide past one another during the remodeling that transforms this simple tissue into a complex structure. But whether destabilization of cell layers actually occurs during cardiac outflow tract formation, and whether other secreted Semaphorins, such as SEMA3C, mediate repulsion at such a close range remain open questions.

In any case, deciphering the functions of Semaphorins during cardiac development promises to be very complex as there is a plethora of Semaphorins expressed in the heart during development. Five class 3 Semaphorins and three PlexinA receptors are expressed in endothelial cells (Serini et al., 2003), and recent data suggest that one of the ways these class 3 Semaphorins function is via autocrine signals that inhibit integrin activation and decrease adhesion between cells and the ECM (Serini et al., 2003). Evidence for this type of cross-talk between integrin and guidance cue signaling is growing, not just for Semaphorins but for the other cues as well (Nakamoto et al., 2004). Elucidating how this cross-talk regulates cell-ECM interactions will be complicated by the observation that cues, such as Netrin (Yebra et al., 2003) and a class 7, GPI-linked Semaphorin (Pasterkamp et al., 2003), directly mediate integrin signaling. Furthermore, studies in chick demonstrate a bifunctional role for a transmembrane member of the class 6 Semaphorins (Toyofuku et al., 2004). SEMA6D mediates endothelial cell migration depending on which region of the heart the cells are derived (Toyofuku et al., 2004). Endothelial cells from the outflow tract are stimulated by SEMA6D, an action opposing the movement directed by SEMA3A. PLXNA1 apparently interacts in these cells with VEGF receptor type 2, allowing SEMA6D to act synergistically with VEGF to promote migration. In contrast, endothelial cells from the ventricular region of the heart are inhibited by SEMA6D, and despite the co-expression of NRP1, this inhibition is attributed to an interaction between PLXNA1 and OTK, a receptor tyrosine kinase shown in *Drosophila* to serve as a PLXNA1 co-receptor (Winberg et al., 2001). Taken together, these results describe dual roles for SEMA6D that are region-specific, opposite in function and dependent on different PLXNA1/ co-receptor interactions. As such, they contribute to the growing data on the elaborate ways in which Semaphorins signal through Plexins and other receptors to influence cardiac morphogenesis.

Ephrins:

Ephrins and Eph receptors are also expressed in the cardiovascular system with one Ephrin and its

receptor expressed in a particularly striking pattern. Transcripts for *Efnb2* are expressed by arteries and not veins, and transcripts for one of its receptors, *Ephb4*, are expressed by veins and not arteries (Wang et al., 1998). The analysis of *Efnb2* and *Ephb4* homozygous null mice reveals similar phenotypes (Gerety et al., 1999; Wang et al., 1998). Early vasculogenesis in both animals appears largely normal since primitive blood vessels form, but major defects occur during angiogenesis when these vessels are remodeled into vascular networks. This shared pattern of phenotypic defects, together with the complementary expression of a ligand and receptor that signal bi-directionally, led to the hypothesis that reciprocal signaling between arteries and veins is required for remodeling the capillary network. This hypothesis was supported by initial studies on mice that express a truncated form of *Efnb2* (*Efnb2*$^{[ICD-]}$) and should therefore be incapable of reverse signaling (Adams et al., 2001). These mice display defects in angiogenesis very similar to those observed in *Efnb2*-/- animals, suggesting that reverse signaling is required for angiogenic remodeling. This conclusion, however, has recently been revised with the generation and analysis of additional lines of mice (Cowan et al., 2004). One line harbors a cytoplasmic domain deletion, similar to the truncation found in *Efnb2*$^{[ICD-]}$ mice, but with the addition of a C-terminal epitope tag (*Efnb2*$^{[ICD-:HA]}$). The second line carries *Efnb2*, in which the cytoplasmic domain is replaced by β-galactosidase (*Efnb2*$^{[ICD-:LacZ]}$). Analysis of these mice shows that when the cytoplasmic domain is truncated, the protein remains trapped within the cell, and is consequently not present at the cell surface to participate in signaling. In contrast, fusing the cytoplasmic domain to β-galactosidase apparently facilitates proper trafficking of the protein to the plasma membrane where it is capable of forward, but not reverse, signaling. Mice expressing this EFNB2/β-gal fusion protein display normal vascular connections, indicating that reverse signaling does not contribute to angiogenesis. These surprising new results lead to a revised hypothesis concerning EFNB2/EPHB4 signaling during angiogenesis in which EFNB2 functions solely as a traditional ligand on arteries to stimulate forward EPHB4 signaling in veins.

The discovery that only forward signaling occurs during vasculogenesis raises the question of how unidirectional signaling leads to similar arterial and venous remodeling defects in the *Efnb2* and *Ephb4* null animals. At least two models, that are not mutually exclusive, can be proposed. One model is based on the observation that EPHB activation by EFNB-Fc fusion proteins induces endothelial sprouting (Adams et al., 1999). These results are consistent with a role for forward signaling in venous remodeling which in turn could stimulate arterial remodeling. If this is the case, arterial defects in *Efnb2*-/- and *Ephb4*-/- mice are secondary to venous defects, and are likely caused by altered or absent blood flow to veins. A second model to explain how unidirectional signaling may lead to symmetrical mutant phenotypes is based on cell mixing experiments using endothelial cells over-expressing either EPHB4 or the truncated form of Ephrin, EFNB2$^{[ICD-]}$ (Fuller et al., 2003). These cells segregate into populations favoring homotypic interactions, suggesting that forward signaling by EFNB2 through EPHB4 restricts cell intermingling by mediating repulsive rather than adhesive interactions. These results are consistent with the functional role proposed for EFNB2/EPHB4 signaling in restricting cell

movement and establishing cell boundaries in adjacent hindbrain rhombomeres (Xu et al., 1999). Accordingly, this activity could establish or maintain the arterial-venous boundary at the interface between populations of endothelial cells expressing EFNB2 and EPHB4. If this is the case, then it suggests that proper boundary formation and maintenance is essential for network remodeling, and in the absence of this forward signaling neither venous nor arterial remodeling occurs.

These and other studies on *Efnb2*-/- and *Ephb4*-/- mice, and on related members of both families, show that EFN/EPH signaling plays additional roles during cardiovascular development. For example, *Ephb2/Ephb3* double null homozygous mice display a variety of defects in vasculogenesis (Adams et al., 1999). And, even though $Efnb^{[ICD-:LacZ]}$ mice do not show defects in vascular remodeling, they display a variety of cardiac valve defects, indicating a role for reverse signaling during heart development (Cowan et al., 2004). Thus, similar to Semaphorin signaling in cardiovascular development, signaling by Ephrins and Eph receptors is complicated, and elucidating the roles of individual members as ligands and as receptors is hindered by the number of family members expressed and by the complexity of their actions.

Kidney Induction: Slit2 "Unmarks" the Spot

This review has highlighted a number of models describing the function of guidance cues during organogenesis--- models that are based primarily on analogous functions of these factors in the nervous system. The complexity of organ development and the number of members of each family expressed in different tissues, however, raises the possibility that interpreting phenotypes based on known activities in the nervous system is misleading. Cues could have entirely novel functions in different contexts. Studies examining SLIT/ROBO signaling during kidney development bring this issue to the fore, with the recent analysis of *Slit2*-/- mice suggesting a new role for SLIT2 signaling in regulating transcription (Grieshammer et al., 2004). In contrast, efforts to demonstrate an established role for SLIT2 as a branching factor in kidney have been unsuccessful (Piper et al., 2002). While much remains to be learned about the new signaling pathway mediated by SLIT in kidney, it raises the specter of novel functions unrelated to the known branching, guidance and adhesive activities associated with this cue.

Kidney organogenesis depends on a series of reciprocal interactions between the epithelial ureteric bud and metanephric mesenchyme. The murine kidney (metanephros) develops around embryonic day eleven when the extending nephric (Wolffian) duct produces an outgrowth called the ureteric bud which invades a specialized region of intermediate mesoderm called the metanephric mesenchyme (Figure 3) (Saxen, 1987). Signaling interactions between the ureteric bud and the metanephric mesenchyme induce the bud to grow and branch so that it arborizes into a tree-like collecting duct system. Signals from the tips of these branches are required for the formation of nephrons, the functional units of the kidney. These signals induce disorganized aggregates of mesenchymal cells to undergo a complex morphogenesis as they change shape and transition into highly organized epithelial tubules.

Ureteric bud formation is elicited by the growth factor, GDNF, which is secreted by the metanephric mesenchyme and signals via its receptors expressed in the duct epithelium (Moore et al., 1996; Pichel et al., 1996; Sanchez et al., 1996). In the absence of *Slit2*, multiple ureteric buds form, and due to a similar phenotype present in *Robo2*-/- mice, the data suggest that SLIT2 signals through ROBO2 to suppress supernumerary bud formation (Grieshammer et al., 2004). Interestingly, a similar phenotype is also observed as a consequence of GDNF treatment, suggesting a link between SLIT/ROBO signaling and GDNF expression (Sainio et al., 1997). Expression analysis reveals *Slit2* transcripts in the nephric duct and in the anterior nephrogenic mesenchyme where *Robo2* is also expressed (Figure 3). In contrast *Gdnf* transcripts are expressed throughout the nephrogenic mesenchyme, but over the course of development they become progressively restricted to the posterior region where the ureteric bud forms (Figure 3).

Given these expression patterns and the chemorepellent activity of SLITS in the nervous system, one appealing model was that SLIT2 /ROBO2 signaling guides *Gdnf*-expressing cells by repelling them from the anterior nephrogenic mesenchyme to the posterior metanephric mesenchyme where they would be appropriately located to secrete GDNF and elicit bud outgrowth. In this model, loss of SLIT2 /ROBO2 signaling would result in supernumerary bud formation since *Gdnf*-expressing cells would be present throughout the mesenchyme rather than properly restricted to the site of ureteric bud growth. Studies were performed to test this model, but it was found that SLIT2 does not appear to act as a chemorepellent for nephrogenic mesenchymal cells (Grieshammer et al., 2004). An alternate model in which SLIT2 acts to eliminate *Gdnf*-positive cells by inducing cell death was also tested. Few or no dying cells, however, were found in the nephrogenic mesenchyme of normal embryos, indicating that this mechanism is not responsible for restricting *Gdnf* expression (Grieshammer et al., 2004). As a result of these studies, the authors favor a third possible model involving the effects of SLIT2 /ROBO2 signaling on *Gdnf* expression. Since GDNF elicits ureteric bud formation, SLIT2 /ROBO2 signaling may function to restrict its expression in anterior nephrogenic mesenchymal cells. Consistent with this model is the observation that *Gdnf* expression is inappropriately maintained in the anterior nephrogenic mesenchyme in *Slit2* and *Robo2* null homozygotes, and reducing *Gdnf* gene dosage in *Slit2*-/- animals rescues the supernumerary ureteric bud phenotype.

Since these experiments do not reveal the mechanism underlying SLIT/ROBO signaling, additional studies are required. One possibility is that SLIT2 acts "in character" through ROBO2 to remodel cell contacts by modulating cell adhesion. This remodeling may indirectly affect the expression of genes by communicating with other signaling pathways, such as integrin, that directly control transcription. Alternatively, these data may reflect a new role for SLIT/ROBO signaling in directly regulating, through as yet uncharacterized transduction pathways, the transcription or translation of genes encoding crucial morphogenetic cues. The idea that ROBO signaling may regulate levels of signaling proteins is supported by recent studies in *Drosophila*. SLIT acts through ROBO to promote terminal asymmetric division of Ganglion Mother Cells by down regulating the

expression of two POU proteins, Nubbin and Mitimere, and consequently allowing the asymmetric localization of Inscuteable (Mehta and Bhat, 2001). In a different context, ROBO signaling in a SLIT independent manner is required for serotonergic neuron differentiation by regulating the expression of a transcription factor, Eagle, required for this process (Couch et al., 2004). While additional studies are required to delineate these pathways, evidence is accumulating that SLIT/ROBO and ROBO mediated signaling does more than just re-organize the cytoskeleton to direct cell motility. Indeed, it appears it may have broad-ranging roles in regulating the transcription and/or translation of key factors that specify cell fates.

Future Directions:

Cells interact with each other in diverse ways to form complex structures during organogenesis. Recent studies analyzing the biological roles of axon guidance cues outside the nervous system demonstrate that these multi-functional cues play diverse roles that profoundly influence the generation of complex tissues. Studies on the function of these molecules in the nervous system provide valuable conceptual clues about their function in other contexts. In general, guidance cues shape the architecture of organs. In the nervous system, cues direct the construction of elaborate networks of connections by guiding neurons and their axonal and dendritic projections. In the heart, mammary gland and lung, cues direct the organization of tissues by regulating cellular interactions. These processes rely on changes in cell-cell or cell-ECM contact and likely occur through transduction pathways similar to those used in axon guidance. These pathways lead to cytoskeletal re-arrangements which, in turn, direct cell motility and adhesion. In contrast, studies in kidney and *Drosophila* on ROBO signaling highlight novel ways for cues to control organ architecture by regulating the expression of crucial morphogenetic factors. Such a role for "axon guidance" molecules expands our notion of their function. As such, it contributes to our broader understanding as biologists of the ways in which relatively few proteins perform wide-ranging functions that depend on *in vivo* context to provide the regulation required to generate an organism.

The next step for developmental biologists is to define the precise activities of these cues and to elucidate their signaling mechanisms. As outlined in this review, this will require increasingly sophisticated genetic manipulations. For example in the lung, the multiplicity of cues that act in functionally-related ways has made it impossible to verify their activity by analyzing animals harboring a deletion in a single gene encoding a cue. Consequently, deciphering the actions of cues that function redundantly will require generating compound homozygous null animals to eliminate the expression of more than one member of a single family and multiple members of different, functionally-related families. A second complication in studying these cues in organs other than the nervous system is that their signaling pathways intersect with other pathways, and in some cases these shared pathways play critical roles in organ development. The example of Semaphorin/VEGF signaling through their Neuropilin co-receptor during cardiovascular development is presented in this review. Distinguishing between the two pathways required structure/function analysis of Neuropilin followed by the

generation of mice expressing a functionally simplified receptor that binds VEGF but not Semaphorin. A second example is bi-directional signaling via transmembrane Ephrin and Eph receptor. To distinguish the operative signaling pathway through these proteins required generating mice that express receptors with cytoplasmic domain truncations, forcing unidirectional signaling. Developmental biologist must undertake more of these state-of-the-art transgenic manipulations to resolve specific signaling pathways during organogenesis. The analysis of these transgenic mice will greatly benefit from advances in high-resolution imaging of organ cultures and whole animals. Together, these investigations promise to reveal the critical ways in which guidance cues mediate cellular interactions as tissues undergo complex morphogenetic changes.

Acknowledgments

Due to space limitation, not all work could be cited and I apologize for limiting citations. This work was supported by a research scholar grant #RSG0218001MGO from the American Cancer Society and Career Grant DAMD170210336 from the U.S. Army Medical Research Command. I am grateful to my reviewers and my colleagues, especially Megan Williams, for their insightful comments.

References

Adams, R. H., Diella, F., Hennig, S., Helmbacher, F., Deutsch, U., and Klein, R. (2001). The cytoplasmic domain of the ligand ephrinB2 is required for vascular morphogenesis but not cranial neural crest migration. Cell *104*, 57-69.

Adams, R. H., Wilkinson, G. A., Weiss, C., Diella, F., Gale, N. W., Deutsch, U., Risau, W., and Klein, R. (1999). Roles of ephrinB ligands and EphB receptors in cardiovascular development: demarcation of arterial/venous domains, vascular morphogenesis, and sprouting angiogenesis. Genes Dev *13*, 295-306.

Anselmo, M. A., Dalvin, S., Prodhan, P., Komatsuzaki, K., Aidlen, J. T., Schnitzer, J. J., Wu, J. Y., and Kinane, T. B. (2003). Slit and robo: expression patterns in lung development. Gene Expr Patterns *3*, 13-19.

Bagnard, D., Lohrum, M., Uziel, D., Puschel, A. W., and Bolz, J. (1998). Semaphorins act as attractive and repulsive guidance signals during the development of cortical projections. Development *125*, 5043-5053.

Behar, O., Golden, J. A., Mashimo, H., Schoen, F. J., and Fishman, M. C. (1996). Semaphorin III is needed for normal patterning and growth of nerves, bones and heart. Nature *383*, 525-528.

Brown, C. B., Feiner, L., Lu, M. M., Li, J., Ma, X., Webber, A. L., Jia, L., Raper, J. A., and Epstein, J. A. (2001). PlexinA2 and semaphorin signaling during cardiac neural crest development. Development *128*, 3071-3080.

Cardoso, W. V. (2000). Lung morphogenesis revisited: old facts, current ideas. Dev Dyn *219*, 121-130.

Chen, H., Bagri, A., Zupicich, J. A., Zou, Y., Stoeckli, E., Pleasure, S. J., Lowenstein, D. H., Skarnes, W. C., Chedotal, A., and Tessier-Lavigne, M. (2000). Neuropilin-2 regulates the development of selective cranial and sensory nerves and hippocampal mossy fiber projections. Neuron *25*, 43-56.

Chen, H., Chedotal, A., He, Z., Goodman, C. S., and Tessier-Lavigne, M. (1997). Neuropilin-2, a novel member of the neuropilin family, is a high affinity receptor for the semaphorins Sema E and Sema IV but not Sema III. Neuron *19*, 547-559.

Childs, S., Chen, J. N., Garrity, D. M., and Fishman, M. C. (2002). Patterning of angiogenesis in the zebrafish embryo. Development *129*, 973-982.

Couch, J. A., Chen, J., Rieff, H. I., Uri, E. M., and Condron, B. G. (2004). robo2 and robo3 interact with eagle to regulate serotonergic neuron differentiation. Development *131*, 997-1006.

Cowan, C. A., Yokoyama, N., Saxena, A., Chumley, M. J., Silvany, R. E., Baker, L. A., Srivastava, D., and Henkemeyer, M. (2004). Ephrin-B2 reverse signaling is required for axon pathfinding and cardiac valve formation but not early vascular development. Dev Biol *271*, 263-271.

de Castro, F., Hu, L., Drabkin, H., Sotelo, C., and Chedotal, A. (1999). Chemoattraction and chemorepulsion of olfactory bulb axons by different secreted semaphorins. J Neurosci *19*, 4428-4436.

Dodelet, V. C., and Pasquale, E. B. (2000). Eph receptors and ephrin ligands: embryogenesis to tumorigenesis. Oncogene *19*, 5614-5619.

Eickholt, B. J., Mackenzie, S. L., Graham, A., Walsh, F. S., and Doherty, P. (1999). Evidence for collapsin-1 functioning in the control of neural crest migration in both trunk and hindbrain regions. Development *126*, 2181-2189.

Engelkamp, D. (2002). Cloning of three mouse Unc5 genes and their expression patterns at mid-gestation. Mech Dev *118*, 191-197.

Feiner, L., Webber, A. L., Brown, C. B., Lu, M. M., Jia, L., Feinstein, P., Mombaerts, P., Epstein, J. A., and Raper, J. A. (2001). Targeted disruption of semaphorin 3C leads to persistent truncus arteriosus and aortic arch interruption. Development *128*, 3061-3070.

Fuller, T., Korff, T., Kilian, A., Dandekar, G., and Augustin, H. G. (2003). Forward EphB4 signaling in endothelial cells controls cellular repulsion and segregation from ephrinB2 positive cells. J Cell Sci *116*, 2461-2470.

Gerety, S. S., Wang, H. U., Chen, Z. F., and Anderson, D. J. (1999). Symmetrical mutant phenotypes of the receptor EphB4 and its specific transmembrane ligand ephrin-B2 in cardiovascular development. Mol Cell *4*, 403-414.

Giger, R. J., Cloutier, J. F., Sahay, A., Prinjha, R. K., Levengood, D. V., Moore, S. E., Pickering, S., Simmons, D., Rastan, S., Walsh, F. S., *et al.* (2000). Neuropilin-2 is required in vivo for selective axon guidance responses to secreted semaphorins. Neuron *25*, 29-41.

Gitler, A. D., Lu, M. M., and Epstein, J. A. (2004). PlexinD1 and semaphorin signaling are required in endothelial cells for cardiovascular development. Dev Cell *7*, 107-116.

Greenberg, J. M., Thompson, F. Y., Brooks, S. K., Shannon, J. M., and Akeson, A. L. (2004). Slit and robo expression in the developing mouse lung. Dev Dyn *230*, 350-360.

Grieshammer, U., Le, M., Plump, A. S., Wang, F., Tessier-Lavigne, M., and Martin, G. R. (2004). SLIT2-mediated ROBO2 signaling restricts kidney induction to a single site. Dev Cell *6*, 709-717.

Gu, C., Rodriguez, E. R., Reimert, D. V., Shu, T., Fritzsch, B., Richards, L. J., Kolodkin, A. L., and Ginty, D. D. (2003). Neuropilin-1 conveys semaphorin and VEGF signaling during neural and cardiovascular development. Dev Cell *5*, 45-57.

Hafner, C., Schmitz, G., Meyer, S., Bataille, F., Hau, P., Langmann, T., Dietmaier, W., Landthaler, M., and Vogt, T. (2004). Differential gene expression of Eph receptors and ephrins in benign human tissues and cancers. Clin Chem *50*, 490-499.

He, Z., and Tessier-Lavigne, M. (1997). Neuropilin is a receptor for the axonal chemorepellent Semaphorin III. Cell *90*, 739-751.

Hong, K., Hinck, L., Nishiyama, M., Poo, M. M., Tessier-Lavigne, M., and Stein, E. (1999). A ligand-gated association between cytoplasmic domains of UNC5 and DCC family receptors converts netrin-induced growth cone attraction to repulsion. Cell *97*, 927-941.

Huber, A. B., Kolodkin, A. L., Ginty, D. D., and Cloutier, J. F. (2003). Signaling at the growth cone: ligand-receptor complexes and the control of axon growth and guidance. Annu Rev Neurosci *26*, 509-563.

Huminiecki, L., Gorn, M., Suchting, S., Poulsom, R., and Bicknell, R. (2002). Magic roundabout is a new member of the roundabout receptor family that is endothelial specific and expressed at sites of active angiogenesis. Genomics *79*, 547-552.

Hurwitz, D. R., Emanuel, S. L., Nathan, M. H., Sarver, N., Ullrich, A., Felder, S., Lax, I., and Schlessinger, J. (1991). EGF induces increased ligand binding affinity and dimerization of soluble epidermal growth factor (EGF) receptor extracellular domain. J Biol Chem *266*, 22035-22043.

Ito, T., Kagoshima, M., Sasaki, Y., Li, C., Udaka, N., Kitsukawa, T., Fujisawa, H., Taniguchi, M., Yagi, T., Kitamura, H., and Goshima, Y. (2000). Repulsive axon guidance molecule Sema3A inhibits branching morphogenesis of fetal mouse lung. Mech Dev *97*, 35-45.

Kagoshima, M., and Ito, T. (2001). Diverse gene expression and function of semaphorins in developing lung: positive and negative regulatory roles of semaphorins in lung branching morphogenesis. Genes Cells *6*, 559-571.

Kawasaki, T., Kitsukawa, T., Bekku, Y., Matsuda, Y., Sanbo, M., Yagi, T., and Fujisawa, H. (1999). A requirement for neuropilin-1 in embryonic vessel formation. Development *126*, 4895-4902.

Kirby, M. L., Gale, T. F., and Stewart, D. E. (1983). Neural crest cells contribute to normal aorticopulmonary septation. Science *220*, 1059-1061.

Kitsukawa, T., Shimizu, M., Sanbo, M., Hirata, T., Taniguchi, M., Bekku, Y., Yagi, T., and Fujisawa, H. (1997). Neuropilin-semaphorin III/D-mediated chemorepulsive signals play a crucial role in peripheral nerve projection in mice. Neuron *19*, 995-1005.

Kolodkin, A. L., Levengood, D. V., Rowe, E. G., Tai, Y. T., Giger, R. J., and Ginty, D. D. (1997). Neuropilin is a semaphorin III receptor. Cell *90*, 753-762.

Kramer, S. G., Kidd, T., Simpson, J. H., and Goodman, C. S. (2001). Switching repulsion to attraction: changing responses to slit during transition in mesoderm migration. Science *292*, 737-740.

Liu, Y., Stein, E., Oliver, T., Li, Y., Brunken, W. J., Koch, M., Tessier-Lavigne, M., and Hogan, B. L. (2004). Novel role for Netrins in regulating epithelial behavior during lung branching morphogenesis. Curr Biol *14*, 897-905.

Livesey, F. J. (1999). Netrins and netrin receptors. Cell Mol Life Sci *56*, 62-68.

Lu, X., le Noble, F., Yuan, L., Jiang, Q., de Lafarge, B., Sugiyama, D., Breant, C., Claes, F., De Smet, F., Thomas, J.-L., *et al.* (2004). The Netrin receptor UNC5B mediates guidance events controlling morphogenesis of the vascular system. Nature *in press*.

Mehta, B., and Bhat, K. M. (2001). Slit signaling promotes the terminal asymmetric division of neural precursor cells in the Drosophila CNS. Development *128*, 3161-3168.

Miao, H. Q., Soker, S., Feiner, L., Alonso, J. L., Raper, J. A., and Klagsbrun, M. (1999). Neuropilin-1 mediates collapsin-1/semaphorin III inhibition of endothelial cell motility: functional competition of collapsin-1 and vascular endothelial growth factor-165. J Cell Biol *146*, 233-242.

Moore, M. W., Klein, R. D., Farinas, I., Sauer, H., Armanini, M., Phillips, H., Reichardt, L. F., Ryan, A. M., Carver-Moore, K., and Rosenthal, A. (1996). Renal and neuronal abnormalities in mice lacking GDNF. Nature *382*, 76-79.

Munarini, N., Jager, R., Abderhalden, S., Zuercher, G., Rohrbach, V., Loercher, S., Pfanner-Meyer, B., Andres, A. C., and Ziemiecki, A. (2002). Altered mammary epithelial development, pattern formation and involution in transgenic mice expressing the EphB4 receptor tyrosine kinase. J Cell Sci *115*, 25-37.

Nakamoto, T., Kain, K. H., and Ginsberg, M. H. (2004). Neurobiology: New connections between integrins and axon guidance. Curr Biol *14*, R121-123.

Nikolova, Z., Djonov, V., Zuercher, G., Andres, A. C., and Ziemiecki, A. (1998). Cell-type specific and estrogen dependent expression of the receptor tyrosine kinase EphB4 and its ligand ephrin-B2 during mammary gland morphogenesis. J Cell Sci *111 (Pt 18)*, 2741-2751.

Ozdinler, P. H., and Erzurumlu, R. S. (2002). Slit2, a branching-arborization factor for sensory axons in the Mammalian CNS. J Neurosci *22*, 4540-4549.

Palmer, A., and Klein, R. (2003). Multiple roles of ephrins in morphogenesis, neuronal networking, and brain function. Genes Dev *17*, 1429-1450.

Park, K. W., Morrison, C. M., Sorensen, L. K., Jones, C. A., Rao, Y., Chien, C. B., Wu, J. Y., Urness, L. D., and Li, D. Y. (2003). Robo4 is a vascular-specific receptor that inhibits endothelial migration. Dev Biol *261*, 251-267.

Pasterkamp, R. J., Peschon, J. J., Spriggs, M. K., and Kolodkin, A. L. (2003). Semaphorin 7A promotes axon outgrowth through integrins and MAPKs. Nature *424*, 398-405.

Pichel, J. G., Shen, L., Sheng, H. Z., Granholm, A. C., Drago, J., Grinberg, A., Lee, E. J., Huang, S. P., Saarma, M., Hoffer, B. J., *et al.* (1996). Defects in enteric innervation and kidney development in mice lacking GDNF. Nature *382*, 73-76.

Piper, M., Nurcombe, V., Wilkinson, L., and Little, M. (2002). Exogenous Slit2 does not affect ureteric branching or nephron formation during kidney development. Int J Dev Biol *46*, 545-550.

Risau, W. (1997). Mechanisms of angiogenesis. Nature *386*, 671-674.

Risau, W., and Flamme, I. (1995). Vasculogenesis. Annu Rev Cell Dev Biol *11*, 73-91.

Sainio, K., Suvanto, P., Davies, J., Wartiovaara, J., Wartiovaara, K., Saarma, M., Arumae, U., Meng, X., Lindahl, M., Pachnis, V., and Sariola, H. (1997). Glial-cell-line-derived neurotrophic factor is required for bud initiation from ureteric epithelium. Development *124*, 4077-4087.

Sanchez, M. P., Silos-Santiago, I., Frisen, J., He, B., Lira, S. A., and Barbacid, M. (1996). Renal agenesis and the absence of enteric neurons in mice lacking GDNF. Nature *382*, 70-73.

Saxen, L. (1987). Organogenesis of kidney (Cambridge, Cambridge University Press).

Serini, G., Valdembri, D., Zanivan, S., Morterra, G., Burkhardt, C., Caccavari, F., Zammataro, L., Primo, L., Tamagnone, L., Logan, M., *et al.* (2003). Class 3 semaphorins control vascular morphogenesis by inhibiting integrin function. Nature *424*, 391-397.

Silberstein, G. B. (2001). Postnatal mammary gland morphogenesis. Microsc Res Tech *52*, 155-162.

Soker, S., Takashima, S., Miao, H. Q., Neufeld, G., and Klagsbrun, M. (1998). Neuropilin-1 is expressed by endothelial and tumor cells as an isoform- specific receptor for vascular endothelial growth factor. Cell *92*, 735-745.

Srinivasan, K., Strickland, P., Valdes, A., Shin, G. C., and Hinck, L. (2003). Netrin-1/neogenin interaction stabilizes multipotent progenitor cap cells during mammary gland morphogenesis. Dev Cell *4*, 371-382.

Stalmans, I., Lambrechts, D., De Smet, F., Jansen, S., Wang, J., Maity, S., Kneer, P., von der Ohe, M., Swillen, A., Maes, C., *et al.* (2003). VEGF: a modifier of the del22q11 (DiGeorge) syndrome? Nat Med *9*, 173-182.

Sundaresan, V., Chung, G., Heppell-Parton, A., Xiong, J., Grundy, C., Roberts, I., James, L., Cahn, A., Bench, A., Douglas, J., *et al.* (1998). Homozygous deletions at 3p12 in breast and lung cancer. Oncogene *17*, 1723-1729.

Takahashi, T., Nakamura, F., Jin, Z., Kalb, R. G., and Strittmatter, S. M. (1998). Semaphorins A and E act as antagonists of neuropilin-1 and agonists of neuropilin-2 receptors. Nat Neurosci *1*, 487-493.

Takashima, S., Kitakaze, M., Asakura, M., Asanuma, H., Sanada, S., Tashiro, F., Niwa, H., Miyazaki Ji, J., Hirota, S., Kitamura, Y., *et al.* (2002). Targeting of both mouse neuropilin-1 and neuropilin-2 genes severely impairs developmental yolk sac and embryonic angiogenesis. Proc Natl Acad Sci U S A *99*, 3657-3662.

Tamagnone, L., and Comoglio, P. M. (2000). Signalling by semaphorin receptors: cell guidance and beyond. Trends Cell Biol *10*, 377-383.

Torres-Vazquez, J., Gitler, A. D., Fraser, S. D., Berk, J. D., Van, N. P., Fishman, M. C., Childs, S., Epstein, J. A., and Weinstein, B. M. (2004). Semaphorin-plexin signaling guides patterning of the developing vasculature. Dev Cell *7*, 117-123.

Toyofuku, T., Zhang, H., Kumanogoh, A., Takegahara, N., Suto, F., Kamei, J., Aoki, K., Yabuki, M., Hori, M., Fujisawa, H., and Kikutani, H. (2004). Dual roles of Sema6D in cardiac morphogenesis through region-specific association of its receptor, Plexin-A1, with off-track and vascular endothelial growth factor receptor type 2. Genes Dev *18*, 435-447.

Wang, H. U., Chen, Z. F., and Anderson, D. J. (1998). Molecular distinction and angiogenic interaction between embryonic arteries and veins revealed by ephrin-B2 and its receptor Eph-B4. Cell *93*, 741-753.

Wang, K. H., Brose, K., Arnott, D., Kidd, T., Goodman, C. S., Henzel, W., and Tessier-Lavigne, M. (1999). Biochemical purification of a mammalian slit protein as a positive regulator of sensory axon elongation and branching. Cell *96*, 771-784.

Webb, S., Qayyum, S. R., Anderson, R. H., Lamers, W. H., and Richardson, M. K. (2003). Septation and separation within the outflow tract of the developing heart. J Anat *202*, 327-342.

Williams, J. M., and Daniel, C. W. (1983). Mammary ductal elongation: differentiation of myoepithelium and basal lamina during branching morphogenesis. Dev Biol *97*, 274-290.

Winberg, M. L., Tamagnone, L., Bai, J., Comoglio, P. M., Montell, D., and Goodman, C. S. (2001). The transmembrane protein Off-track associates with Plexins and functions downstream of Semaphorin signaling during axon guidance. Neuron *32*, 53-62.

Xian, J., Clark, K. J., Fordham, R., Pannell, R., Rabbitts, T. H., and Rabbitts, P. H. (2001). Inadequate lung development and bronchial hyperplasia in mice with a targeted deletion in the Dutt1/Robo1 gene. Proc Natl Acad Sci U S A *98*, 15062-15066.

Xu, Q., Mellitzer, G., Robinson, V., and Wilkinson, D. G. (1999). In vivo cell sorting in complementary segmental domains mediated by Eph receptors and ephrins. Nature *399*, 267-271.

Yebra, M., Montgomery, A. M., Diaferia, G. R., Kaido, T., Silletti, S., Perez, B., Just, M. L., Hildbrand, S., Hurford, R., Florkiewicz, E., *et al.* (2003). Recognition of the neural chemoattractant Netrin-1 by integrins alpha6beta4 and alpha3beta1 regulates epithelial cell adhesion and migration. Dev Cell *5*, 695-707.

Yuan, L., Moyon, D., Pardanaud, L., Breant, C., Karkkainen, M. J., Alitalo, K., and Eichmann, A. (2002). Abnormal lymphatic vessel development in neuropilin 2 mutant mice. Development *129*, 4797-4806.

Zisch, A. H., Stallcup, W. B., Chong, L. D., Dahlin-Huppe, K., Voshol, J., Schachner, M., and Pasquale, E. B. (1997). Tyrosine phosphorylation of L1 family adhesion molecules: implication of the Eph kinase Cek5. J Neurosci Res *47*, 655-665.

Zou, Y. (2004). Wnt signaling in axon guidance. Trends Neurosci *27*, 528-532.

Figure Legends

Figure 1: Domain structure of guidance cues and their receptors. Members of a family of guidance cues may be secreted from the cell or tethered to the membrane via GPI or transmembrane linkages. Receptors are all single-pass transmembrane proteins. Abbreviations: EGF, epidermal growth factor; Ig, immunoglobulin; CUB, complement-homology domain; MAM, meprin/A5/mu-phosphatase homology domain, PDZ refers to a motif that was originally discovered in three proteins PSD-95, Dlg1 and ZO-1.

Figure 2: The expression patterns of Semaphorins, Netrins and their receptors along with their attractive versus repulsive functions may create push-pull forces that shape the architecture of a lung bud (after, Kagoshima and Ito, 2001). In this model, Netrins function proximally to restrict ectopic budding. *Ntn1* and *Ntn4* transcripts are expressed together in the stalk region (red), and the proteins encoded by these transcripts are deposited into the basal lamina surrounding the bud stalk (red –). Transcripts of the components of the repellent receptor complex, *Unc5b* and *Dcc*, are expressed in an overlapping manner in the stalk epithelium, and are present to receive this restrictive cue (red). Transcripts of *Sema3a* are expressed distally in the mesenchyme and function to fine-tune the size and shape of emerging buds (purple). Transcripts of the SEMA3A receptor, *Nrp1*, are present to receive this restrictive signal in the epithelium of terminal buds (blue). These repulsive activities are balanced by the attractive function of SEMA3C, transcripts of which are expressed in the epithelium of terminal buds (blue), and the protein encoded by these transcripts is deposited into the basal lamina surrounding the terminal bud (blue +). To receive this positive cue, transcripts of the SEMA3C receptor, *Nrp2*, are expressed in an overlapping manner with the transcripts of *Sema3c* in the epithelium of terminal buds (blue).

Figure 3: SLIT2 restricts ectopic ureteric buds by signaling through ROBO2 to inhibit *Gdnf*-expression in the anterior mesenchyme (after, Grieshammer et al., 2004). *Slit2* transcripts (red gradient) are detected at a high level throughout the nephric duct and at relatively lower levels in the nephrogenic mesenchyme. In contrast, *Robo2* transcripts are expressed at a high level throughout the nephrogenic mesenchyme where *Gdnf* expression is suppressed. During development transcripts for *Gdnf* become restricted to the posterior region where the ureteric bud forms in the metanephric mesenchyme (blue cloud surrounding the ureteric bud). These patterns of expression are consistent with a model in which SLIT2, signaling through ROBO2, restricts the anterior expression of *Gdnf*. In the posterior region, lack of ROBO2 prevents SLIT signaling, allowing *Gdnf* expression and consequently the appropriate outgrowth of the ureteric bud.

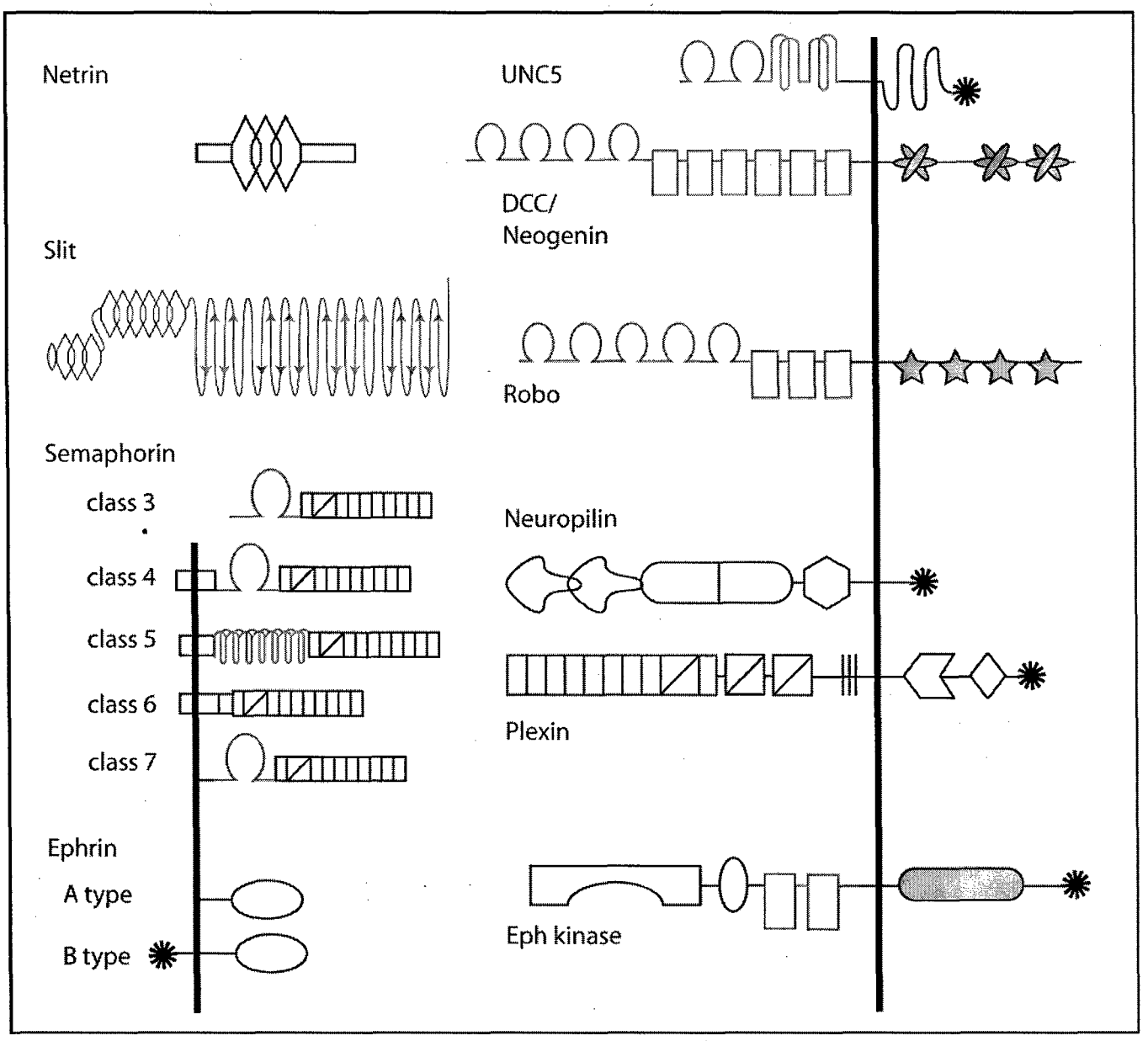

Key:

- EGF-like repeat
- leucine rich repeat
- Ig domain
- thrombospondin domain
- sema domain with met related sequence
- ligand binding domains
- fibronectin type III repeat
- CUB domain
- coagulation factor homology domain
- MAM domain
- signaling domains
- sex-plexin domain
- kinase domain
- PDZ domain binding motif

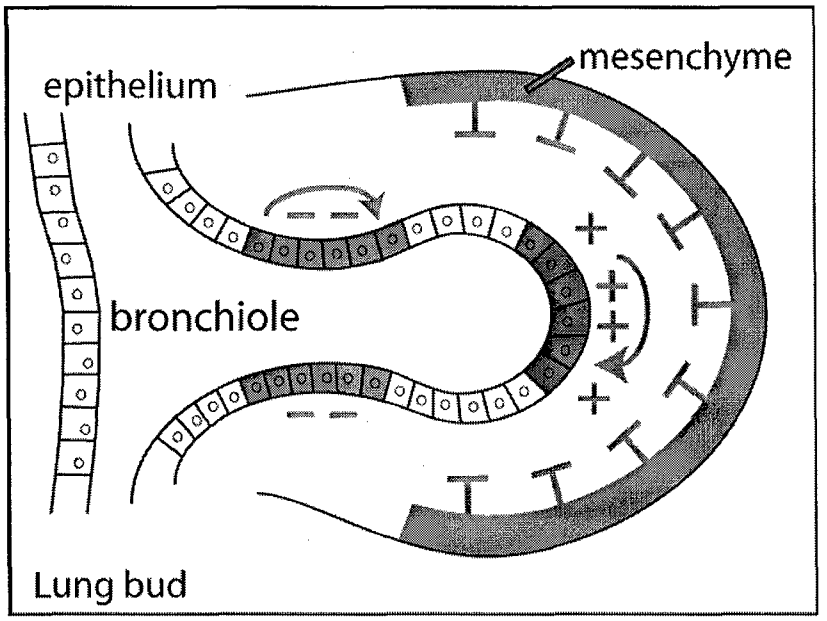
epithelium
mesenchyme
bronchiole
Lung bud

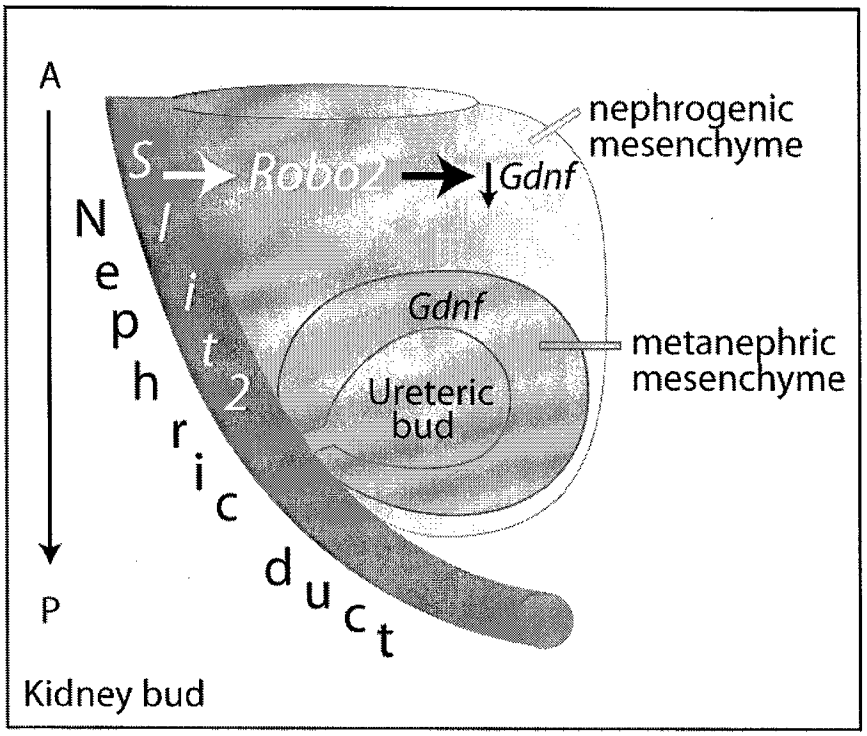
A
P
Slit2
Robo2
Gdnf
nephrogenic mesenchyme
Gdnf
metanephric mesenchyme
Ureteric bud
Nephric duct
Kidney bud

Slit2 and Netrin1 Act Synergistically as Adhesive Cues to Generate Tubular Bi-layers during Ductal Morphogenesis

Phyllis Strickland[1]§, Grace C. Shin[1]§, Andrew Plump[2], Marc Tessier-Lavigne[3] and Lindsay Hinck[1]*

[1]Department of Molecular, Cell and Developmental Biology University of California, Santa Cruz Santa Cruz, CA 95064, [2]Merck Research Laboratories, 126 East Lincoln Avenue, Rahway, New Jersey 07065, [3]Genentech, Incorporated, 1 DNA Way, South San Francisco, CA 94080

* Corresponding author: hinck@biology.ucsc.edu

§ These authors contributed equally to the work

Running title: **Slit2 and Netrin1 in Mammary Ductal Morphogenesis**

Key Words: Slit, Robo, Netrin, Neogenin, mammary

SUMMARY

Development of many organs, including mammary glands, involves ductal morphogenesis. Mammary ducts are bi-layered tubular structures comprising an outer layer of cap/myoepithelial cells and an inner layer of luminal epithelial cells. *Slit2* is expressed by cells in both layers, with secreted SLIT2 broadly distributed throughout the epithelial compartment. In contrast, *Robo1* is expressed specifically by cap/myoepithelial cells. Loss-of-function mutations in *Slit2* and *Robo1* yield similar phenotypes characterized by disorganized end buds reminiscent of those present in *Ntn1-/-* glands, suggesting that SLIT2 and NTN1 function in concert during mammary development. Analysis of *Slit2-/-;Ntn1-/-* glands demonstrates an enhanced phenotype that extends through the ducts and is characterized by separated cell layers and occluded lumens. Aggregation assays show that *Slit2-/-;Ntn1-/-* cells, in contrast to wildtype cells, do not form bi-layered organoids, a defect rescued by addition of SLIT2. NTN1 has no effect alone, but synergistically enhances this rescue. Thus, our data establish a novel role for SLIT2 as an adhesive cue, acting in parallel with NTN1 to generate cell boundaries along ducts during bi-layered tube formation.

INTRODUCTION

Dramatic changes in shape and form occur during organogenesis as tissues are molded into three-dimensional structures. These changes involve a variety of rearrangements as cells disperse, condense, or form sheets. Cells within structures project internally or externally to form protrusions, internal boundaries develop to restrict cell mixing, and canalization occurs to generate lumens. Together, these developmental processes produce the functionally coordinated array of tissues that characterize multicellular organisms.

The mammary gland undergoes an elaborate and regulated morphogenesis, establishing a tree-like epithelial structure (Silberstein, 2001). This epithelium is a bi-layered tube comprising an outer layer of myoepithelial cells which ultimately contracts under the influence of hormones to squeeze milk into a central lumen from an inner layer of secretory epithelial cells (Fig. 1A). Before birth, only a simple ductal structure forms which is transformed during puberty into a mammary tree by the process of ductal elongation, end bud bifurcation, and secondary branching. This morphogenesis requires the continuous addition of new cells to both

layers, coordinated with the simultaneous formation of a lumen. The enlarged termini of ducts, termed end buds, are responsible for both growth and primary structure of the gland (Fig. 1A). Growth is driven by proliferation of a single layer of multi-potent progenitor cap cells at the tip of the bud, and by the underlying luminal cells. Cap cells differentiate into myoepithelial cells, generating the outer tubular layer, and at the same time, luminal cells are remodeled, generating a hollowed lumen from a relatively solid mass of cells present in the end bud.

These modifications in shape and form of the gland during ductal morphogenesis require coordinated cellular interactions. In generating this double-layered structure, cells interact with each other and with the extracellular matrix. Cadherins mediate interactions between cells within a given layer. E-cadherin provides adhesion between luminal cells in the body of the end bud and in the inner layer of the duct, and P-cadherin acts between cap cells at the tip of the end bud and myoepithelial cells along the duct (Daniel et al., 1995). Interactions between the cell layers, at least in the end bud, are provided by the secreted cue netrin-1 (*Ntn1*), which is expressed by luminal cells, and binds its receptor neogenin (*Neo1*), present on the surface of cap cells (Srinivasan et al., 2003). Loss-of-function mutations in *Ntn1* and *Neo1* result in disorganized end buds, characterized by inappropriate spaces between cap and luminal cell layers. Significantly, this disorganization does not extend into the ducts which appear normal (Srinivasan et al., 2003). Consequently, the identity of the adhesion system, if any, that mediates interactions between the myoepithelial and luminal epithelial bi-layers during ductal morphogenesis is uncertain. Desmosomal constituents are present during postnatal mammary gland development, but they appear diffuse within cells and may not be organized into mature plaques (Dulbecco et al., 1984). This suggests that desmosomal components of cell adhesion are held in store, and their assembly is delayed during development, perhaps allowing flexible movement of cells during tissue extension and tube formation. Later, in the mature gland, adhesion between myoepithelial cells and luminal cells is via desmosomes which provide strong adhesion to maintain tissue architecture (Runswick et al., 2001).

SLITs, like NTNs, are well known axon guidance proteins, acting as cues to guide neurons and their axons to targets during neural development. While SLITs and NTNs are structurally dissimilar, they share some of the same characteristics. They are both proteins that, while secreted, are not freely diffusible, but instead

immobilized in association with cell membranes or components of the extracellular matrix (Kappler et al., 2000; Zhang et al., 2004). Both act as bifunctional cues, capable of eliciting attractive and repulsive behaviors from cells expressing their receptors (Colamarino and Tessier-Lavigne, 1995; Englund et al., 2002; Kennedy et al., 1994; Kidd et al., 1999; Kramer et al., 2001). Furthermore, both have receptors that contain extracellular immunoglobulin domains and fibronectin type III repeats. In many proteins, these motifs act adhesively. Consequently it is not surprising that, in addition to their chemotropic guidance functions, SLITs and NTNs act chemotactically at close range to positively and negatively modulate cell-cell and cell-ECM interactions (Deiner et al., 1997; Kang et al., 2004; Simpson et al., 2000; Srinivasan et al., 2003).

Here we demonstrate a functional role for SLIT2 and its ROBO1 receptor during mammary gland morphogenesis. We show that SLIT2 is distributed throughout the epithelial compartment whereas ROBO1 expression is restricted to cap/myoepithelial cells. The analysis of glands carrying loss-of-function mutations reveals similar defects, suggesting this ligand/receptor pair function in the same pathway. *Slit2-/-* and *Robo1-/-* end buds display inappropriate spaces between cap and luminal cell layers, a defect reminiscent of the phenotypes observed in outgrowths deficient for *Ntn1* and *Neo1*(Srinivasan et al., 2003). Consequently, we generated glands with homozygous deletions in both *Slit2* and *Ntn1* and observe, in addition to defects in end bud structure, a synergistic strengthening of the single-mutant phenotypes characterized by severe ductal abnormalities that appear to stem from insufficient adhesion between myoepithelial and luminal cells. In vitro assays confirm that *Slit2-/-*; *Ntn1-/-* cells are severely compromised in their ability to form bi-layered organoids, and this deficiency is rescued by addition of purified SLIT2. Addition of NTN1 does not rescue on its own, but its addition with SLIT2, dramatically enhances both the number and size of bi-layered organoids generated, confirming a strong synergism between NTN1 and SLIT2. These results identify a novel, short-range function for SLIT2 as an adhesive cue acting through its ROBO1 receptor during ductal morphogenesis. Furthermore our results support a model in which dual "axon" guidance systems (SLIT2/ROBO1and NTN1/NEO1) mediate interactions between cells to preserve the structure of the gland during periods of rapid growth and morphogenetic modeling.

Materials and Methods:

Animals: The study conformed to guidelines set by the UCSC animal care committee(CARC). *Ntn1* severe hypomorphs, and *Slit1, Slit2, Slit3*, *Robo1*, and *Robo2* nulls were generated and genotyped as described (Serafini et al., 1996, Leighton et al., 2001, Plump et al., 2002, and Long et al.,2004). Double mutants were generated by crossing double heterozygotes.

Transplant techniques: Mammary anlage rescue from E16-20 embryos were performed as described (Robinson et al., 2000). Mammary fragments from the embryo were transplanted into precleared fat pads of athymic nude females. Tissue fragments from the resulting outgrowths were transplanted into precleared hosts to generate null and wild type tissue controls (Srinivasan et al., 2003).

Tissue analysis: Whole gland preparations were stained for ß-galactosidase activity as described (Brisken et al., 1999). Phenotypes were characterized on 6μm longitudinal serial sections stained with anti-smooth muscle actin (SMA) and counterstained with hematoxylin. Standard error was reported when data from multiple transplant lines were pooled in penetrance and expressivity studies.

Expression Studies: The promoters for *Slit1*, *Slit3*, *Robo1*, and *Robo2* drives the expression of *lacZ*. Their expression was assessed by whole gland ß-galactosidase staining (Brisken et al.,1999). The *Slit2* promoter drives the expression of GFP. Expression was assessed by anti-GFP immunhistochemistry.

Immunohistochemistry: Tissue was fixed in 4%paraformaldehyde at 4C, overnight. Paraffin embedded tissue was sectioned at 6μm and mounted serially. The following antibodies were used for analysis: anti-SMA, 1:500 (Sigma), anti-E-cadherin, 1:500 (BD Transduction Labs), anti-GFP, 1:50 (Molecular Probes), anti-Robo1, 1:250 (DUTT1. gift from Pamela Rabbits), and anti-Slit2, 1:25 (SCBT). Standard protocols were followed and Vector ABC kits were used to amplify the signals.

RT-PCR of mouse mammary glands: Mammary glands from *Robo1*+/+ 5 week old female mice were used and total RNA was prepared using a Micro-to-Midi Total RNA Purification System (Invitrogen). cDNA was made from total RNA using iScript™ cDNA Synthesis Kit (Bio-Rad) and used for reverse-transcriptase reactions (1μg). *Robo1* and *Dutt1* specific primers were generated as previously described (Clark et al., 2002). Products were separated on a 2.5% agarose gel.

Rotary cultures: Primary mammary epithelial cells were prepared from mild overnight collagenase and dispase digestion of *Slit2-/-;Ntn1-/-* and +/+ mammary glands, as described (Darcy et al., 2000). Differential trypsinization was performed to separate myoepithelial from luminal cells and these fractions were then combined at a ratio of 4:1 (myoepithelial:luminal) and rotated at 60rpm at 37C, 5% CO_2 for up to 3 days in growth medium, at a density of 10^6 cells/ml. SLIT2 and NTN1 were added directly to the cells prior to rotation. Rotary aggregates were fixed in 4% paraformaldehyde. Immunostaining of aggregates was performed on 30μm thick cryosections using a Mouse on Mouse (M.O.M.) kit (Vector Laboratories) with anti-SMA (1:500) and also DAPI. Aggregate size was categorized as follows: less than 10 cells, 10-20 cells, and more than 20 cells. Aggregates were also categorized based on whether none or one (or more) myoepithelial cells were present on the outside. At least 10 aggregates were counted for each experiment.

Ductal phenotype quantification: TEB arrays were embedded in paraffin and longitudinal 6μm serial sections were immunostained for SMA to delineate the myoepithelial cells layer and counterstained with hematoxylin. Slides were scanned for TEBs displaying the null phenotype with subtending ducts that could be followed in serial section. These were selected for analysis. Alternate sections were photographed and scored for severity of the phenotype and distance the ductal phenotype could be detected from the TEB. These were categorized as sporadic loss of luminal cells if discontinuous lengths of luminal cells from 20-50μm were present. Epithelial separation was characterized by lengths of intact luminal cells, ranging from 40-1000μm, detached from the myoepithelial cell layer. Ducts with more than one aberration were scored with the most severe phenotype.

RESULTS

Slit2 and Robo1 are Expressed in the Mammary Gland during Ductal Elongation.

To begin an investigation into whether SLITs and ROBOs play a role in mammary gland development, we examined the expression patterns of *Slit1*, *Slit2*, *Slit3*, *Robo1* and *Robo2*. Since *Robo4* expression is reported to be specific to the vasculature (Huminiecki et al., 2002; Park et al., 2003), we did not examine this family member, nor did we pursue *Rig1*(*Robo3*) since it likely functions as a negative regulator of SLIT responsiveness rather than as a signaling receptor (Sabatier et al., 2004).

We found using immunohistochemistry that SLIT2 is broadly distributed in wildtype (+/+) tissue throughout the epithelial compartment during the period of ductal outgrowth (5 weeks). It is present in and around both myoepithelial and luminal epithelial cells in the end bud (Fig. 1B). Little or no background immunostaining was observed in *Slit2*-/- outgrowths (Fig 1C). To identify the cells that express Slit2, we took advantage of the expression of *GFP* under the control of the endogenous promoters in mice targeted for *Slit2* and assayed for GFP expression using immunohistochemistry. At 5 weeks of age, we observed GFP expression in *Slit2*-/- tissue in cap cells of the end bud (Fig 1D, arrowheads) and in luminal cells (Fig 1D, arrows). Along the duct, we also observed GFP immunostaining in both myoepithelial (Fig 1F, arrowheads) and luminal epithelial cells (Fig 1F, arrow). As this immunostaining was performed on knock-out tissue, the morphological structure of the end bud and duct was abnormal; these defects are described in detail in the next section. Wildtype (+/+) control tissue displays the normal end bud structure, and we observed little or no background GFP staining, indicating that the detection method was specific (Fig. 1E, G). Next, we examined the expression of other *Slit* family members. We did not detect *Slit1* expression either during development or in the mature animal during any stage of pregnancy, lactation or involution (data not shown). In contrast, taking advantage of the expression of *lacZ* under the control of the endogenous promoter in mice targeted for *Slit3*, we observed accumulation of the β-galactosidase reaction product in myoepithelial cells (Fig. 1H, arrowheads), and ductal luminal cells (Fig. 1H, arrow) of the mature virgin *Slit3*-/- gland, and during pregnancy in luminal and myoepithelial cells of alveoli (Fig. 1I). *Slit3*, however, was not expressed during ductal outgrowth. Moreover, no morphological defects were detected in *Slit3*-/- mammary glands (unpublished observations, P.S., G.S., L.H), likely due to the presence of residual SLIT2 which is expressed early and may compensate for a lack of SLIT3 later in development.

Next, we examined the expression of *Robo1* and *Robo2* which are the receptors that mediate both the attractant and repellent effects of SLITS. Immunohistochemical analysis on wildtype (+/+) tissue demonstrated ROBO1 expression specifically on cap cells in the end bud (Fig. 2A) and myoepithelial cells of the duct (data not shown) with little or no background immunostaining observed in *Robo1*-/- tissue (Fig. 2B). Once again, we took advantage of the expression of *lacZ* under the control of the endogenous *Robo1* promoter in -/- and -/+

tissue to confirm our immunohistochemical results. We observed the accumulation of the β-galactosidase reaction product specifically in cap cells of the end bud (Fig. 2C, arrowheads) and myoepithelial cells in the duct where it co-localized with the marker, smooth muscle actin (SMA) (Fig. 2D). Since the expression of two isoforms of *Robo1* has been reported during mouse development (Clark et al., 2002), we determined which isoform is expressed during mammary development by performing RT-PCR analysis on mRNA. Total brain mRNA was used as a control since both isoforms are expressed in this tissue, but we found the *Dutt1* isoform is specifically expressed in developing mammary gland (Fig. 2E). Next we examined *Robo2* expression by staining *Robo2*+/- tissue for the β-galactosidase reaction product, and, similar to *Slit3*, found it was not expressed during ductal outgrowth (data not shown), but was expressed later in development in a subset of ductal myoepithelial cells in the mature virgin animal (Fig. 2F, arrowheads) and during pregnancy in alveoli (Fig. 2G, arrows).

Loss of Either *Slit2* or *Robo1* Results in Abnormal End Buds that are Morphologically Similar to *Ntn1*-/- and *Neo1*-/- End Buds.

To investigate the role of SLIT proteins in mammary gland development, we analyzed glands carrying loss-of-function alleles of *Slit2* and *Robo1*. The perinatal lethality of the *Slit2*-/- mutation prevented the study of mammary glands in mice carrying the homozygous mutation. Consequently, we followed standard protocols and harvested mammary anlage from *Slit2*-/- embryos and transplanted the tissue into fat pads of immunocompromised mice that had been cleared of their epithelial tissue. The contralateral fat pad received control anlage from +/+ embryos from the same litter (Robinson et al., 2000; Young, 2000). To ensure that only the epithelial compartment of the anlage was transplanted, we performed serial transplants of tissue fragments to generate outgrowths. At least three independently derived lines were isolated and serially transplanted for up to three generations to provide tissue for the experiments. In all studies, littermate control +/+ outgrowths were generated on the contralateral side for comparison. This ensured that both the +/+ and -/- outgrowths were subjected to the same systemic environment.

We sectioned *Slit2*-/- outgrowths 2-3 weeks post-transplantation to analyze end buds since wholemount analysis revealed no obvious morphological defects (data not shown). The sections were stained with an antibody directed against SMA to visualize cap and myoepithelial cells (Fig. 3 A-G). Compared with an end bud from control outgrowths (Fig. 3A), which displayed close apposition of the cap and luminal layers, *Slit2*-/- end buds displayed severe abnormalities. In *Slit2*-/- end buds, the cap cells were significantly pulled away from the luminal cells, creating an exaggerated subcapsular space, ranging from 5-15 μm compared to the subcapsular space of 0.1-1 μm typically observed in +/+ end buds (Fig. 3, compare A and B). Frequently there were dissociated cells present in this space and immunostaining with anti-SMA identified these loose cells as cap cells (Fig. 3B). In some end buds, we observed regions where luminal cells were completely detached from cap cells, leaving a cap cell layer devoid of underlying luminal cells (Fig. 3C, between arrows). These single layers of cap cells commonly folded inward, resulting in double-layered invaginations that compromised the structure of the end bud by disorganizing the underlying luminal cells and occluding the inner luminal space (Fig. 3D, between arrowheads). The phenotype was 100% penetrant with approximately 60% of the end buds in every outgrowth affected (59.1 +/– 26.5%, n= 98 end buds, 12 outgrowths).

A similar analysis was performed on *Robo1*-/- glands. Since mice carrying the *Robo1* mutation were viable, intact glands were examined, although we confirmed that a similar phenotype was present when *Robo1*-/- tissue was transplanted (data not shown). For these experiments, glands from +/+ littermates served as control tissue. End buds in *Robo1*-/- glands were disorganized, displaying a phenotype that was indistinguishable from the phenotype displayed in *Slit2*-/- end buds, characterized by the formation of subcapsular spaces, dissociation of cap cells, and invagination of the cap cell layer (Fig. 3F, G). As is the case for *Slit2*-/- outgrowths, the penetrance of the phenotype was 100% with approximately 60% of the end buds in every end bud array affected (62%+/- 23%, n=74 end buds, 4 outgrowths).

A noteworthy aspect of the defects observed in *Slit2*-/- and *Robo1*-/- end buds was their striking similarity to the defects observed in *Ntn*-/- and *Neo1*-/- end buds (Srinivasan et al., 2003). One major similarity was that end buds from each homozygous null animal exhibited loss of adhesion between the cap and luminal cell layers, with dissociated cap cells present in the resulting subcapsular space (Fig. 3B, F). These shared

defects created the impression that *Ntn1*-/-, *Neo1*-/-, *Slit2*-/-, and *Robo1*-/- phenotypes were identical, but we detected two unique characteristics in *Slit2*-/- and *Robo1*-/- end buds. The first was that the cap cell layer of *Slit2*-/- and *Robo1*-/- end buds folded into the luminal compartment (Fig. 3D, G), and this was not observed in *Ntn1*-/- and *Neo1*-/- glands (Srinivasan et al., 2003). Second, the basal lamina surrounding *Slit2*-/- and *Robo1*-/- end buds were intact (Fig. 3 and data not shown), whereas breaks were observed in *Ntn1*-/- and *Neo1*-/- glands (Srinivasan et al., 2003). Despite these differences, the overall appearance of end buds from each knock-out suggested the defects were due to a general loss of cell-cell adhesion between cap and luminal cell layers (Srinivasan et al., 2003). End buds are highly proliferative structures that undergo active remodeling and are consequently more likely to be sensitive to impaired cell adhesion. Since we discovered disorganization in this sensitive structure when either NTN/NEO or SLIT2/ROBO1 signaling system was lost, we expect, if these guidance systems functionally compensate for one another, that loss of both systems simultaneously will lead to disrupted cell contacts in more stable regions of the gland that are insensitive to the loss of either system alone.

Loss of Both *Slit2* and *Ntn1* Results in Disrupted Ductal Structure in Addition to Abnormal End Buds.

To investigate whether SLIT2 and NTN1 function in parallel to maintain interactions between the cap/myoepithelial and luminal cell layers during mammary gland development, we generated double homozygous null outgrowths. We sectioned *Slit2*-/-;*Ntn1*-/- outgrowths 2-3 weeks post-implantation to analyze end buds. The end buds displayed abnormalities with combined characteristics of both *Ntn1*-/- and *Slit2*-/- outgrowths (Fig. 4). Consequently, in addition to the subcapsular space and dissociated cells typically exhibited in outgrowths harboring homozygous loss-of-function alleles at either gene locus (Fig. 4B), we observed cap cell layers devoid of underlying luminal cells (Fig. 4A, between arrowheads) and cap cell layer enfolding (Fig. 4C, between arrowheads), both characteristic of defects observed in *Slit2*-/- outgrowths. Moreover, we also observed breaks in the basal lamina (Fig. 4B, box), a defect exhibited in *Ntn1*-/- outgrowths (Srinivasan et al., 2003). The phenotype was 100% penetrant with approximately 80% of the end buds affected (82.6% +/- 15.4% n= 103 end buds, 8 outgrowths). This represented an approximately 20% increase in expressivity compared to the expressivity exhibited in *Slit2*-/- end buds (Fig. 3) or *Ntn1*-/- end buds (Srinivasan et al., 2003). Together

with the observation that the *Slit2-/-;Ntn1-/-* phenotype was more severe in end buds (Fig. 4) and ducts (see below) compared to the phenotype exhibited in outgrowths carrying single homozygous null alleles, our analysis suggests that NTN/NEO and SLIT/ROBO pathways function in parallel to mediate contacts between epithelial cell layers.

In addition to abnormal end buds, the ducts of *Slit2-/-;Ntn1-/-* glands displayed severe adhesion defects. Compared to the ductal structure displayed in +/+ tissue, which illustrates the typically close apposition between luminal and myoepithelial cell layers (Fig. 5D), SMA immunostaining of double homozygous deficient outgrowths showed significant loss of adhesion between these layers (Fig. 5 A, B). In the mildest form, a few luminal cells were sporadically detached from the myoepithelial cell layer (Fig. 5A, arrows). A more severe defect was observed when this modest detachment of cells expanded to encompass substantial lengths of the duct, with the luminal cell layer essentially peeled away from the myoepithelial cell layer (Fig. 5B, double arrowheads). Although the contralateral control glands never displayed abnormal tissue morphology, we addressed the possibility that at least some aspects of the phenotype were due to the experimental protocol of fixing tissue post-harvest by perfusing animals with paraformaldehyde prior to tissue harvest. All aspects of the phenotype were preserved under these conditions.

We categorized the ductal phenotype as mild (+, sporadic loss of luminal cells) and more severe (++, separation of myoepithelial and luminal epithelial cell layers), (Fig. 5C). The ducts were characterized by identifying abnormal end buds and then, when longitudinal sections allowed, tracing the subtending duct back for up to 2mm. While we never observed ductal abnormalities in *Ntn1-/-* outgrowths, ductal abnormalities were readily apparent in *Slit2-/-* (n=12) and double *Slit2-/-;Ntn1-/-* (n=18) outgrowths (compare Fig. 5G with 5E, A, B). The loss of *Slit2* resulted in both sporadic luminal cell loss (50%) and separation of the epithelial cell layers (50%). In contrast, the more severe phenotype of epithelial separation was the major phenotype present (89%) in the absence of both *Slit2* and *Ntn1*. Taken together, the data showed that loss of either *Slit2-/-* or *Ntn1-/-* results in cell-cell adhesion defects between cap and luminal cell layers in the end bud (Fig. 3) (Srinivasan et al., 2003). This loss in adhesion extends into the duct in *Slit2-/-*, but not *Ntn1-/-*, outgrowths (Fig. 5E, G). The subtle role for NTN1 in ductal morphogenesis is only revealed by the additional removal of *Ntn1* in a *Slit2-/-*

background which increases the severity of the ductal defects (Fig. 5A, B). This suggests that, while SLIT2 plays a primary role in mediating interactions between luminal and myoepithelial cell layers during ductal morphogenesis, NTN1 synergistically contributes to these interactions.

SLIT2 and NTN1 Mediate Contacts between Luminal and Myoepithelial Cell Layers.

In the mammary gland, cadherin based cell adhesion mediates interactions between cells within the two cell layers, with P-cadherin mediating cap and myoepithelial cell adhesion, and E-cadherin mediating luminal cell adhesion (Daniel et al., 1995). Since we observe adhesive defects predominantly in the luminal compartment of *Slit2-/-;Ntn1-/-* outgrowths, we examined whether E-cadherin-mediated cell adhesion between cells of this layer was intact or disrupted. Immunohistochemistry on +/+ control glands with an E-cadherin antibody revealed, as expected, membrane staining around luminal cells (Fig. 6B, D). Similar robust immunostaining was observed between luminal cells of *Slit2-/-;Ntn1-/-* ducts (Fig. 6A, C). Thus, the appearance of cadherin-mediated contacts did not appear altered in double homozygous null tissue despite the presence of morphological abnormalities associated with loss of *Slit2* and *Ntn1*.

Since contacts between luminal cells appeared normal in *Slit2-/-;Ntn1-/-* outgrowths, we examined contacts between luminal and myoepithelial cells. It has been shown that desmosomes mediate contacts between these cell layers in mature ducts (Runswick et al., 2001), so we performed immunohistochemical staining with antibodies directed against desmosomal components. Punctate staining characteristic of desmosomes was not observed, suggesting that even in wildtype tissue, desmosomes are not fully assembled during branching morphogenesis (data not shown) (Dulbecco et al., 1984). Consequently, to investigate the interaction between luminal and myoepithelial cells, we used in vitro aggregation assays to examine whether primary cells, harvested from *Slit2-/-;Ntn1-/-* outgrowths, were impaired in their ability to generate bi-layered epithelial structures. Previous studies have shown that mixtures of wildtype, primary mammary cells form aggregates of luminal cells surrounded by single layers of myoepithelial cells (Runswick et al., 2001). This process appears to be a timed aggregation with luminal cells forming clusters that myoepithelial cells attach to

and surround. In agreement with these previous studies, we confirmed that wildtype cells formed bi-layered organoids (Fig. 7A).

Next, we generated aggregates from *Slit2-/-;Ntn1-/-* cells and observed that, while luminal aggregates formed, few were surrounded by myoepithelial cells. To quantify this assay, we considered a structure bi-layered when there were one or more myoepithelial cells surrounding the luminal cell aggregate. Even with this lenient definition, we found that 70% of *Slit2-/-;Ntn1-/-* aggregates lacked a bi-layer (Fig. 7B). Of the 30% *Slit2-/-;Ntn1-/-* aggregates categorized as having a bi-layer, many contained just one or only a few myoepithelial cells on the outer surface, compared to +/+ aggregates which generally displayed fully-formed myoepithelial cell layers (Fig. 7A). A second characteristic of *Slit2-/-;Ntn1-/-* aggregates was that they appeared smaller than wildtype aggregates. To quantify aggregate size, we counted the number of cells comprising each and categorized them as: fewer than 10 cells, between 10 and 20 cells, and greater than 20 cells (Fig. 7K). All wildtype organoids contained greater than 10 cells and the majority contained greater than twenty. In contrast, the majority of aggregates composed of *Slit2-/-;Ntn1-/-* cells were small, containing less than 10 cells, consistent with a role for the myoepithelial cell layer, which does not form when *Slit2-/-;Ntn1-/-* aggregate, in stabilizing clustered luminal cells in rotary culture. We never observed myoepithelial cells inappropriately mixed into the luminal cell aggregates, a situation that occurs when desmosomal adhesion in disrupted (Runswick et al., 2001). Thus while *Slit2-/-;Ntn1-/-* luminal cells aggregated properly, *Slit2-/-;Ntn1-/-* myoepithelial cells are severely deficient in their ability to adhere to the outside of luminal cell aggregates even though they express the ROBO1 and NEO1 receptors (Fig. 2) (Srinivasan et al., 2003),.

To confirm this deficiency is due to the lack of SLIT2 and NTN1, we repeated the experiment in the presence of 3μg/ml and 6μg/ml of SLIT2 and NTN1 to determine whether bi-layered organoids were formed under these conditions. With 3μg/ml of each protein, the percent of aggregates forming bi-layered structures increased from 30% to 70% with the majority of organoids exhibiting fully-formed myoepithelial layers (Fig. 7C). With 6μg/ml of each protein, bi-layered aggregation was fully rescued (Fig. 7D). To evaluate whether SLIT2 or NTN1 alone were sufficient to rescue the phenotype, we performed the rescue experiment with 3μg/ml, 6μg/ml, or 12μg/ml of each protein alone. At 3μg/ml and 6μg/ml of SLIT2, 40% of the *Slit2-/-;Ntn1-/-*

aggregates formed bi-layered structures, at 12μg/ml this number increased to 80% (Fig. 7E-G). While these organoids were relatively large with the majority composed of greater than 10 cells (Fig. 7K), they lacked the fully formed myoepithelial cell layers that were observed when the rescue experiment was performed with both SLIT2 and NTN1 (Fig. 7 compare C, D with E-G). Addition of NTN1 alone yielded only small aggregates with just 10% considered bi-layered because one or two myoepithelial cells clung to the outer perimeter (Fig. 7H-J). Interestingly, this 10% bi-layered aggregation in the presence of NTN1 was less than the 30% bi-layered aggregation observed under control conditions in the absence of NTN1 and SLIT2, suggesting that NTN1 alone had a modest inhibitory effect on aggregation. Taken together, the data demonstrated that SLIT2, acting through its ROBO1 receptor on myoepithelial cells (Fig. 2), mediates contacts between luminal and myoepithelial cells. This contact formation is synergistically enhanced in the presence of NTN1 whose receptor, NEO1, is also specifically expressed on myoepithelial cells (Srinivasan et al., 2003). At 3μg/ml and 6μg/ml of SLIT2, 40% of the aggregates were bi-layered, a number that increased to 70% and 100%, respectively, with the addition of NTN1 (Fig. 7C-F). The observation that NTN1 acted in concert with SLIT2 to rescue bi-layered aggregation in vitro was consistent with the phenotypes observed in vivo. A ductal phenotype was observed in *Slit2-/-*, and not *Ntn1-/-* outgrowths, but the defects were synergistically strengthened by the additional loss of *Ntn1* in a *Slit2-/-* background (Fig. 5). Thus, SLIT2 and NTN1 function in concert during mammary ductal morphogenesis to generate tubular bi-layers by mediating interactions between distinct epithelial cell layers.

DISCUSSION

During development, bi-layered ducts of mammary epithelium are generated as end buds invade the fat pad forming an elaborately branched structure. Taking advantage of the relatively simple model system of mammary ductal development, we examined the role of two different families of "axon guidance" cues during epithelial morphogenesis. Using a combination of in vivo and in vitro approaches, we provide evidence that SLIT2 and NTN1 act synergistically to generate adhesive contacts between the two distinct epithelial cell layers comprising a tubular bi-layer. Our data support a model in which these cues work in parallel at short-range as

adhesive cues to maintain tissue structure while allowing cell movement and re-organization during periods of rapid tissue growth and remodeling.

Members of Functionally-Related Families Act Synergistically during Mammary Ductal Morphogenesis

During mammary ductal development, only the *Slit2* and *Robo1* members of these gene families are expressed in the gland. While secreted SLIT2 protein is widely distributed throughout the epithelial compartment, ROBO1 is expressed specifically in cap and myoepithelial cells (Figs. 1, 2). Glands harboring loss-of-function mutations in either gene exhibit similar phenotypes, strongly supporting a model in which SLIT2 signals through its ROBO1 receptor at this stage of development. Defects in *Slit2-/-* and *Robo1-/-* glands are confined to the end bud and are relatively modest, but the observed loss of cell-cell interactions in this growth structure is consistent with the loss of stabilizing interactions (Fig. 3). *Slit2-/-* and *Robo1-/-* end buds exhibit a general disorganization in cell contacts with inappropriate spaces forming between the cap and luminal cell layers. Dissociated cells fill these subcapsular spaces and layers of cap cells fold inward, occluding lumenal space. Taken together these results suggest that SLIT2-mediated activation of ROBO1 is required to maintain the proper positioning of cap and luminal cell layers in the end bud.

Our previous studies have already implicated the NTN/NEO guidance system in maintaining proper positioning of cap cells at the leading edge of the end bud (Srinivasan et al., 2003). We proposed that NTN1, expressed by luminal cells, acts adhesively as a short-range attractant to maintain proper positioning of NEO1-expressing cap cells. The similarity in the defects exhibited by *Ntn1-/-* and *Slit2-/-* end buds prompted us to investigate the consequences of genetically interrupting the expression of genes encoding both guidance cues. We show that loss of *Ntn1* in a *Slit2-/-* background results in a synergistic strengthening of the single-mutant phenotypes (Figs. 4, 5). Moreover addition of NTN1 synergistically enhances the ability of SLIT2 to rescue bi-layered aggregation of primary *Slit2-/-;Ntn1-/-* mammary cells (Fig. 7). Our results are consistent with a model in which two different guidance systems act in parallel to mediate interactions between distinct epithelial cell types during organ development, although we have not excluded the possibility that some cross-regulation between these systems occurs (Stein and Tessier-Lavigne, 2001).

SLIT2 Signals through ROBO1 as a Short-Range Adhesive Cue

Our experiments support a positive role for SLIT2 in the developing gland. First, the loss of cell-cell interactions observed in *Slit2*-/- and *Robo1*-/- end buds is consistent with the loss of a stabilizing interaction (Fig. 3). Second, the observation that simple addition of purified SLIT2 rescues the ability of *Slit2*-/-; *Ntn1*-/- cells to form bi-layered organoids (with NTN1 contributing synergistically to this rescue), support an adhesive, rather than instructive, role for SLIT2 since cues do not need to be presented in a way that provides directional information (Fig. 7). Such a short-range adhesive role has been already proposed for NTN1 and NEO1 (Srinivasan et al., 2003). Since SLIT2 is broadly distributed throughout the epithelial compartment (Fig. 1F), it seems likely that it associates with luminal cells via heparin sulfate proteoglycans which have been shown to bind and stabilize SLITs (Ronca et al., 2001; Steigemann et al., 2004). Candidates are glypican and syndecan which are expressed by mammary cells (Delehedde et al., 2001). Moreover, there may be a requirement for proteoglycans on cells that bind, concentrate and present SLITs as well as on receptor expressing cells since, in *Drosophila*, genetic studies have shown that syndecan serves as a necessary co-receptor for ROBO in transducing the SLIT signal (Steigemann et al., 2004).

While most studies have focused on the inhibitory and chemorepulsive influence of SLIT/ROBO signaling on cell migration and axon guidance, a few examples demonstrate its outgrowth promoting activities and chemoattractive functions. For example, human vascular endothelial cells are attracted to SLIT-expressing tumors (Wang et al., 2003), and *Drosophila* mesodermal cells are attracted to SLIT-expressing muscle attachment sites (Kramer et al., 2001). SLITs are also positive regulators of elongation and branch formation for both rat sensory neurons and *Drosophila* tracheal cells (Englund et al., 2002; Wang et al., 1999). While none of these studies demonstrate SLIT acting to increase cell-cell interactions at short-range, the process of guidance at long-range must involve a series of local interactions as cells or axons move up a gradient toward the source of cue. Similarly processes such as branch formation must involve local interactions since a restricted portion of the target membrane preferentially protrudes and becomes stabilized. In the mammary gland, our data suggest that SLIT2, secreted by target cells, is available on cell surfaces in the epithelium where it interacts with

ROBO1 present on the surface of cap/myoepithelial cells. Their interaction maintains tissue architecture and restricts inappropriate intermingling by mediating contacts between distinct epithelial cells layers.

These examples establish positive roles for SLITs and ROBOs in cell migration, branch formation and interepithelial interactions, but studies on the repellent activity of SLITs have supplied details concerning the mechanisms by which the SLIT/ROBO signal is transduced. The intracellular domain of ROBO1 contains four motifs that have been shown to interact with a number of signaling proteins including the actin binding protein ENABLED (murine MENA) (Bashaw et al., 2000; Yu et al., 2002), the nonreceptor Abelson tyrosine kinase, c-ABL (Bashaw et al., 2000), the adaptor DOCK (Fan et al., 2003), and the GTPase-activating protein srGAP1 (Wong et al., 2001). All these signaling proteins are candidates for mediating the attractive and adhesive activities of ROBO. Indeed, before their roles as negative regulators of ROBO signaling were revealed, DOCK was identified as a positive regulator in axon outgrowth and synapse formation (Desai et al., 1999; Garrity et al., 1996), and MENA was shown to promote actin dependent motility (Krause et al., 2002). All these signaling proteins are also candidates for mediating the interaction of ROBO1 with the cytoskeleton, leading to changes in the mobility or adhesiveness of cells. We hypothesize that SLIT2 signals through ROBO1, leading to cytoskeletal remodeling that modulates adhesive contacts between distinct epithelial cell types. Similar signaling would also occur between NTN1 and NEO1. At least in the mammary gland, this signaling is not necessarily instructive since the movement of cap and myoepithelial cells into stroma away from luminal cells is severely restricted by basal lamina (Warburton et al., 1982).

Concluding Remarks

Our discovery that members of functionally-related families act in similar ways during development suggests an explanation for the observation that single loss-of-function mutations and even multiple loss-of-function mutations in family members of genes encoding "axon guidance" cues have failed to yield phenotypes in many vertebrate organ systems. For example, lungs of embryos carrying loss-of-function alleles in both *Ntn1* and *Ntn4* display no apparent phenotype even though treatment of lung explants in vitro with either NTN1 of NTN4 dramatically reduces lung bud formation (Liu et al., 2004). Similarly, early vascular development in

embryos carrying loss-of-function alleles in *Ntn1* appears normal even though treatment of vascular smooth muscle cells and endothelial cells with NTN1 stimulates proliferation, induces migration and promotes adhesion of these cells (Park et al., 2003). In our studies, the phenotypes exhibited in glands harboring homozygous deletions of either *Slit2* or *Netrin1* are relatively mild and largely confined to the highly specialized end bud (Fig. 3) (Srinivasan et al., 2003)). A more dramatic phenotype required deletion of both these guidance cues since they both appear to mediate adhesive, short-range associations between neighboring cell types (Figs. 4, 5). Taken together, these results suggest that deciphering the actions of "axon" guidance cues that function in similar ways, for example adhesively during organ development, will require the analysis of compound homozygous null animals to eliminate the expression of more than one member of functionally-related families. Future studies in the mammary gland and other organ systems may elucidate other combinations of Netrins, Slits, Semaphorins or Ephrins that function synergistically to mediate cell contacts during development.

Acknowledgments

We thank the following people for their generous contributions: Pamela Rabbitts for her kind gift of antibodies generated against ROBO1/DUTT1, Santa Cruz Biotech for antibodies directed against SLITs, David Garrod for antibodies directed against desmosomal constituents, Christelle Sabatier for SLIT2 protein, David Ornitz for *Slit3*-/- mice, Gary Silberstein and Andrew Chisholm for comments on the manuscript. This work was supported by a research scholar grant #RSG0218001MGO from the American Cancer Society, Career grant DAMD170210336 from the U.S. Army Research Command, and research grant 10PB-0188 from the California Breast Cancer Research Program.

Fig. Legends

Fig. 1. Expression patterns of *Slit2* and *Slit3* during mammary gland development.

(A) Schematic of an EB with subtending duct.

(B, C) SLIT2 immunostaining on (B) +/+ and (C) *Slit2*-/- end buds.

(D, E) GFP immunostaining on (B) *Slit2*-/- and (C) +/+ end buds.

(F, G) GFP immunostaining on (D) *Slit2*-/- and (E) +/+ ducts.

(H, I) *Slit3*-/- outgrowth stained for ß-galactosidase activity.

(H) *Slit3* expression in mature virgin duct.

(I) *Slit3* expression in aveoli during pregnancy.

Arrowheads point to examples of positively stained cells in the cap cell layer of the end bud (B, D) and in the myoepithelial cell layer of the duct (F, H). Arrows point to examples of positively stained cells in the luminal compartment of the end bud (D) and duct (F, H).

L, lumen; scale bar = 10μm.

Fig. 2. Expression patterns of *Robo1* and *Robo2* during mammary gland development.

(A, B) ROBO1 immunostaining on (A) +/+ and (B) *Robo1*-/- end buds.

(C, D) *Robo1*-/- outgrowth stained for ß-galactosidase activity in the (C) end bud and (D) duct. (D) shows a grazing, longitudinal section through a duct. Arrowheads identify examples of myoepithelial cells co-expressing *Robo1* (blue) and SMA (brown).

(E) Total RNA was extracted from the mammary gland of 5wk female mice. cDNA was generated and used for RT-PCR using *Dutt1* and *Robo1* specific primers. Lane 1: P4 cerebellum (control), Lane 2: mammary gland. 100bp ladder (NEB) was used as a marker, as shown on the left hand side. *Dutt1* generates a 571bp PCR fragment and *Robo1* generates a 428bp PCR fragment.

(F, G) *Robo2*+/– glands stained for ß-galactosidase activity in the mature virgin duct (F) and aveoli during pregnancy (G).

Arrowheads point to examples of positively stained cells in the cap cell layer of the end bud (A, C) and myoepithelial cell layer of the duct (D, F). Arrows (G) point to examples of positively stained *Robo2*-expressing cells.

L, lumen; scale bar = 10μm.

Fig. 3. Loss of either *Slit2* or *Robo1* leads to similarly abnormal end buds.

(A-G) End buds immunostained with an antibody directed against SMA to identify cap and myoepithelial cell layers.

(A, E) Wildtype (+/+) end bud morphology shows tight juxtaposition of cap and luminal cell layers.

(B-D) Longitudinal sections through *Slit2*-/- end buds.

(B) Exaggerated space between the cap and luminal cell layers (double arrowhead) and dissociated cells detected in subcapsular space.

(C) Loss of luminal cells underlying the cap cell layer (between arrows).

(D) Complete disruption of end bud morphology characterized by the infolding of cap cells into the luminal compartment (arrowheads) leading to lumen loss.

(F, G) Longitudinal sections through *Robo1*-/- end buds.

(F) Exaggerated space between the cap and luminal cell layers (double arrowheads), dissociated cells in the subscapular space, and infolding of the cap cell layer into the luminal compartment (arrowheads).

(G) Complete disruption of end bud morphology characterized by the infolding of cap cells into the luminal compartment (arrowheads) leading to lumen loss.

(A-D) *Slit2*-/- outgrowths were generated by transplantation with contralateral +/+ control outgrowths.

(E-G) *Robo1*-/- and +/+ mammary glands were from littermates.

L, lumen; scale bar = 10μm.

Fig. 4. Combined loss of *Slit2* and *Ntn1* leads to abnormal end bud morphology with characteristics of both *Slit2*-/-and *Ntn1*-/- end buds.

All end buds immunostained with antibody generated against SMA.

(A-C) *Slit2*-/-;*Ntn1*-/- end buds.

(A) Loss of luminal cells underlying the cap cell layer (between arrowheads).

(B) Separation of the cap cell layer from the luminal cell layer (double arrowhead) and breaks in the basal lamina (rectangles).

(C) Complete disruption of end bud morphology characterized by the infolding of cap cells into the luminal compartment (arrowhead) leading to lumen loss.

(D) +/+ end bud.

L, lumen; scale bar = 10μm.

Fig. 5. Loss of both *Slit2* and *Ntn1* and leads to separation of epithelial cell layers in the duct.

All ducts immunostained with antibody generated against SMA.

(A,B) *Slit2-/-;Ntn1-/-* ducts.

(A) Moderate disruption characterized by sporadic loss of luminal cells (arrows).

(B) Separation of epithelial layer (double arrowhead).

(C) Table quantifying the severity of ductal disruption. *Ntn1-/-* ducts are normal whereas *Slit2-/-* and *Slit2-/-;Ntn1-/-* ducts display increasingly severe disorganization.

(+) Modest disruption is characterized by sporadic loss of luminal cells in short (~50mm) length of duct. (++) More severe disruption is characterized by significant stretches (~50-2000mm) of separation of myoepithelial and luminal cell layers.

(D) *Slit2+/+;Ntn1* +/+ duct from contralateral transplant shows tight juxtaposition of myoepithelial and luminal epithelial cell layers and an unobstructed lumen.

(E,F) Loss of *Slit2* (E) leads to sporadic loss of luminal cells (arrows) in the duct, compared to *Slit2* +/+ duct (F) from contralateral transplant duct.

(G,H) *Ntn1-/-* duct (G) appears morphologically indistinguishable compared to *Ntn1-/-* +/+ duct (H) from contralateral transplant.

L, Lumen; scale bar=10μm.

Fig. 6. E-cadherin adhesion system is intact in *Slit2;Ntn1-/-* ducts.

(A-D) Immunostaining on ducts with anti-E-cadherin. Luminal cells display normal E-cadherin staining in (A) *Slit2-/-;Ntn1-/-* and (B) +/+ ducts. (C, D) Magnified image (5X) of the ducts, indicated by the white rectangle in (A) and (B), respectively.

(E, F) Phase contrast image of (E) *Slit2-/-;Ntn1-/-* duct and (F) +/+ ducts, as shown in (A) and (B), respectively. Double arrowhead (A, E) represent separation of myoepithelial cell layer from luminal cell layer.

L, Lumen; scale bar=10μm.

Fig. 7. *Slit2-/-;Ntn1-/-* myoepithelial cells are unable to form bi-layered aggregates in vitro.

(A-J) Aggregates are stained with SMA (red) and DAPI (blue), a nuclear stain. (A) +/+ aggregates are bi-layered, forming luminal cell aggregates surrounded by a layer of myoepithelial cells. (B) *Slit2-/-;Ntn1-/-* aggregates are bi-layered 30% of the time and are smaller in size, compared to +/+. Bi-layered is defined as having 1 or more myoepithelial cells surrounding the luminal cell aggregate. Addition of (C) 3μg/ml or (D) 6μg/ml of SLIT2 and NTN1 restores bi-layered structure of the aggregates. Addition of (E) 3μg/ml, (F) 6μg/ml, and (G) 12μg/ml of SLIT2 alone partially restores the ability of aggregates to form bi-layered structures. However, aggregates are unable to form bi-layered structures in the presence (H) 3μg/ml, (I) 6μg/ml, and (J) 12μg/ml of NTN1 alone. The percentage of aggregates that exhibit bi-layered morphology is shown below each aggregate.

(K) Quantification of aggregate formation in the absence or presence of SLIT2 and NTN1. *Slit2-/-;Ntn1-/-* cells form larger numbers of smaller aggregates compared to +/+ aggregates (black). However, addition of either 3μg/ml or 6μg/ml of SLIT2 and NTN1 rescues bi-layered morphology and allows *Slit2-/-;Ntn1-/-* cells to form larger aggregates (purple). Addition of SLIT2 alone (blue) partially rescues bilayered morphology and allows *Slit2-/-;Ntn1-/-* cells to form larger aggregates, but addition of NTN1 alone (orange) does not restore the ability of *Slit2-/-;Ntn1-/-* cells to form larger aggregates. Scale bar = 10μm.

References:

Bashaw, G. J., Kidd, T., Murray, D., Pawson, T. and Goodman, C. S. (2000). Repulsive axon guidance: Abelson and Enabled play opposing roles downstream of the roundabout receptor. *Cell* 101, 703-15.

Clark, K., Hammond, E. and Rabbitts, P. (2002). Temporal and spatial expression of two isoforms of the Dutt1/Robo1 gene in mouse development. *FEBS Lett* 523, 12-6.

Colamarino, S. A. and Tessier-Lavigne, M. (1995). The axonal chemoattractant netrin-1 is also a chemorepellent for trochlear motor axons. *Cell* 81, 621-9.

Daniel, C. W., Strickland, P. and Friedmann, Y. (1995). Expression and functional role of E- and P-cadherins in mouse mammary ductal morphogenesis and growth. *Dev Biol* 169, 511-9.

Deiner, M. S., Kennedy, T. E., Fazeli, A., Serafini, T., Tessier-Lavigne, M. and Sretavan, D. W. (1997). Netrin-1 and DCC mediate axon guidance locally at the optic disc: loss of function leads to optic nerve hypoplasia. *Neuron* 19, 575-89.

Delehedde, M., Lyon, M., Sergeant, N., Rahmoune, H. and Fernig, D. G. (2001). Proteoglycans: pericellular and cell surface multireceptors that integrate external stimuli in the mammary gland. *J Mammary Gland Biol Neoplasia* 6, 253-73.

Desai, C. J., Garrity, P. A., Keshishian, H., Zipursky, S. L. and Zinn, K. (1999). The Drosophila SH2-SH3 adapter protein Dock is expressed in embryonic axons and facilitates synapse formation by the RP3 motoneuron. *Development* 126, 1527-35.

Dulbecco, R., Allen, W. R. and Bowman, M. (1984). Lumen formation and redistribution of inframembranous proteins during differentiation of ducts in the rat mammary gland. *Proc Natl Acad Sci U S A* 81, 5763-6.

Englund, C., Steneberg, P., Falileeva, L., Xylourgidis, N. and Samakovlis, C. (2002). Attractive and repulsive functions of Slit are mediated by different receptors in the Drosophila trachea. *Development* 129, 4941-51.

Fan, X., Labrador, J. P., Hing, H. and Bashaw, G. J. (2003). Slit stimulation recruits Dock and Pak to the roundabout receptor and increases Rac activity to regulate axon repulsion at the CNS midline. *Neuron* 40, 113-27.

Garrity, P. A., Rao, Y., Salecker, I., McGlade, J., Pawson, T. and Zipursky, S. L. (1996). *Drosophila* photoreceptor axon guidance and targeting requires the dreadlocks SH2/SH3 adapter protein. *Cell* 85, 639-50.

Huminiecki, L., Gorn, M., Suchting, S., Poulsom, R. and Bicknell, R. (2002). Magic roundabout is a new member of the roundabout receptor family that is endothelial specific and expressed at sites of active angiogenesis. *Genomics* 79, 547-52.

Kang, J. S., Yi, M. J., Zhang, W., Feinleib, J. L., Cole, F. and Krauss, R. S. (2004). Netrins and neogenin promote myotube formation. *J Cell Biol* 167, 493-504.

Kappler, J., Franken, S., Junghans, U., Hoffmann, R., Linke, T., Muller, H. W. and Koch, K. W. (2000). Glycosaminoglycan-binding properties and secondary structure of the C-terminus of netrin-1. *Biochem Biophys Res Commun* 271, 287-91.

Kennedy, T. E., Serafini, T., de la Torre, J. R. and Tessier-Lavigne, M. (1994). Netrins are diffusible chemotropic factors for commissural axons in the embryonic spinal cord. *Cell* 78, 425-35.

Kidd, T., Bland, K. S. and Goodman, C. S. (1999). Slit is the midline repellent for the robo receptor in Drosophila. *Cell* 96, 785-94.

Kramer, S. G., Kidd, T., Simpson, J. H. and Goodman, C. S. (2001). Switching repulsion to attraction: changing responses to slit during transition in mesoderm migration. *Science* 292, 737-40.

Krause, M., Bear, J. E., Loureiro, J. J. and Gertler, F. B. (2002). The Ena/VASP enigma. *J Cell Sci* 115, 4721-6.

Liu, Y., Stein, E., Oliver, T., Li, Y., Brunken, W. J., Koch, M., Tessier-Lavigne, M. and Hogan, B. L. (2004). Novel role for Netrins in regulating epithelial behavior during lung branching morphogenesis. *Curr Biol* 14, 897-905.

Park, K. W., Morrison, C. M., Sorensen, L. K., Jones, C. A., Rao, Y., Chien, C. B., Wu, J. Y., Urness, L. D. and Li, D. Y. (2003). Robo4 is a vascular-specific receptor that inhibits endothelial migration. *Dev Biol* 261, 251-67.

Robinson, G. W., Accili, D. and Hennighausen, L. (2000). Rescue of Mammary Epithelium of Early Lethal Phenotypes by Embryonic Mammary Gland Transplantation as Exemplified with Insulin Receptor Null Mice. New York: Kluwer Academic/Plenum Press.

Ronca, F., Andersen, J. S., Paech, V. and Margolis, R. U. (2001). Characterization of Slit protein interactions with glypican-1. *J Biol Chem* 276, 29141-7.

Runswick, S. K., O'Hare, M. J., Jones, L., Streuli, C. H. and Garrod, D. R. (2001). Desmosomal adhesion regulates epithelial morphogenesis and cell positioning. *Nat Cell Biol* 3, 823-30.

Sabatier, C., Plump, A. S., Ma, L., Brose, K., Murakami, F., Lee, E. Y. and Tessier-Lavigne, M. (2004). The divergent Robo family protein Rig-1 is a negative regulator of Slit responsiveness requried for midline crossing by commissural axons. *Cell* 117, 157-169.

Silberstein, G. B. (2001). Postnatal mammary gland morphogenesis. *Microsc Res Tech* 52, 155-62.

Simpson, J. H., Kidd, T., Bland, K. S. and Goodman, C. S. (2000). Short-range and long-range guidance by slit and its Robo receptors. Robo and Robo2 play distinct roles in midline guidance. *Neuron* 28, 753-66.

Srinivasan, K., Strickland, P., Valdes, A., Shin, G. C. and Hinck, L. (2003). Netrin-1/neogenin interaction stabilizes multipotent progenitor cap cells during mammary gland morphogenesis. *Dev Cell* 4, 371-82.

Steigemann, P., Molitor, A., Fellert, S., Jackle, H. and Vorbruggen, G. (2004). Heparan sulfate proteoglycan syndecan promotes axonal and myotube guidance by slit/robo signaling. *Curr Biol* 14, 225-30.

Stein, E. and Tessier-Lavigne, M. (2001). Hierarchical organization of guidance receptors: silencing of netrin attraction by slit through a Robo/DCC receptor complex. *Science* 291, 1928-38.

Wang, B., Xiao, Y., Ding, B. B., Zhang, N., Yuan, X., Gui, L., Qian, K. X., Duan, S., Chen, Z., Rao, Y. et al. (2003). Induction of tumor angiogenesis by Slit-Robo signaling and inhibition of cancer growth by blocking Robo activity. *Cancer Cell* 4, 19-29.

Wang, K. H., Brose, K., Arnott, D., Kidd, T., Goodman, C. S., Henzel, W. and Tessier-Lavigne, M. (1999). Biochemical purification of a mammalian slit protein as a positive regulator of sensory axon elongation and branching. *Cell* 96, 771-84.

Warburton, M. J., Mitchell, D., Ormerod, E. J. and Rudland, P. (1982). Distribution of myoepithelial cells and basement membrane proteins in the resting, pregnant, lactating, and involuting rat mammary gland. *J Histochem Cytochem* 30, 667-76.

Wong, K., Ren, X. R., Huang, Y. Z., Xie, Y., Liu, G., Saito, H., Tang, H., Wen, L., Brady-Kalnay, S. M., Mei, L. et al. (2001). Signal transduction in neuronal migration: roles of GTPase activating proteins and the small GTPase Cdc42 in the Slit-Robo pathway. *Cell* 107, 209-21.

Young, L. J. T. (2000). The Cleared Mammary Fat Pad and the Transplantation of Mammary Gland Morphological Structures and Cells. New York: Kluwer Academic/Plenum Press.

Yu, T. W., Hao, J. C., Lim, W., Tessier-Lavigne, M. and Bargmann, C. I. (2002). Shared receptors in axon guidance: SAX-3/Robo signals via UNC-34/Enabled and a Netrin-independent UNC-40/DCC function. *Nat Neurosci* 5, 1147-54.

Zhang, F., Ronca, F., Linhardt, R. J. and Margolis, R. U. (2004). Structural determinants of heparan sulfate interactions with Slit proteins. *Biochem Biophys Res Commun* 317, 352-7.

Figure 1

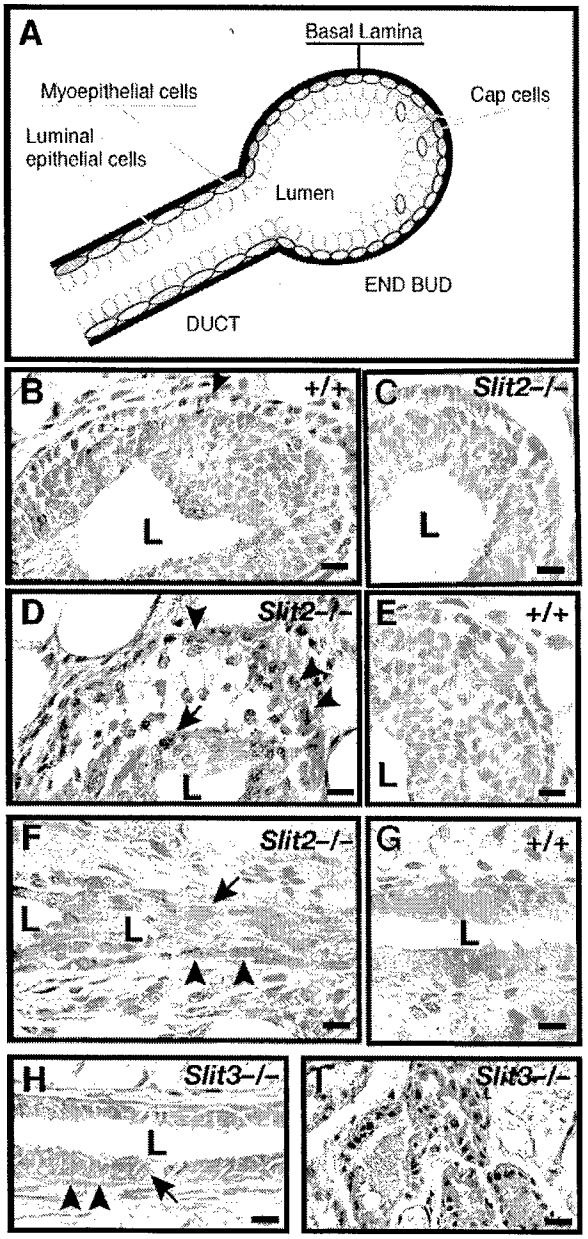
A
Basal Lamina
Myoepithelial cells
Cap cells
Luminal epithelial cells
Lumen
END BUD
DUCT
B
+/+
L
C
Slit2-/-
L
D
Slit2-/-
L
E
+/+
L
F
Slit2-/-
L
L
G
+/+
L
H
Slit3-/-
L
I
Slit3-/-

Figure 2

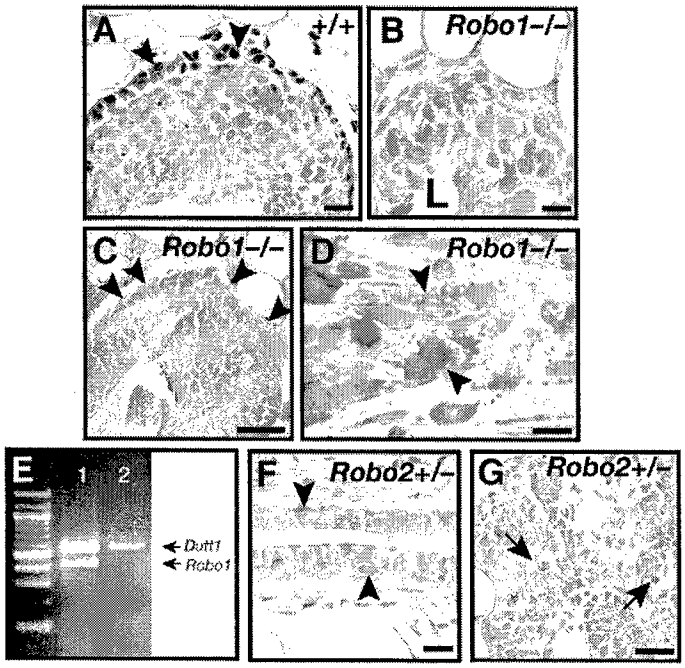

Figure 3

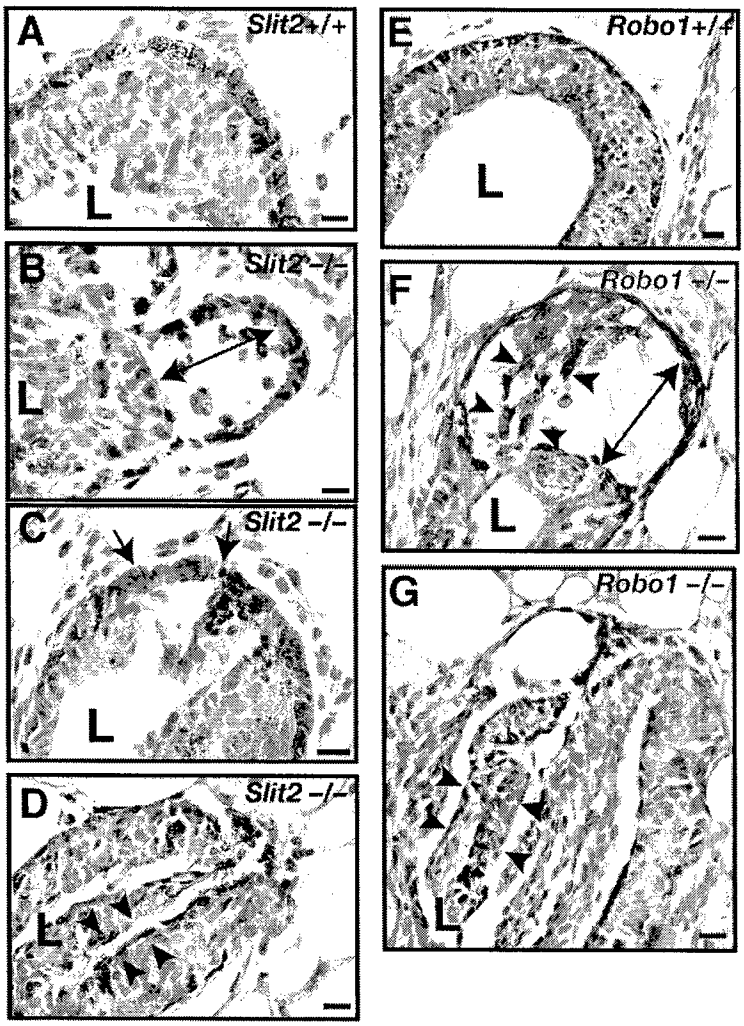

Figure 4

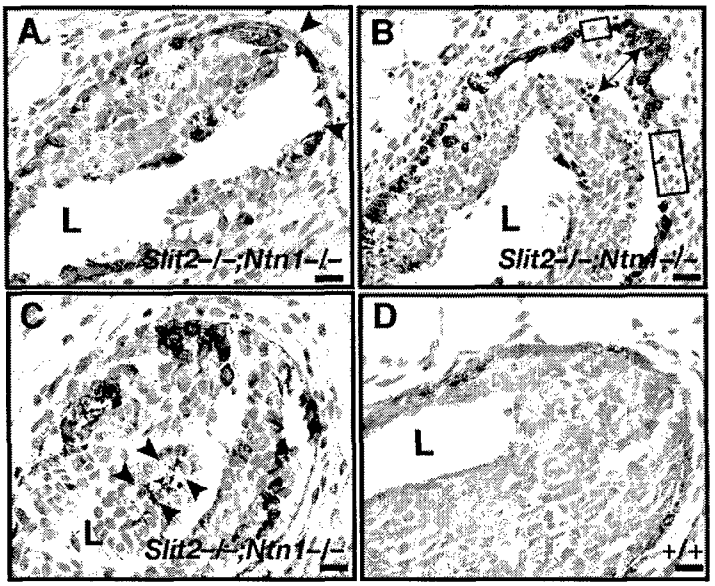

Figure 5

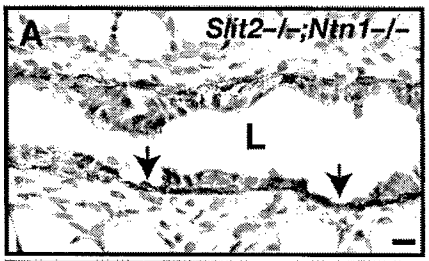

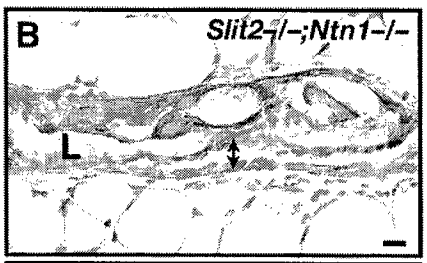

C	+ sporadic loss of luminal cells	++ separation of epithelial layers
Slit2-/-;Ntn1-/-	11%	89%
Slit2-/-	50%	50%
Ntn1-/-	0%	0%

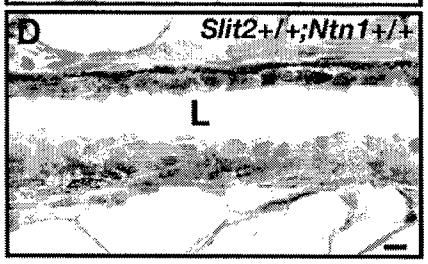

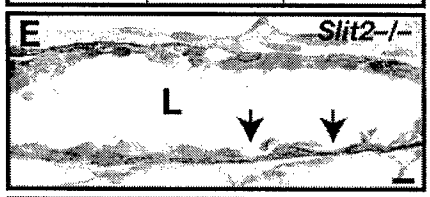

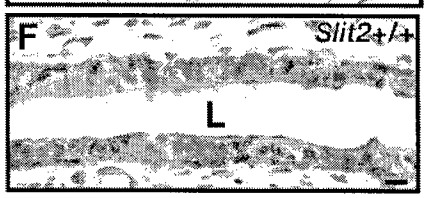

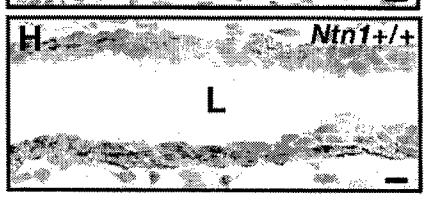

Figure 6

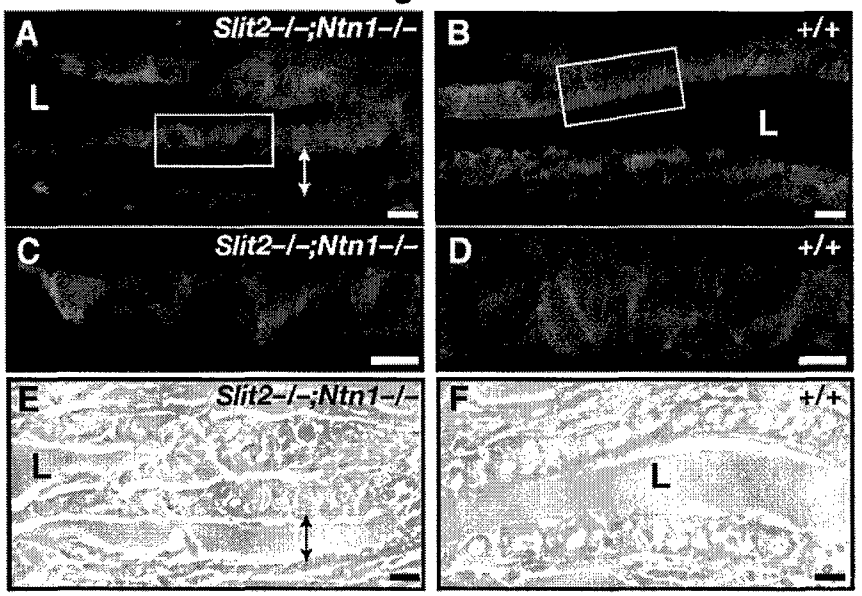

Figure 7

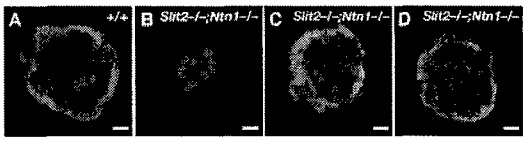

SLIT2	0μg/ml	0μg/ml	3μg/ml	6μg/ml
NTN 1	0μg/ml	0μg/ml	3μg/ml	6μg/ml
% of bi-layered aggregates*	100%	30%	70%	100%

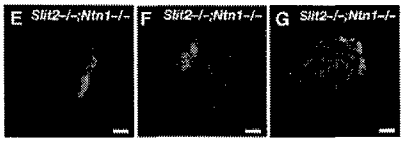

SLIT2	3μg/ml	6μg/ml	12μg/ml
NTN 1	0μg/ml	0μg/ml	0μg/ml
% of bi-layered aggregates*	40%	40%	80%

SLIT2	0μg/ml	0μg/ml	0μg/ml
NTN 1	3μg/ml	6μg/ml	12μg/ml
% of bi-layered aggregates*	10%	10%	10%